

INFORMATION TO USERS

This manuscript has been reproduced from the microfilm master. UMI films the text directly from the original or copy submitted. Thus, some thesis and dissertation copies are in typewriter face, while others may be from any type of computer printer.

The quality of this reproduction is dependent upon the quality of the copy submitted. Broken or indistinct print, colored or poor quality illustrations and photographs, print bleedthrough, substandard margins, and improper alignment can adversely affect reproduction.

In the unlikely event that the author did not send UMI a complete manuscript and there are missing pages, these will be noted. Also, if unauthorized copyright material had to be removed, a note will indicate the deletion.

Oversize materials (e.g., maps, drawings, charts) are reproduced by sectioning the original, beginning at the upper left-hand corner and continuing from left to right in equal sections with small overlaps. Each original is also photographed in one exposure and is included in reduced form at the back of the book.

Photographs included in the original manuscript have been reproduced xerographically in this copy. Higher quality 6" x 9" black and white photographic prints are available for any photographs or illustrations appearing in this copy for an additional charge. Contact UMI directly to order.

U·M·I

University Microfilms International
A Bell & Howell Information Company
300 North Zeeb Road, Ann Arbor, MI 48106-1346 USA
313/761-4700 800/521-0600

Order Number 9321216

**Phase relations in the system $\text{CeO}_2\text{-Al}_2\text{O}_3\text{-SiO}_2$ in inert and
reducing atmospheres**

Tas, Ahmet Cuneyt, Ph.D.

Iowa State University, 1993

U·M·I

300 N. Zeeb Rd.
Ann Arbor, MI 48106

Phase relations in the
system CeO_2 - Al_2O_3 - SiO_2 in
inert and reducing atmospheres

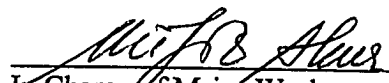
by

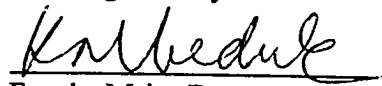
Ahmet Cuneyt Tas

A Dissertation Submitted to the
Graduate Faculty in Partial Fulfillment of the
Requirements for the Degree of
DOCTOR OF PHILOSOPHY

Department: Materials Science and Engineering
Major: Ceramic Engineering

Approved :


In Charge of Major Work


For the Major Department


For the Graduate College

Iowa State University
Ames, Iowa

1993

TABLE OF CONTENTS

	Page
GENERAL INTRODUCTION	1
PAPER I: CERIUM OXYGEN APATITE ($\text{Ce}_{4.67}[\text{SiO}_4]_3\text{O}$) X-RAY DIFFRACTION PATTERN REVISITED	4
ABSTRACT	6
INTRODUCTION	7
EXPERIMENTAL PROCEDURE	9
RESULTS AND DISCUSSION	14
SUMMARY	22
REFERENCES	23
PAPER II: PHASE RELATIONS IN THE SYSTEM Al_2O_3 - $\text{Ce}_2\text{Si}_2\text{O}_7$ IN THE TEMPERATURE RANGE 900° TO 1925°C IN INERT ATMOSPHERE	24
ABSTRACT	26
INTRODUCTION	27
EXPERIMENTAL PROCEDURE	29
RESULTS AND DISCUSSION	35
CONCLUSIONS	52
REFERENCES	53
APPENDIX 1. X-RAY DIFFRACTION PATTERN OF MONOCLINIC $\text{Ce}_2\text{Si}_2\text{O}_7$	55
APPENDIX 2. X-RAY DIFFRACTION PATTERN OF TETRAGONAL $\text{Ce}_2\text{Si}_2\text{O}_7$	63
PAPER III: PHASE RELATIONS IN THE SYSTEM Ce_2O_3 - $\text{Ce}_2\text{Si}_2\text{O}_7$ IN THE TEMPERATURE RANGE 1150° TO 1970°C IN REDUCING AND INERT ATMOSPHERES	67
ABSTRACT	69
INTRODUCTION	70
EXPERIMENTAL PROCEDURE	73
RESULTS AND DISCUSSION	80
CONCLUSIONS	107
REFERENCES	108
PAPER IV: PHASE RELATIONS AND STRUCTURES IN THE SYSTEM Ce_2O_3 - Al_2O_3 IN INERT AND REDUCING ATMOSPHERES	111
ABSTRACT	113
INTRODUCTION	114

	Page
EXPERIMENTAL PROCEDURE	119
RESULTS AND DISCUSSION	121
CONCLUSIONS	149
ACKNOWLEDGEMENTS	151
REFERENCES	152
 PAPER V: STRUCTURAL INVESTIGATION OF PURE AND N-DOPED CERIUM OXYGEN APATITE ($\text{Ce}_{4.67}[\text{SiO}_4]_3\text{O}$) BY NEUTRON DIFFRACTION	 156
ABSTRACT	158
INTRODUCTION	159
EXPERIMENTAL PROCEDURE	161
RESULTS AND DISCUSSION	163
CONCLUSIONS	177
ACKNOWLEDGEMENT	178
REFERENCES	179
 GENERAL SUMMARY	 181
 ACKNOWLEDGEMENTS	 185
 APPENDIX A. SCHEMATIC OF THE QUENCHING FURNACE AND DTA ACCESSORIES USED IN THIS STUDY	 186
 APPENDIX B. LISTINGS OF THE PROGRAMME WRITTEN IN BASIC FOR THE DTA MODULES OF THIS STUDY	 190
 APPENDIX C. X-RAY DIFFRACTION PATTERN OF Ce_2SiO_5	 212
 APPENDIX D. SAMPLES OF DTA CALIBRATION RUNS	 217

GENERAL INTRODUCTION

The most abundant and the least expensive of all the rare earth elements, Cerium, has received little scientific interest when compared to the other members of the rare earth family. The interest paid to the cerium silicates and aluminates, mainly over the decade of 60's, by the Soviet researchers and few others has generally been limited to the preparation and synthesis of compounds and the subsequent structural studies. The illustrious valency change observed in cerium between the 3+ (inert / reducing) and 4+ (oxidising) states has also been one of the causes of such lack of interest among the phase equilibria researchers towards cerium-silicates, -aluminates, and -aluminosilicates.

It is one of the prerequisites in ceramic science that in the synthesis and preparation of better ceramics, especially with new materials, a beforehand fundamental understanding of the phase relations and equilibria between the component phases and scrupulous characterisation of individual phases in their pure forms should be available prior to the assesment of the performance characteristics of the final product. A quite contrary approach has been illustrated in the synthesis of Y- or Ce-SIALON ceramics. Y_2O_3 or CeO_2 have been added, together with small amounts of Al_2O_3 , to a Si_3N_4 matrix to form Y- or Ce-aluminosilicate liquids at the boundaries of Si_3N_4 grains at typical hot-pressing temperatures in excess of 1650°C. Upon cooling from the synthesis temperatures, researchers reported the formation of crystalline Y- or Ce-silicate phases which were also found to be detrimental to the mechanical

properties of the final products. The characterisation of those crystalline silicate phases, especially in the case of Ce-SIALON's, was attempted in the absence of a phase diagram showing the high temperature phase relations among all the known silicate phases of the Ce_2O_3 - SiO_2 system and in the absence of any information on the ternary phase equilibria in the Ce_2O_3 - Al_2O_3 - SiO_2 system. As a result of this, many researchers have reported the observation of some or all of the Ce-silicate phases in their final products of similar compositions without being able to predict their stability regions at elevated temperatures.

Similar difficulties have been encountered in recent years in ceramic systems with compositions able to crystallise the binary compounds (i.e., CeAlO_3 and $\text{CeAl}_{11}\text{O}_{18}$) of the Ce_2O_3 - Al_2O_3 system at elevated temperatures. The formation of $\text{CeAl}_{11}\text{O}_{18}$, in relatively small amounts, has been observed in CeO_2 - Al_2O_3 - ZrO_2 ceramics. The X-ray characterisation of this phase has usually resorted to an assumed structural similarity with the other lanthanide hexaaluminates largely because no diffraction and structure data have been available for this compound.

This study was targeted, at first, to address the above-mentioned difficulties in the literature. Considering the fact that any systematic information available on the crystallographic and microstructural behaviour of materials as a function of temperature and composition would make it possible to exploit these materials to the fullest extent, it is hoped that this work will broaden the basic understanding of the cerium-silicates and -aluminates.

Explanation of the Dissertation Format

The five sections in this dissertation are self-contained papers corresponding to five distinct phases of research. The papers are presented here in the chronological order they were written. The first paper has already been published in Powder Diffraction (Vol. 7, 219-222, 1992). The second paper has been presented at the 94th Annual Convention of the American Ceramic Society and has been accepted for publication in the Journal of the American Ceramic Society. The remaining three papers were submitted for publication in the Journal of the American Ceramic Society. There is a general summary following the last paper. Though Dr. M. Akinc appears as co-author in these papers, A.C. Tas is the principal investigator and author of the work presented here. All experiments were performed by the principal investigator with the exception of neutron diffraction and Rietveld analyses which were performed by Dr. V.G. Young, Jr. For his contributions, Dr. Young appears as co-author in the last paper.

PAPER I: CERIUM OXYGEN APATITE ($\text{Ce}_{4.67}[\text{SiO}_{4.3}\text{O}]$) X-RAY DIFFRACTION
PATTERN REVISITED

Cerium Oxygen Apatite ($\text{Ce}_{4.67}[\text{SiO}_4]_3\text{O}$) X-Ray Diffraction Pattern Revisited

Submitted by

A. Cuneyt Tas and Mufit Akinc

Department of Materials Science and Engineering

Iowa State University

Ames, Iowa 50011

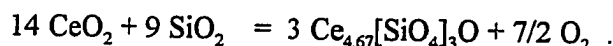
This manuscript has been published in Powder Diffraction in December 1992.

ABSTRACT

A new X-ray diffraction pattern for the compound cerium oxygen apatite, $\text{Ce}_{4.67}[\text{SiO}_4]_3\text{O}$ is suggested. The compound was prepared by the solid state reaction of the oxides, CeO_2 and SiO_2 and has a hexagonal crystal structure with the lattice constants $a = 9.6578 \text{ \AA}$ and $c = 7.1187 \text{ \AA}$. The sample of the most recent PDF pattern 31-0336* (Visser, 1978) for this compound is believed to be contaminated with significant quantities of N owing to the fact that it was prepared by mixing Ce_2O_3 and Si_3N_4 and its very close resemblance to the pattern displayed in the PDF 33-0333 given for the cerium "nitrogen" apatite, $\text{Ce}_3[\text{SiO}_4]_3\text{N}$.

INTRODUCTION

The apatite ($\text{Ca}_5[\text{PO}_4]_3\text{F}$) -type compound, cerium (III) orthosilicate ($\text{Ce}_{4.67}[\text{SiO}_4]_3\text{O}$) in the CeO_2 - SiO_2 binary system forms according to the following reaction (Felsche, 1969):



Depending on the gas atmosphere, the forward reaction is favoured at elevated temperatures (i.e., $T > 1550^\circ\text{C}$) from pure oxides in a vacuum atmosphere. The evolution of the gaseous O_2 was confirmed by mass spectrometer and with an appropriate amount of weight loss by thermogravimetry. The XRD pattern of this compound was indexed by Felsche (1969) as hexagonal belonging either to P6_3 or $\text{P6}_3/\text{m}$ space group with lattice dimensions equal to $a = 9.659$ and $c = 7.121 \text{ \AA}$ with two formula units per unit cell. Felsche's pattern was later published as PDF 22-0169. This pattern was then replaced by that of Visser (1978). Visser's pattern (#31-0336*) was given a star quality and it identified the Ce-apatite to belong to the $\text{P6}_3/\text{m}$ space group. Lattice constants were given as $a = 9.6387$ and $c = 7.1812 \text{ \AA}$.

The difference between the patterns of Felsche and Visser was that the latter included about 10 additional weak reflections, slight shift in d-spacings resulting in a slight difference in the lattice constants.

The primary purpose of the present study was to investigate the phase relations in the CeO_2 - SiO_2 - Al_2O_3 system in inert atmosphere. As a prerequisite for this investigation, a systematic study into the synthesis and structural characterisation of compounds in the

CeO_2 - SiO_2 and CeO_2 - Al_2O_3 binaries was done. This report addresses the discrepancy observed for Ce-Apatite, $\text{Ce}_{4.67}[\text{SiO}_4]_3\text{O}$, phase.

EXPERIMENTAL PROCEDURE

Stoichiometric $\text{Ce}_{4.67}[\text{SiO}_4]_3\text{O}$ was synthesized by combining appropriate quantities of CeO_2 (99.87% pure, Cerac) and fumed SiO_2 (99.98% pure, Sigma) in acetone and wet mixing in plastic jars for 50 minutes followed by overnight drying at 80 °C. Powders were pressed into pellets in a tungsten carbide lined steel die at about 140 MPa. Pellets were prefired at 950 °C for 4 hours in air, followed by heating on a platinum sample holder in a vertical tube furnace at 1560 °C in a pre-purified flowing argon atmosphere for 6 hours, followed by quenching in water. When the homogeneity of the product or the completeness of the reaction is in doubt, the samples were reground, pressed and fired for another 6 hours. Analysis of the product by laser source mass spectroscopy indicates that only carbon (5400 ppm), nitrogen (1200 ppm) and boron (150 ppm) impurities are present at significant quantities. All other elements are below the 50 ppm level. Carbon is believed to have been introduced during quenching. The water quench bath is covered with a low vapour pressure oil layer which forms a char layer upon the pellet. The source of boron and nitrogen is unknown. One possible source for nitrogen could be an impurity in the flowing argon gas.

The XRD patterns of the product were obtained using a Guinier camera and monochromatic $\text{CuK}\alpha_1$ radiation. Experimental procedures are summarised in Table 1. The XRD pattern of the single phase $\text{Ce}_{4.67}[\text{SiO}_4]_3\text{O}$ sample along with the lattice constants are given in Table 2. The standard errors in lattice constants are 3.46×10^{-4} and 4.40×10^{-4} for a

Table 1. Powder diffraction data for phase characterisation

Name :	Cerium Oxygen Apatite or Cerium Oxide Silicate
Empirical Formula :	$\text{Ce}_{4.667}[\text{SiO}_4]_3\text{O}$
Chemical Analysis :	Yes
Source/preparation :	Synthetic; fusion of binary oxides CeO_2 and SiO_2 under inert atmosphere
Radiation type, source :	X-rays, Cu
Wavelength used :	1.5406 Å $K\alpha_1$, Monochromatic
Camera :	Guinier
Camera radius :	57.16 mm
Guinier geometry :	$\text{DELTA} = A1 \cdot L + A2$ ($L = L(\text{MEASURED}) - L(\text{PRIM})$)
	$A1 = 0.181\text{E-}02$ $A2 = -0.121\text{E+}00$
	$\text{DELTA} = A1 \cdot L^2 + A2 \cdot L + A3$
	$A1 = 0.168\text{E-}04$ $A2 = -0.170\text{E-}02$ $A3 = 0.425\text{E-}01$
Temperature (°C) :	25 ± 1
Range of 2θ from :	$5^\circ 2\theta$ to $85^\circ 2\theta$
Internal 2θ standard :	Si (NBS 640a)
Lattice parameter of 2θ standard :	5.4308 Å
2θ error correction procedure :	Interpolation from 2θ 's of standard
Intensity meas. technique :	Peak heights
Method of cell detn. :	Cell and structure known from Felsche (1969)
Cell refinement method :	Least-squares. Appleman and Evans (1973)

Table 2. Powder diffraction data for $\text{Ce}_{4.67}[\text{SiO}_4]_3\text{O}$

$2\Theta_{\text{obs}}$	I/I_0	d_{obs}	hkl	$2\Theta^*$
18.370	4	4.8257	110	+0.013
21.238	30	4.1801	200	+0.010
22.235	24	3.9948	111	+0.008
25.000	16	3.5588	002	+0.003
27.206	37	3.2751	102	0.000
28.207	42	3.1611	210	+0.001
30.922	100	2.8895	211	-0.003
31.188	53	2.8654	112	-0.003
32.072	34	2.7884	300	-0.005
33.015	3	2.7109	202	-0.005
38.789	7	2.3196	310	+0.002
39.374	4	2.2865	221	0.000
40.878	3	2.2058	311	-0.004
41.084	5	2.1952	302	-0.007
42.407	10	2.1297	113	-0.001
43.227	6	2.0912	400	-0.005
43.837	1	2.0635	203	+0.007
45.346	31	1.9983	222	-0.004
46.701	16	1.9434	312	0.000
47.887	38	1.8980	213	-0.007
49.132	19	1.8528	321	-0.003
49.922	29	1.8253	410	-0.004
50.586	32	1.8029	402	0.000
51.290	11	1.7798	004	-0.004
54.336	2	1.6870	322	+0.071
56.177	4	1.6360	204	+0.058
56.606	2	1.6246	412	-0.020
58.339	5	1.5804	420	+0.009
58.763	9	1.5700	331	0.000

Table 2. (continued)

$2\Theta_{\text{obs}}$	I/I_0	d_{obs}	hkl	$2\Theta^*$
59.559	10	1.5509	214	-0.004
59.874	2	1.5435	421	-0.019
61.173	13	1.5138	502	+0.006
61.724	2	1.5016	510	+0.027
61.788	5	1.5002	304	-0.005
62.165	8	1.4920	323	+0.001
63.216	7	1.4697	511	+0.006
63.365	9	1.4666	332	+0.001
64.336	2	1.4468	413	-0.005
67.643	2	1.3839	512	+0.006
68.140	4	1.3750	430	+0.001
69.258	3	1.3555	404	-0.015
69.563	2	1.3503	431	-0.014
70.236	2	1.3390	520	+0.018
70.660	4	1.3320	333	+0.004
71.639	8	1.3162	521	+0.001
72.350	3	1.3050	324	-0.010
72.802	11	1.2980	602	-0.001
74.375	22	1.2744	414	-0.014
74.732	3	1.2692	513	+0.003
75.711	8	1.2552	611	+0.021
75.839	14	1.2534	522	+0.007
77.840	1	1.2261	225	+0.022
78.388	2	1.2189	504	-0.002
79.304	3	1.2071	440	+0.010
81.336	6	1.1820	424, 006	-0.016
81.983	2	1.1743	106	+0.032
83.952	4	1.1517	116	+0.043

* $2\Theta_{\text{obs}} - 2\Theta_{\text{calc}}$

and c, respectively. These values are roughly half of those calculated either from Visser's or Felsche's data.

RESULTS AND DISCUSSION

Comparison of x-ray diffraction pattern of our samples resulted in better agreement with that of the deleted PDF pattern of Felsche (1969) than that of current Visser (1978) pattern. The observed d-spacings obtained by Visser, Felsche and by us along with calculated lattice constants are given in Table 3 for comparison. The overall agreement between our data and that of Felsche is not only in better matching of the d-spacings but also in missing reflections. Furthermore, our data extend down to 1.152 Å whereas Felsche's and Visser's data go down to 1.47 Å, with 20 fewer reflections than ours. Visser reports reflections at 5.44 (101), 2.409 (220), 1.915 (320), 1.697 (223), 1.683 (114), 1.670 (500), and 1.664 (313) Å. Of these all but three (1.915, 1.683, 1.664 Å) peaks were marked by Visser as coincidence peaks with those of $\text{Ce}_4\text{Si}_2\text{O}_7\text{N}_2$ apparently present in his sample. Our repeated attempts in a very carefully run experiment failed to generate these peaks. Since the intensities of these peaks are very weak even in Visser's data and we were able to detect even weaker peaks in other reflections, we believe the coincidence peaks reported by Visser do not belong to the oxygen apatite phase, $\text{Ce}_{4.67}[\text{SiO}_4]_3\text{O}$.

Deviation between our data and those of Felsche and of Visser was calculated from each peak by the following expression :

$$T - i = (d_T - d_i) / d_T \quad (1)$$

where d_T and d_i represent the observed d-spacings for a given plane by this study and others (i.e., d_F for Felsche, d_V for Visser). In general, agreement between us and Felsche was

Table 3. Comparison of the d-spacings

hkl	Visser	Felsche	This study
101	5.44	--	--
110	4.82	4.83	4.8257
200	4.17	4.18	4.1801
111	4.00	4.00	3.9948
002	3.591	3.56	3.5588
102	3.298	3.28	3.2751
210	3.155	3.16	3.1611
211	2.889	2.889	2.8895
112	2.879	--	2.8654
300	2.782	2.788	2.7884
202	2.721	2.711	2.7109
220	2.409	--	--
310	2.314	2.319	2.3196
221	2.284	2.286	2.2865
311	--	--	2.2058
302	2.199	2.195	2.1952
113	2.143	2.130	2.1297
400	2.087	2.091	2.0912
203	2.076	--	2.0635
222	2.001	1.998	1.9983
312	1.945	1.944	1.9434
320	1.915	--	--
213	1.907	1.898	1.8980
321	1.851	1.853	1.8528
410	1.821	1.825	1.8253
402	1.805	1.803	1.8029
004	1.795	1.780	1.7798
223	1.697	--	--

Table 3. (Continued)

hkl	Visser	Felsche	This study
322	1.690	--	1.6870
114	1.683	--	--
500	1.670	--	--
313	1.664	1.659	--
204	1.649	--	1.6360
412	--	--	1.6246
420	1.575 (403)	1.581	1.5804
331	1.567	1.570	1.5700
214	1.560	1.551	1.5509
421	1.541	--	1.5435
502	1.514	1.514	1.5138
304	1.509	--	1.5016
510	--	1.500	1.5002
323	1.495	1.492	1.4920
511	1.467	--	1.4697
332	--	1.467	1.4666

Lattice parameters :

	a (Å)	c (Å)	V(Å ³)
VISSER	9.6387	7.1812	577.7830
FELSCHE	9.6590	7.1210	575.1450
THIS STUDY	9.6578	7.1187	575.0260

consistently an order of magnitude better than that with us and Visser. The average deviation from Felsche's pattern was found to be 123 ppm whereas that from Visser's was 2675 ppm. This comparison clearly indicates that our data agree with that of Felsche much better than with that of Visser. The only information on the PDF pattern indicates that the sample employed by Visser was prepared by Mah et al. (1978) at Wright Patterson by hot pressing a Ce_2O_3 and Si_3N_4 mixture. It is also mentioned that "the sample contained $\text{Ce}_4\text{Si}_2\text{O}_7\text{N}_2$, the lines of which were omitted". As mentioned above at least several peaks that were considered as "coincidence" peaks (belonging to both $\text{Ce}_4\text{Si}_2\text{O}_7\text{N}_2$ and $\text{Ce}_{4.67}[\text{SiO}_4]_3\text{O}$) do actually belong to $\text{Ce}_4\text{Si}_2\text{O}_7\text{N}_2$ but not to the cerium oxygen apatite. In Visser's sample Si_3N_4 was employed as one of the reactants. The fact that sample did contain nitrogen bearing phases raises a question as to whether his apatite phase is really cerium oxygen apatite ($\text{Ce}_{4.67}[\text{SiO}_4]_3\text{O}$) or cerium nitrogen apatite ($\text{Ce}_5[\text{SiO}_4]_3\text{N}$). No chemical analysis is provided and it is likely that his sample contained large amounts of nitrogen. Some of the reflections such as 220, 320, 500, 313 and 403 which were observed by Visser but neither by us nor Felsche show up in our samples after treating our sample at 1520°C for 6 hours in "nitrogen" atmosphere rather than argon atmosphere. Alternatively, we added small quantities of Si_3N_4 (>98%, Grade KSN-10M-TX, Shin-Etsu) in our starting oxide mixture while retaining the total Ce:Si stoichiometric ratio (4.667 : 3.00) to see if we could duplicate Visser's pattern. Indeed, in addition to previously observed cerium oxygen apatite peaks, we did see reflections at 5.50, 1.9155, 1.666, 1.651 Å which were also observed by Visser and indexed as "101", "320", "313", "204" reflections. An X-ray powder diffraction pattern of cerium nitrogen apatite

($\text{Ce}_5[\text{SiO}_4]_3\text{N}$) provided by Guha (1980) (PDF 33-0333) is compared to Visser's cerium oxygen apatite ($\text{Ce}_{4.67}[\text{SiO}_4]_3\text{O}$, PDF 31-0336) in Table 4. Comparison of the two sets of data clearly indicates that these two samples have nearly identical x-ray diffraction patterns.

Assuming that the sample used by Visser is the same as that described by Mah et al. (1979), one can easily explain the formation of cerium nitrogen apatite. Mah et al. prepared their sample from a 10 % CeO_2 and 90 % Si_3N_4 mixture. They claimed to grow $\text{Ce}_{4.67}[\text{SiO}_4]_3\text{O}$ crystals on the surface of a hot pressed (under N_2) sample. Upon heating a mixture of CeO_2 and Si_3N_4 , as above, regardless of the gas atmosphere used, the first thing that will form (at about 1400°C) is an oxynitride liquid. This liquid will then act as a flux during the formation of crystalline cerium nitrogen apatite. It is unlikely that the "cerium apatite" that forms under these conditions could be free of nitrogen contamination.

Although there is little doubt that Visser's sample contained considerable nitrogen and the differences observed in XRD can be attributed to nitrogen, very little can be said about the site (s) these nitrogens occupy. Guha (1980) gives his composition as $\text{Ce}_5[\text{SiO}_4]_3\text{N}$ (actually for a unit cell it should read: $\text{Ce}_{10}[\text{SiO}_4]_6\text{N}_2$). There is no evidence that nitrogen actually occupies the (0,0,1/4) and (0,0,3/4) sites. These sites are surrounded by three Ce atoms in the defect free compound. However, it is quite possible that some of the nitrogen atoms can occupy the oxygen sites in SiO_4 tetrahedra. In fact, Gaude (1987) obtained an apatite-like phase by reacting CeO_2 , CeN , SiO_2 and Si at 1350°C in N_2 atmosphere. They claimed their product has the formula: $\text{Ce}_{10}[\text{SiO}_{3.61}\text{N}_{0.39}]_6\text{O}_{1.83}\square_{0.17}$. Gaude (1987) explained this structure using the concept of SiO_3N tetrahedra units, however, they also admitted that

Table 4. Comparison of Visser's data to that of Guha

hkl	d (Å)		I/I ₀	
	Visser	Guha	Visser	Guha
101	5.44	--	6!	--
110	4.82	4.83	10!	5
200	4.17	4.18	35	15
111	4.00	4.00	25	12
002	3.591	3.590	12	8
102	3.298	3.300	55	45
210	3.155	3.159	35	40
211	2.889	2.890	100	100
112	2.879	--	70	--
300	2.782	2.783	35	35
202	2.721	2.721	8	3
220	2.409	2.411	2!	2
310	2.314	2.316	8	5
221	2.284	2.284	4	2
302	2.199	2.200	6	6
113	2.143	2.145	10	10
400	2.087	2.088	4	5
203	2.076	--	2	--
222	2.001	2.003	25	45
312	1.945	1.946	16	12
320	1.915	1.915	4	10
213	1.907	1.908	30	40
321	1.851	1.851	14	12
410	1.821	1.822	20	20
402	1.805	1.803	25	40
004	1.795	1.795	16	20
223	1.697	1.698	4!	2

Table 4. (continued)

hkl	Visser	Guha	Visser	Guha
322	1.690	--	2	--
114	1.683	1.683	2	2
500	1.670	--	1!	--
313	1.664	--	6	--
204	1.649	1.649	2!	3
412	--	1.624	--	2
403	1.575	(420) 1.579	4	3
331	1.567	1.567	8	5
214	1.560	1.561	10	6
421	1.541	--	<1	--
502	1.514	--	10	--
304	1.509	1.510	6	10
323	1.495	1.495	6	5
511	1.467	(332) 1.466	8	8
105	--	1.416	--	2
512	--	1.385	--	2
430	--	1.374	--	2
404	--	1.360	--	2
333	--	1.334	--	3
215	--	1.308	--	7
602	--	1.296	--	3
414	--	1.278	--	12
513	--	1.271	--	5
522		1.252		8
603		1.203		4

without neutron diffraction data one could not assert the precise position of N. Nitrogen substitution for oxygen (relatively close ionic sizes of O^{2-} (1.40 Å) and N^{3-} (1.71 Å)) does not create any point defects to maintain the charge neutrality. Instead, more cerium ions will occupy the vacancy sites in oxygen apatite ($Ce_{4.67}\square_{0.33}[SiO_4]_3O$) to form the cerium nitrogen apatite ($Ce_5[SiO_4]_3N$). Lange (1979,1980) in a similar system, pointed out that XRD data can not differentiate between various oxygen and nitrogen containing apatites. Solid solubility between the two forms makes the distinction impossible by XRD techniques.

One final question remains to be answered with respect to the crystal structure of cerium oxygen apatite. Does the apatite structure exhibit $P6_3$ or $P6_3/m$ symmetry? The reflections $00l$ with $l \neq 2n$ were found to be absent in the pattern. This particular extinction condition is applicable to both of the above space groups in a hexagonal system. Gaude et al. (1975) claims that the space group is $P6_3$ not $P6_3/m$ for $Sm_{10}Si_6N_2O_{24}$. Again, there is no direct evidence provided for the site occupancy of the nitrogen atoms in the structure. However, the application of symmetry operation (based on the atomic coordinates of the $Ce_{4.67}[SiO_4]_3O$ structure (Belokoneva et al., 1972)) on $P6_3$ (#173) generates 8 sites for 10 lanthanide (Sm or Ce) atoms and 18 O sites for 24 tetrahedral oxygen atoms, whereas $P6_3/m$ (#176) generates 10 sites for 10 lanthanide atoms and 24 sites for 24 tetrahedral O atoms. It is, therefore, reasonable to assume the space group for either nitrogen or oxygen apatite to be $P6_3/m$ in unison with the fluoroapatite structure.

SUMMARY

X-ray diffraction pattern of cerium oxygen apatite, $\text{Ce}_{4.67}[\text{SiO}_4]_3\text{O}$, has been revisited. It appears that the x-ray diffraction pattern of cerium oxygen apatite has been incorrectly replaced by cerium nitrogen apatite in the PDF. Our analysis indicates that Visser's data which claims to be cerium oxygen apatite is actually cerium nitrogen apatite ($\text{Ce}_5[\text{SiO}_4]_3\text{N}$) and matches very closely to that of Guha. Both compounds show the same structure and space group symmetry but with different lattice constants. Exact site occupancy of nitrogen atoms will have to await the neutron diffraction experiments.

REFERENCES

1. Felsche, J. (1969). *Naturwissenschaften*, 22, 325-326.
2. Visser, J. (1978). *JCPDS Grant-in-Aid Report, JCPDS File Card #31-0336*, Technisch Physische Dienst, Delft, Netherlands.
3. Appleman, D.E. & Evans, H.T. (1973). *U.S. Geological Survey, Computer Contribution 20*, U.S. National Technical Information Service, Document PB-216188.
4. Mah T et al., Air Force Materials Laboratory, Wright-Patterson Air Force Base, Ohio, USA, *JCPDS File # 31-0336*.
5. Guha, J.P. (1980). *J.Mater.Sci.*, 15, 521-522.
6. Mah, T., Mazdiyasn, K.S. & Ruh, R. (1979). *J.Amer.Ceram.Soc.*, 62, 12-16.
7. Gaude, J. (1987). *Revue de Chimie Minerale*, 24, 22-27.
8. Lange, F.F. & Davis, B.I. (1979). *J.Amer.Ceram.Soc.*, 62, 629-630.
9. Lange, F.F. (1980). *Amer.Ceram.Soc.Bull.*, 59, 239-240, 249.
10. Gaude, J., L'Haridon, P., Hamon, C., Marchand, R. & Laurent, Y. (1975). *Bull. Soc. fr. Mineral. Cristallogr.*, 98, 214-217.
11. Belokoneva, E.L., Petrova, T.L., Simonov, M.A. & Belov, N.V. (1972). *Soviet Physics-Crystallography*, 17, 429-431.

PAPER II: PHASE RELATIONS IN THE SYSTEM Al_2O_3 - $\text{Ce}_2\text{Si}_2\text{O}_7$ IN THE
TEMPERATURE RANGE 900° TO 1925° C IN INERT
ATMOSPHERE

Phase Relations in the System Al_2O_3 - $\text{Ce}_2\text{Si}_2\text{O}_7$ in the Temperature Range 900° to 1925°C in Inert Atmosphere

Submitted by

A. Cuneyt Tas and Mufit Akinc

Department of Materials Science and Engineering

Iowa State University

Ames, Iowa 50011

This manuscript has been accepted for publication in the Journal of the American Ceramic Society.

ABSTRACT

Equilibrium relationships in the system Al_2O_3 - $\text{Ce}_2\text{Si}_2\text{O}_7$ in inert atmosphere have been investigated in the temperature range 900° to 1925°C. A simple eutectic reaction was found at 1375°C and 51 mol% $\text{Ce}_2\text{Si}_2\text{O}_7$. A high-low polymorphic transformation in $\text{Ce}_2\text{Si}_2\text{O}_7$ was observed at 1274°C. New XRD patterns are suggested for both polymorphs of cerium pyrosilicate. The melting point of $\text{Ce}_2\text{Si}_2\text{O}_7$ was found to be 1788°C. A value for $\Delta H_{\text{m,Ce}_2\text{Si}_2\text{O}_7}^\circ$ of 36.81 kJ/mol was calculated from the initial slope of the experimentally determined liquidus in equilibrium with the pyrosilicate phase.

INTRODUCTION

The present study is concerned with the phase relations between cerium pyrosilicate (disilicate), $\text{Ce}_2\text{Si}_2\text{O}_7$, and Al_2O_3 . $\text{Ce}_2\text{Si}_2\text{O}_7$ has been shown to have two polymorphs, a pseudo-orthorhombic high-temperature¹ and a tetragonal low-temperature form^{2,3}. The high-temperature form has been reported first to have an orthorhombic space group of $Pna2_1$ (or $Pnam$) by Felsche and Hirsiger⁴. This space group has later been changed to the monoclinic space group of $P2_1/n$, by Felsche¹, after very weak reflections $h0l$ with $h \neq 2n$ had been observed on over-exposed precession photographs. Though Felsche¹ pointed out to the significant resemblance of the structure of the high-temperature form of cerium pyrosilicate to that of $\alpha\text{-Ca}_2\text{P}_2\text{O}_7$, which was identified⁵ by the lattice constants, $a = 12.66 \text{ \AA}$, $b = 8.542 \text{ \AA}$, $c = 5.315 \text{ \AA}$ and a monoclinic angle $\beta = 90.3^\circ$, he reported the compound to have a monoclinic angle of 90° , and preferred to describe it as pseudo-orthorhombic. The high-to-low transition has been reported to be extremely sluggish.^{1,2} The melting point of $\text{Ce}_2\text{Si}_2\text{O}_7$ has been reported to be $1770 \pm 25^\circ\text{C}$.⁶ It has been reported⁷ that, under strongly oxidising conditions, the cerium ion remains in the 4+ state (CeO_2) and does not react with SiO_2 to form the pyrosilicate. However, it has also been shown⁸ that, when high purity CeO_2 and fumed SiO_2 are mixed together in stoichiometric pyrosilicate proportions and heated to $T > 1550^\circ\text{C}$ in air for extended periods, pyrosilicate forms and can be quenched to room temperature, with small amounts of $\text{Ce}_{4.67}[\text{SiO}_4]_3\text{O}$ being present as an impurity phase (the absent SiO_2 either being combined with a glassy phase or having sublimed as SiO). On the

other hand, if, instead of quenching, the heated mixture is subjected to slow cooling from 1550°C to 1300°C in air, the result is decomposition of the pyrosilicate phase into CeO_2 and α -cristobalite.⁸ This necessitates the use of an inert or neutral atmosphere in a study of the high-temperature phase relations of the Ce^{3+} silicates and aluminosilicates. The lack of detailed data in the CeO_2 - SiO_2 binary, especially those concerning the thermal stability range of the pyrosilicate phase, makes it appropriate for such a study to begin with the synthesis and characterisation of $\text{Ce}_2\text{Si}_2\text{O}_7$.

Very few studies⁸⁻¹¹ have been found in the literature that focus on the synthesis of cerium containing aluminosilicate glasses and crystalline materials. These have commonly been studies at one temperature (1500°-1550°C) and one or two different compositions in the ternary system CeO_2 - Al_2O_3 - SiO_2 and, hence, were far from being phase equilibria studies in terms of scope. O'Brien and Akinc⁸ were the first to report the coexistence in air of the solid phases $\text{Ce}_2\text{Si}_2\text{O}_7$ and Al_2O_3 in a liquid matrix containing CeO_2 , SiO_2 , and Al_2O_3 . This finding provided the impetus for the present study, which is hoped to broaden the understanding of this binary system.

EXPERIMENTAL PROCEDURE

Compositions in the Al_2O_3 - $\text{Ce}_2\text{Si}_2\text{O}_7$ system of specific atomic ratios of Al:Ce:Si were prepared by mixing the appropriate amounts of the oxides CeO_2 , Al_2O_3 and SiO_2 under acetone in an agate mortar for approximately one hour. The chemical analyses, the mean particle sizes, and surface areas of the starting oxides are given in Table I. Chemical analyses were determined using laser source mass spectrometry, particle size analyses using light absorbance (Model CAPA 700, Horiba) and surface area using nitrogen adsorption (Model 4200, Leeds and Northrup). The oxides were heated in air at 975°C for 12 hours prior to weighing. The compositions studied are indicated in Table II. For each composition, approximately 2 g samples of the mixture were weighed and uniaxially pressed into 1.27-cm-diameter pellets in a tungsten carbide-lined steel die at about 200 MPa. For compositions close to the end members, the oxide mixtures were cold isostatically pressed at 200 MPa following uniaxial dry pressing at 35 MPa.

The pellets were equilibrated at a predetermined temperature in a MoSi_2 quench furnace with a vertical 120-cm-long alumina reaction tube. The inert atmosphere in the furnace tube was maintained by constant flow of either prepurified argon or argon + 10% H_2 gases. The pellets were contained in envelopes made from thin foils of Pt (for argon) or Mo (for argon + 10% H_2). At the end of the specified equilibration times, the samples were quenched by dropping into an ice-water bath, covered with a thin layer of vacuum pump oil, which also

Table I. Chemical Analysis of Starting Materials

Oxide	CeO ₂ ^a	Fumed SiO ₂ ^b	Al ₂ O ₃ ^c
Al ₂ O ₃	94 ppm	9 ppm	99.96 wt%
SiO ₂	235 ppm	99.98 wt%	88 ppm
Na ₂ O	121 ppm	18 ppm	76 ppm
CeO ₂	99.87 wt%	-	-
Fe ₂ O ₃	114 ppm	4 ppm	49 ppm
CaO	112 ppm	59 ppm	30 ppm
MgO	13 ppm	2 ppm	20 ppm
Ga ₂ O ₃	121 ppm	< 1 ppm	50 ppm
MnO	10 ppm	< 1 ppm	5 ppm
Cr ₂ O ₃	88 ppm	< 1 ppm	4 ppm
CuO	25 ppm	< 1 ppm	10 ppm
Li ₂ O	9 ppm	< 1 ppm	37 ppm
ZnO	5 ppm	2 ppm	25 ppm
NiO	11 ppm	3 ppm	3 ppm
TiO ₂	8 ppm	17 ppm	-
Sc ₂ O ₃	15 ppm	15 ppm	-
K ₂ O	24 ppm	7 ppm	-
La ₂ O ₃	152 ppm	-	-
Pr ₆ O ₁₁	36 ppm	-	-
Gd ₂ O ₃	12 ppm	6 ppm	-
B ₂ O ₃	68 ppm	13 ppm	-
C	89 ppm	400 ppm	-
Cl ⁻	20 ppm	33 ppm	-

Table I. (Continued)

Surface Area	6.2 m ² /gm	400 m ² /gm	7.5 m ² /gm
Mean Particle Size	0.7 μm	0.007 μm	0.4 μm

^a CERAC, Inc. WI, Lot No. 36171-A-1

^b SIGMA Chem. Co., MO, Lot No. 114F-0070

^c REYNOLDS, Inc, VA, Lot No. BM-2415

served to seal the bottom end of the furnace tube. The minimum equilibration time during preliminary experiments was 17 hours. After 17 hours of heating, the samples were quenched, examined by XRD for phase analysis, re-pelletised, and heated for an additional 17 hours followed by quenching and phase analysis. The minimum time required for a certain composition to reach equilibrium at a certain temperature was deduced when XRD traces showed no detectable changes in kinds and amounts of the phases present. The temperature in the furnace tube was controlled to within $\pm 6^{\circ}\text{C}$. The temperature in the hot zone was monitored with a B-type thermocouple which was calibrated after every 120 hours of heating against the melting points of Au (1064°C) and Pd (1554°C) under a moderate flow of argon.

Table II. Results of Equilibration Runs in the System Al_2O_3 - $\text{Ce}_2\text{Si}_2\text{O}_7$

Composition	Temperature (°C)	Time (h)	Phase(s) Observed
PYRO 5 ^a	1560	40	Liquid + Al_2O_3
PYRO 10	1560	40	Liquid + Al_2O_3
PYRO 15	1560	40	Liquid + Al_2O_3
PYRO 20	1560	40	Liquid + Al_2O_3
PYRO 30	1560	40	Liquid + Al_2O_3
PYRO 40	1560	40	Liquid
PYRO 44	1560	40	Liquid
PYRO 48	1560	40	Liquid
PYRO 50	1560	40	Liquid
PYRO 51	1560	40	Liquid
PYRO 52	1560	40	Liquid
PYRO 54	1560	40	Liquid
PYRO 56	1560	40	Liquid
PYRO 58	1560	40	Liquid
PYRO 60	1560	40	Liquid
PYRO 70	1560	40	Liquid + Monoc. $\text{Ce}_2\text{Si}_2\text{O}_7$
PYRO 75	1560	40	Liquid + Monoc. $\text{Ce}_2\text{Si}_2\text{O}_7$
PYRO 80	1560	40	Liquid + Monoc. $\text{Ce}_2\text{Si}_2\text{O}_7$
PYRO 85	1560	40	Liquid + Monoc. $\text{Ce}_2\text{Si}_2\text{O}_7$
PYRO 90	1560	40	Liquid + Monoc. $\text{Ce}_2\text{Si}_2\text{O}_7$
PYRO 95	1560	40	Liquid + Monoc. $\text{Ce}_2\text{Si}_2\text{O}_7$
PYRO 100	1560	> 7	Monoc. $\text{Ce}_2\text{Si}_2\text{O}_7$
PYRO 15	1480	70	Liquid + Al_2O_3
PYRO 30	1480	65	Liquid + Al_2O_3
PYRO 50	1480	50	Liquid
PYRO 70	1480	60	Liquid + Monoc. $\text{Ce}_2\text{Si}_2\text{O}_7$
PYRO 90	1480	70	Liquid + Monoc. $\text{Ce}_2\text{Si}_2\text{O}_7$
PYRO 15	1400	85	Liquid + Al_2O_3
PYRO 30	1400	75	Liquid + Al_2O_3
PYRO 50	1400	50	Liquid
PYRO 70	1400	65	Liquid + Monoc. $\text{Ce}_2\text{Si}_2\text{O}_7$
PYRO 90	1400	75	Liquid + Monoc. $\text{Ce}_2\text{Si}_2\text{O}_7$
PYRO 15	1300	120	Al_2O_3 + Monoc. $\text{Ce}_2\text{Si}_2\text{O}_7$
PYRO 30	1300	90	Al_2O_3 + Monoc. $\text{Ce}_2\text{Si}_2\text{O}_7$
PYRO 50	1300	75	Al_2O_3 + Monoc. $\text{Ce}_2\text{Si}_2\text{O}_7$
PYRO 70	1300	80	Al_2O_3 + Monoc. $\text{Ce}_2\text{Si}_2\text{O}_7$
PYRO 90	1300	100	Al_2O_3 + Monoc. $\text{Ce}_2\text{Si}_2\text{O}_7$
PYRO 30	1560	40	
	1200	96	[Cooling rate : 8 °C/h] Al_2O_3 + Tetra. $\text{Ce}_2\text{Si}_2\text{O}_7$
PYRO 75	1560	40	
	1200	96	[Cooling rate : 8 °C/h] Al_2O_3 + Tetra. $\text{Ce}_2\text{Si}_2\text{O}_7$

^a PYRO 5 : 5 mol% $\text{Ce}_2\text{Si}_2\text{O}_7$ - 95 mol% Al_2O_3

For phase analysis, every quenched, ground sample was examined using XRD in the 5° - 85° 2Θ range using an x-ray powder diffractometer^a with a maximum scanning rate of 0.4° 2Θ /min. Silicon (NBS640a) was used as an external standard. The diffraction patterns given in this study were produced with a scan rate of 0.1° 2Θ /min in the same 2Θ range. Microstructural analyses were carried out using SEM^b and reflected light microscopy. The chemical compositions of the microstructural features observed in SEM were examined with EDXS^c, and are believed to be accurate to within ± 4 atomic percent.

Differential Thermal Analysis (DTA) experiments were carried out to monitor the phase transitions in this system. The DTA runs were performed either in Mo foil crucibles in a tungsten-mesh vacuum furnace^d (P_{O_2} being less than 6×10^{-9} atm) using type C thermocouples or in Pt crucibles in an argon atmosphere in a MoSi₂ furnace using type B thermocouples. Two heating rates (3° and 6° C/min) were used for every composition. The thermocouples (Type C) of the vacuum DTA unit^e were calibrated against the melting points of Au (1064° C), Li₂SiO₃ (1204° C), Pd (1554° C), and Pt (1772° C). The sample for each DTA run was first equilibrated at 1560° C for 40 hours in Ar atmosphere, water-quenched, and then

^a XDS 2000, Scintag, Inc., CA, USA ^b JSM-840 or JSM-6100, JEOL, Inc., MA, USA

^c Model Delta-5, Kevex Corp., CA, USA ^d Centorr Associates, Inc., NH, USA

^e Oxy-Gon Industries, Inc., NH, USA

ground to a fine powder, followed by X-ray analysis. For each composition selected for DTA analysis, the first run scanned the whole temperature range (900-1925°C). Upon reaching the maximum temperature, the furnace contents were quenched to room temperature by shutting off the power to the furnace. The quenched samples were then analysed by XRD and by SEM. The second run for the same composition (with a fresh, equilibrated powder sample) scanned between 900°C and the temperature at which the first thermal event ended as observed in the initial DTA run. The furnace-quenched second sample was also subjected to XRD analysis to determine the phases present and the nature of that thermal event. The subsequent run, analysed as before, covered the temperature range between 900°C and the temperature at which the second thermal event commenced (if there was one).

RESULTS AND DISCUSSION

The high temperature monoclinic polymorph of $\text{Ce}_2\text{Si}_2\text{O}_7$, with the lattice parameters $a = 13.080 \text{ \AA}$, $b = 8.727 \text{ \AA}$, $c = 5.405 \text{ \AA}$, and $\beta = 90.13^\circ$, was synthesized as a single phase silicate without any difficulty at 1560°C in argon using a heating rate of $4^\circ\text{C}/\text{min}$ to the peak temperature, with a hold for 7 hours followed by quenching. For holding times less than 7 hours, small amounts of $\text{Ce}_{4.67}[\text{SiO}_4]_3\text{O}$ (cerium oxygen apatite) were found to be present in our samples. Monoclinic $\text{Ce}_2\text{Si}_2\text{O}_7$ could be cooled down to 1350°C at a typical rate of $4^\circ\text{C}/\text{min}$ under flowing purified argon; however, below 1350°C , it partially decomposed to $\text{Ce}_{4.67}[\text{SiO}_4]_3\text{O}$. Monoclinic cerium pyrosilicate could be preserved as the stoichiometric phase only when it was cooled down to 900°C in vacuum or in an argon+10% H_2 atmosphere.

We hereby present a new XRD pattern (Am. Ceram. Soc. Depository Service) for the monoclinic $\text{Ce}_2\text{Si}_2\text{O}_7$ phase. This pattern, although still points out to a similar-sized unit cell by that given by JCPDS PDF pattern 23-0318, after Felsche and Hirsiger¹, reveals, for the first time, the monoclinic nature of $\text{Ce}_2\text{Si}_2\text{O}_7$, with a small monoclinic angle of 90.13° , owing to its high resolution. The 135 reflections observed in the $5 - 85^\circ 2\theta$ range also showed the characteristic peak splitting that could be seen in a monoclinic structure. The 18 strongest reflections of this pattern were displayed in Table III of this article. This finding for $\text{Ce}_2\text{Si}_2\text{O}_7$, therefore, warrants the further structural investigation of the high-temperature forms of pyrosilicate phases of the remaining light rare earth elements, i.e., La, Pr, Nd and Sm, which

Table III. Brief XRD Patterns of Tetragonal and Monoclinic Forms of $\text{Ce}_2\text{Si}_2\text{O}_7$

Tetragonal $\text{Ce}_2\text{Si}_2\text{O}_7$: $a = 6.792 \text{ \AA}$, $c = 24.700 \text{ \AA}$, $V = 1139.4 \text{ \AA}^3$, $Z = 8$, SG : $P4_1 (76)$

Monoclinic $\text{Ce}_2\text{Si}_2\text{O}_7$: $a = 13.080 \text{ \AA}$, $b = 8.727 \text{ \AA}$, $c = 5.405 \text{ \AA}$, $\beta = 90.13^\circ$, $Z = 4$,
 $V = 617.03 \text{ \AA}^3$, SG : $P21/n (14)$

Tetragonal $\text{Ce}_2\text{Si}_2\text{O}_7$				Monoclinic $\text{Ce}_2\text{Si}_2\text{O}_7$			
hkl	d_{calc}	d_{obs}	I/I_0	hkl	d_{calc}	d_{obs}	I/I_0
101	6.55	6.54	11	110	7.26	7.27	38
110	4.80	4.80	13	200	6.54	6.55	11
112	4.48	4.47	16	021	3.395	3.396	100
113	4.15	4.14	24	-121	3.288	3.289	29
115	3.443	3.441	22	121	3.284	3.283	20
201	3.364	3.365	95	-311	3.168	3.167	10
202	3.274	3.274	70	311	3.158	3.156	6
008	3.087	3.086	100	-320	3.084	3.085	24
211	3.014	3.013	25	-411	2.669	2.669	9
117	2.849	2.848	32	411	2.660	2.659	11
205	2.798	2.797	14	-131	2.515	2.515	10
206	2.619	2.620	12	131	2.513	2.512	8
221	2.390	2.389	13	040	2.182	2.182	10
310	2.148	2.149	12	140	2.152	2.152	13
304	2.125	2.125	18	-322	2.036	2.036	13
314	2.028	2.028	32	-412	2.030	2.030	21
227	1.985	1.985	12	-621	1.837	1.837	10
229	1.807	1.806	12	341	1.834	1.835	10

were reported by Felsche¹ to have similar pseudo-orthorhombic structures with the same space group, $P2_1/n$.

The low-temperature tetragonal polymorph of $\text{Ce}_2\text{Si}_2\text{O}_7$ was synthesized by very slow (4°C/h) cooling of the high-temperature form (monoclinic phase) from 1560° to 1175°C in a purified argon + 10% H_2 atmosphere followed by 60 hours of annealing at 1175°C followed by quenching. Felsche¹ was not able to produce this phase by cooling the monoclinic form from 1550°C at 30°C/h to below 1200°C . We also tried this cooling rate and confirmed Felsche's observation. Heindl *et al.*² were the first to synthesize this compound by slow cooling (5°C/h) the high temperature form, and they found that the lattice parameters of the tetragonal polymorph fall between those of the tetragonal forms of $\text{La}_2\text{Si}_2\text{O}_7$ and $\text{Pr}_2\text{Si}_2\text{O}_7$ in the light lanthanide pyrosilicate series. Very recently, Van Hal and Hintzen³ claimed that they found "a new $\text{Ce}_2\text{Si}_2\text{O}_7$ compound never reported before for cerium silicates" and suggested an XRD pattern for the tetragonal polymorph of $\text{Ce}_2\text{Si}_2\text{O}_7$. Van Hal and Hintzen used almost the same starting materials as did Heindl *et al.*,² i.e, $\text{Ce}(\text{NO}_3)_3$ and reactive forms of SiO_2 , and both carried out their anneals in a H_2 (7% and 5%, respectively)- N_2 atmosphere. As we have shown¹² in a previous study on another cerium silicate, $\text{Ce}_{4.67}[\text{SiO}_4]_3\text{O}$, this phase is susceptible to taking nitrogen into the structure by substituting for oxygen. Nitrogen can be incorporated into the structure not only from nitrogen-bearing starting materials, as was the case in the studies of Heindl *et al.*² and Van Hal and Hintzen³, but also from the annealing atmosphere, as was also the case in both studies. Our previous work¹² showed that annealing a stoichiometric mixture of CeO_2 (or Ce_2O_3) and SiO_2 in a N_2 atmosphere causes nitrogen to be

incorporated into the structure and changes certain d-spacings in the diffraction pattern significantly. Although we have not yet studied the effect of the presence of nitrogen on the structure of $\text{Ce}_2\text{Si}_2\text{O}_7$, we suggest that caution be exercised in regard to the purity of the cerium silicates prepared from nitrogen-containing starting materials and nitrogen-bearing annealing atmospheres. Table III displays the 18 strongest reflections of the XRD pattern of tetragonal $\text{Ce}_2\text{Si}_2\text{O}_7$ prepared from high-purity CeO_2 and fumed SiO_2 in a nitrogen-free atmosphere. The complete XRD pattern of this phase can be obtained from the American Ceramic Society depository service.

The polymorphic transformation temperature for $\text{Ce}_2\text{Si}_2\text{O}_7$ was found to be at $1274^\circ \pm 3^\circ\text{C}$. To determine this temperature, we performed four separate DTA runs with 350-mg samples of the tetragonal phase in vacuum ($P_{\text{O}_2} \leq 6 \times 10^{-9}$ atm) in Mo crucibles with a heating rate of $1^\circ\text{C}/\text{min}$. Three of these runs consistently produced a small endothermic event at this temperature, as is shown in the sample DTA trace labeled as PYRO100 in Figure 1. These three runs were terminated at 1350°C , and the recovered samples were analysed by XRD. The resultant patterns indicated the presence of the high-temperature monoclinic form of $\text{Ce}_2\text{Si}_2\text{O}_7$. The fourth 350-mg portion of the same tetragonal sample was heated only to 1210°C in the DTA unit and furnace quenched from this temperature. The resultant XRD pattern showed only the tetragonal form of the pyrosilicate.

Calibration of the DTA thermocouples were checked against the Pt melting point and was measured to be at $1772 \pm 1^\circ\text{C}$ just prior to the determination of the melting point of $\text{Ce}_2\text{Si}_2\text{O}_7$. We carried out two runs at a heating rate of $3^\circ\text{C}/\text{min}$ under vacuum with 320-mg

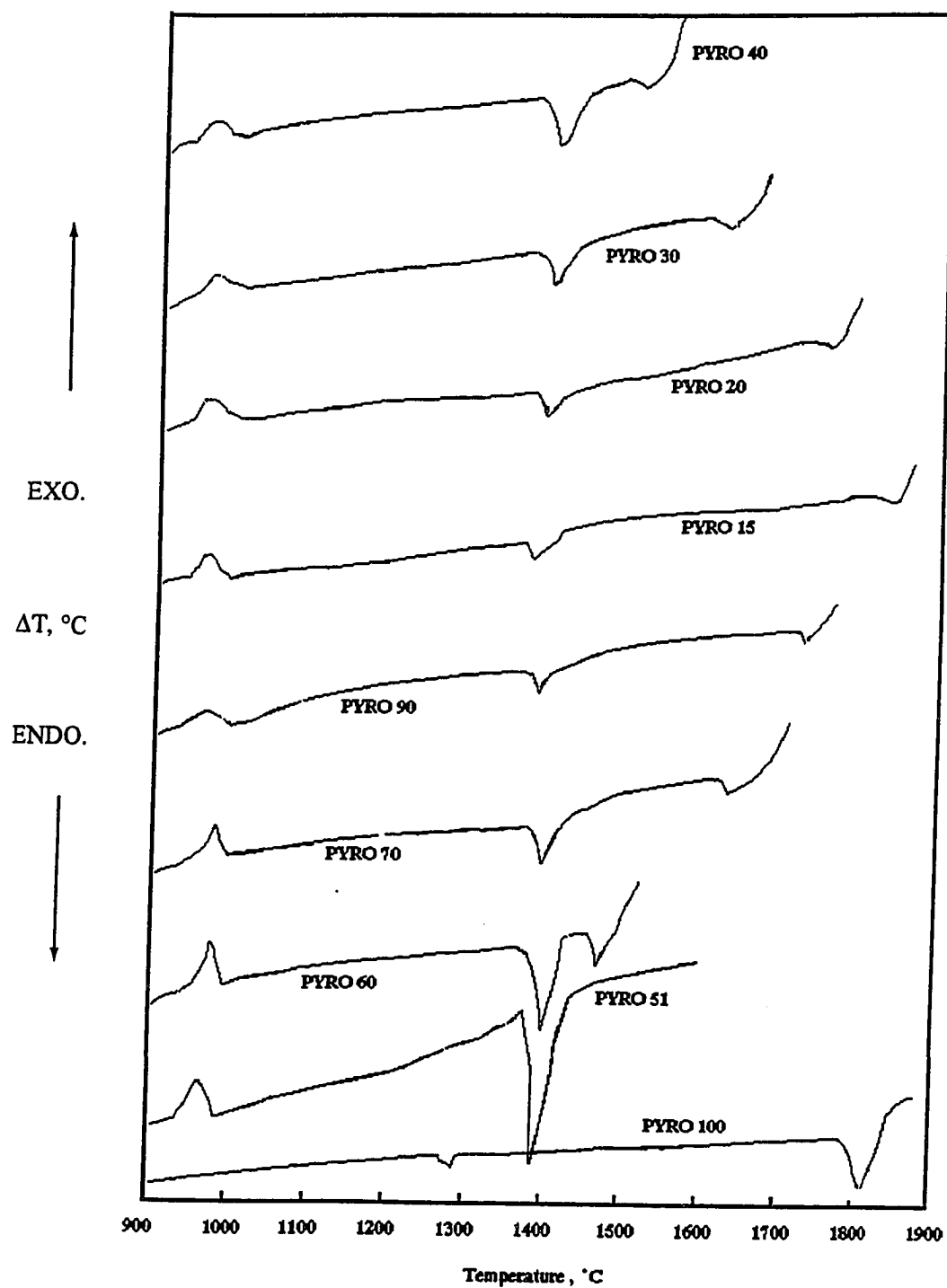


Figure 1. DTA traces of selected compositions in the $\text{Al}_2\text{O}_3 - \text{Ce}_2\text{Si}_2\text{O}_7$ system

samples of single-phase tetragonal and single-phase monoclinic $\text{Ce}_2\text{Si}_2\text{O}_7$. While the monoclinic sample did not yield any event at the polymorphic transformation temperature, both the tetragonal and monoclinic phases indicated the beginning of melting at temperature $1788 \pm 5^\circ\text{C}$. This temperature correlates well with the previously reported value of $1770 \pm 25^\circ\text{C}$ of Toropov *et al*.⁶

In the Al_2O_3 - $\text{Ce}_2\text{Si}_2\text{O}_7$ binary, the first 21 compositions of Table II were used for the construction of the phase diagram. After numerous preliminary experiments to determine the required time for the equilibrium phases to form at a given temperature (i.e., 1560° , 1480° , 1400° and 1300°C), we selected the still conservative time of 40 hours for 1560°C . All the compositions were annealed at this temperature for 40 hours in purified argon and ice-water quenched. Each sample was thoroughly ground and examined with XRD (0.4° $2\Theta/\text{min}$, 5° - 85° 2Θ) to determine the phases present. A small portion of each sample was saved for microstructural analysis by SEM and optical microscopy. The phases observed for this series of samples are summarised in Table II.

The next temperature we chose for the equilibration runs was 1480°C . The five compositions annealed at this temperature (Pyro 15,30,50,70,and 90), produced two solid phases: α - Al_2O_3 and monoclinic $\text{Ce}_2\text{Si}_2\text{O}_7$, as indicated by powder XRD and verified by microscopic analysis. When the equilibration temperature was decreased to 1400°C , the annealing times needed to be increased (as shown in Table II) to form the equilibrium phases. For example, the sample of Pyro 15 composition after annealing at 1400°C for 65 hours contained minor amounts of tetragonal CeAlO_3 and hexagonal Ce_2O_3 , 11 Al_2O_3 (cerium

hexaaluminate) in addition to the major crystalline $\alpha\text{-Al}_2\text{O}_3$ phase. For an annealing time of 85 hours at 1400°C , however, the only crystalline phase in the sample was $\alpha\text{-Al}_2\text{O}_3$. In the case of Pyro 90 sample (1400°C , 60 hours), cerium oxygen apatite ($\text{Ce}_{4.67}[\text{SiO}_4]_3\text{O}$) appeared as a metastable phase, which disappeared upon increasing the annealing time from 60 to 75 hours. Reduction in the amount of liquid formed by lowering the annealing temperature slows the reaction kinetics. As a result, longer times are needed for reaching the equilibrium phases.

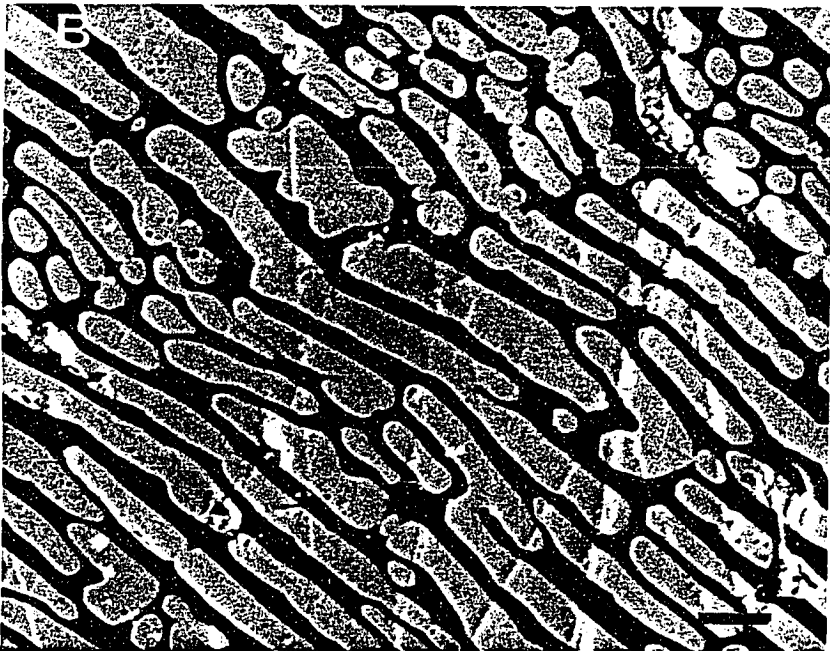
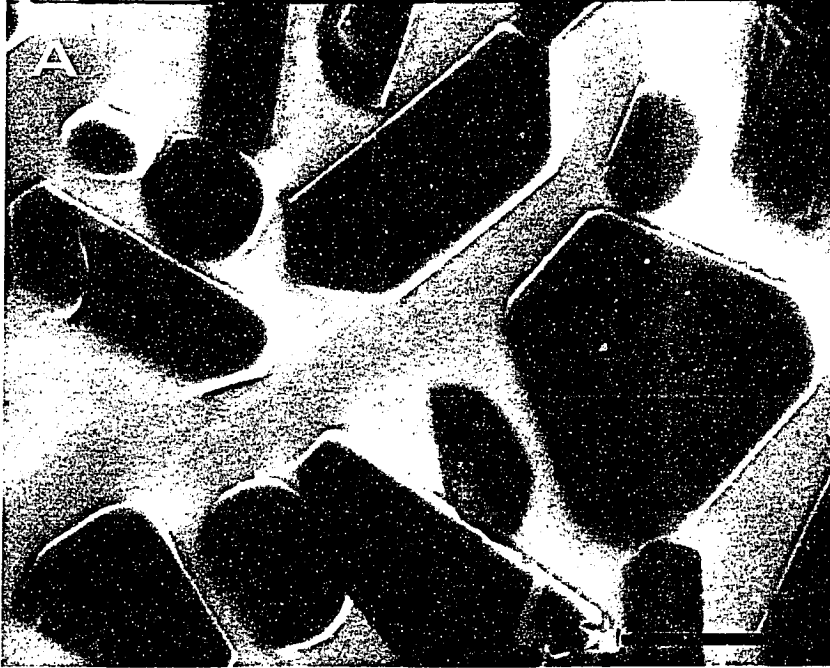
A back scattered electron (BSE) micrograph of Pyro 30 sample (1400°C , 75 hours, quenched) is shown in Figure 2a, which displays the $\alpha\text{-Al}_2\text{O}_3$ grains dispersed in a liquid matrix which contains Ce, Si and Al. Figure 2b, on the other hand, shows the characteristic microstructure of a Pyro 90 sample (1400°C , 75 hours, quenched) with the $\text{Ce}_2\text{Si}_2\text{O}_7$ phase dispersed in the darker liquid matrix.

At an annealing temperature of 1300°C , it took over 100 hours for the liquid to completely crystallise into $\alpha\text{-Al}_2\text{O}_3$ and monoclinic $\text{Ce}_2\text{Si}_2\text{O}_7$ for the Pyro 15 and Pyro 90 compositions, respectively. Figure 2c shows the microstructure of a Pyro 15 sample that was first annealed at 1560°C for 40 hours and slowly cooled ($20^\circ\text{C}/\text{h}$) to 1300°C , where it was annealed for 80 hours, and then quenched. It is apparent from this BSE micrograph that the liquid crystallizes primary $\alpha\text{-Al}_2\text{O}_3$, followed by the crystallisation of the eutectic liquid. It is also observed that the rather sluggish eutectic microstructure formation has been initiated at the most favourable spots in the sample, i.e., at the solid ($\alpha\text{-Al}_2\text{O}_3$)-liquid interfaces. Figure 2d depicts the BSE micrograph of a sample with the eutectic composition (51 mol% pyrosilicate) first equilibrated at 1560°C and then cooled ($35^\circ\text{C}/\text{h}$) to 1300°C , followed by

Figure 2. Backscattered electron images of samples in the Al_2O_3 - $\text{Ce}_2\text{Si}_2\text{O}_7$ system

- (A) Pyro 30 : Dark alumina grains on a gray once-liquid matrix. 1400°C, 75 hours, Quenched
- (B) Pyro 90 : Bright monoclinic pyrosilicate streaks on a darker once-liquid matrix. 1400°C, 75 hours, Quenched
- (C) Pyro 15 : Dark alumina grains, eutectic reaction is continuing. 1560°C, 40 hours, 20°C/h to 1300°C, 80 hours, Quenched
- (D) Pyro 51 : Eutectic microstructure, darker features are alumina. 1560°C, 40 hours, 35°C/h to 1300°C, 50 hours, Quenched
- (E) Pyro 95 : Darker liquid phase between the coarse monoclinic pyrosilicate grains. 1560°C, 40 hours, Quenched
- (F) Pyro 95 : Unpolished section; monoclinic pyrosilicate grains are bonded to each other with a darker liquid phase. 1560°C, 40 hours, Quenched

BAR LENGTHS = 10 μm



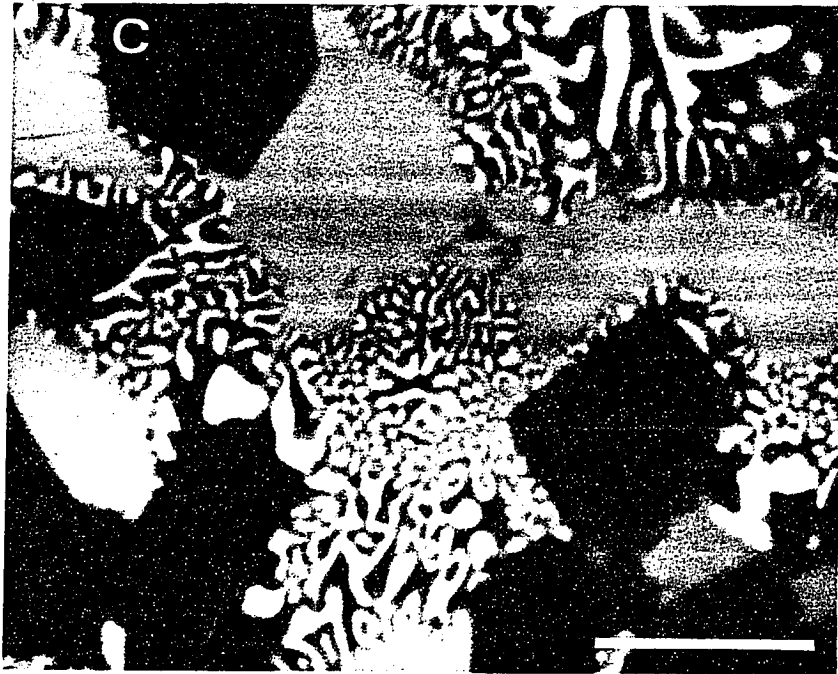


Figure 2. Continued



Figure 2. Continued

quenching in water. The bright features are monoclinic $\text{Ce}_2\text{Si}_2\text{O}_7$, whereas the dark are $\alpha\text{-Al}_2\text{O}_3$. Figure 2e displays the BSE micrograph of a Pyro 95 sample where the scarce dark phase is the liquid and the bright phase is monoclinic $\text{Ce}_2\text{Si}_2\text{O}_7$. Figure 2f shows an unpolished section of the same sample (Pyro 95) in which the well crystallised monoclinic $\text{Ce}_2\text{Si}_2\text{O}_7$ grains are cemented together with the darker liquid phase. In this microstructure Al was found to be confined to the bonding liquid phase.

In order to produce the equilibrium solid phase mixture below the polymorphic transformation temperature of $\text{Ce}_2\text{Si}_2\text{O}_7$, we annealed the two samples (Pyro 30 and Pyro 75, Table II) in an argon +10% H_2 atmosphere in Mo crucibles. These samples were first equilibrated at 1560°C and then slowly (8°C/h) cooled to 1200°C, followed by 96 hours of annealing at that temperature. Although we doubled the cooling rate compared to that employed in the case of pure $\text{Ce}_2\text{Si}_2\text{O}_7$ (to achieve the polymorphic transformation), the presence of the liquid phase helped to improve the transformation kinetics in these samples, and we were able to obtain the solid phases $\alpha\text{-Al}_2\text{O}_3$ and tetragonal $\text{Ce}_2\text{Si}_2\text{O}_7$ in the same microstructure.

DTA of the compositions investigated in this study (Table II) were run at both 3°C/min and 6°C/min heating rates in vacuum. Some selected traces from these runs are displayed in Figure 1. All of the traces shown in this figure represent the heating rate of 3°C/min. The faster DTA scans consistently produced an average of 3-4°C higher temperatures for the eutectic temperature. The eutectic was found to be at 51 mol% (± 0.5 mol%) $\text{Ce}_2\text{Si}_2\text{O}_7$ and a temperature of $1375 \pm 5^\circ\text{C}$. Powder XRD analysis coupled with the DTA experiments

indicated that the relatively small exothermic event occurring around $960 \pm 30^\circ\text{C}$, which was common to all of the DTA traces, was due to the formation of crystalline phases from the glassy starting material. For instance, for a sample of Pyro 30, that peak corresponded to the crystallisation of $\text{Ce}_2\text{Si}_2\text{O}_7$, as indicated by the XRD analysis of a sample recovered from a DTA run which was terminated at 1025°C ; whereas, for a sample of Pyro 70 composition, this peak belonged to the crystallisation of $\alpha\text{-Al}_2\text{O}_3$. For all the DTA traces shown in Figure 1, the second, endothermic event indicated the first liquid formation in the system, while the third thermal event (if there was one) represented the disappearance of the solid phase completely. The rather drastic change observed in the slope of the DTA lines at and beyond this point, preceded by a significant endothermic-like disturbance to the baseline, indicated the presence of a rising/crawling up liquid along the inner walls, eventually emptying the inside of the sample pan. Upon the prevalence of this condition, the thermal balance between the sample and the reference pans (which had dictated the slope of the baseline until that point) had been lost, and the baseline began to display a sharp rise with increasing temperature. Based on the phase information gathered from the equilibration runs and the DTA data, the binary phase diagram of $\text{Al}_2\text{O}_3\text{-Ce}_2\text{Si}_2\text{O}_7$ shown in Figure 3 was constructed. The phase diagram displays a simple eutectic reaction with a polymorphic transformation in $\text{Ce}_2\text{Si}_2\text{O}_7$ below the eutectic temperature.

Assuming ideal mixing in the liquid phase and complete immiscibility of $\alpha\text{-Al}_2\text{O}_3$ in solid $\text{Ce}_2\text{Si}_2\text{O}_7$, the enthalpy of melting of $\text{Ce}_2\text{Si}_2\text{O}_7$ can be calculated from the experimentally

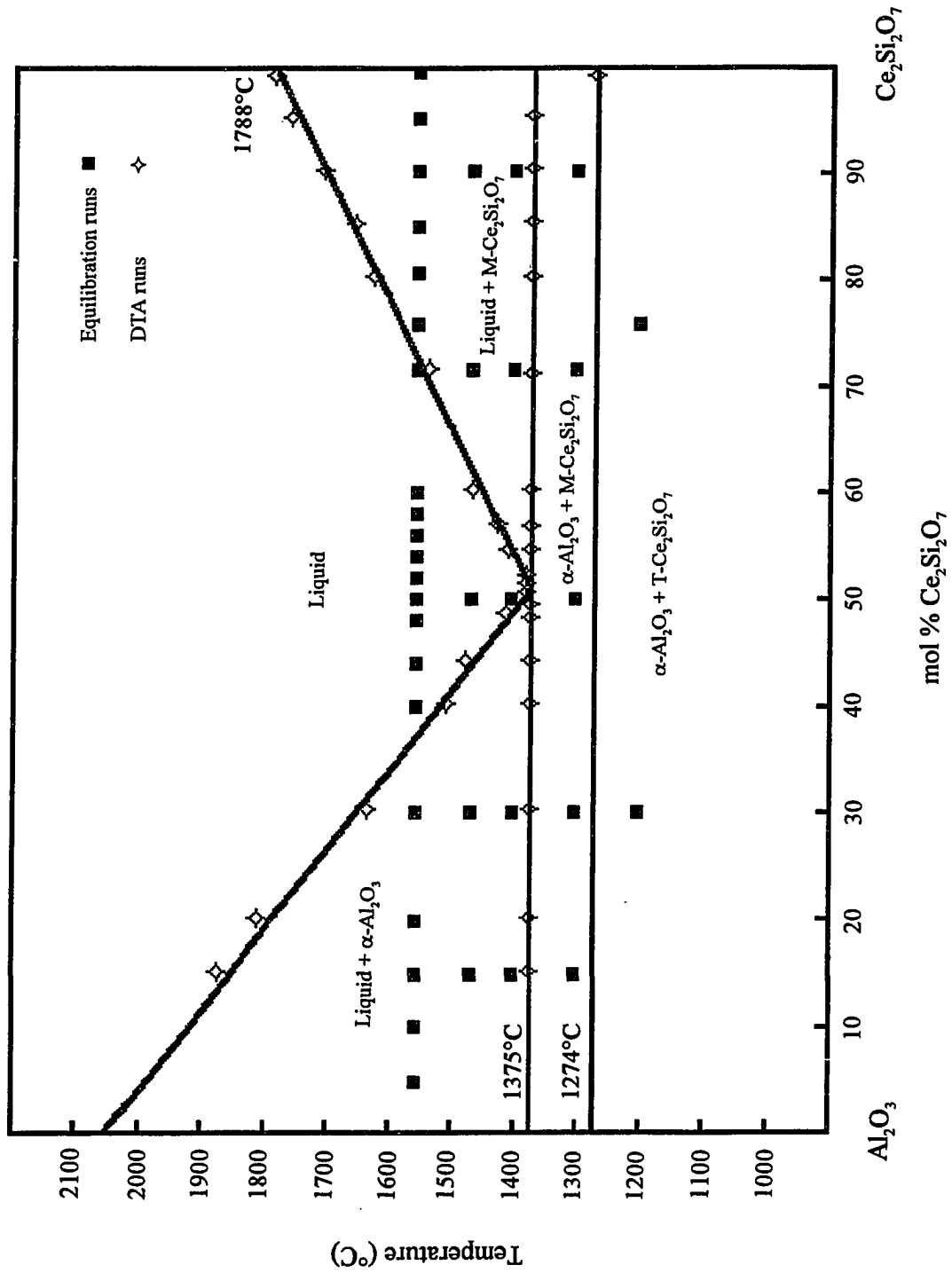
determined liquidus line, using the freezing point depression of $\text{Ce}_2\text{Si}_2\text{O}_7$ by the addition of Al_2O_3 , according to

$$\log X_A = - \frac{\Delta H_{m,A}}{R} \left[\frac{(T_{m,A} - T_L)}{T_{m,A} \cdot T_L} \right] \quad (1),$$

where $A = \text{Ce}_2\text{Si}_2\text{O}_7$.

Therefore, a plot of $\log X_{\text{Ce}_2\text{Si}_2\text{O}_7}$ (liquidus) against the term $[(T_{\text{m,Ce}_2\text{Si}_2\text{O}_7} - T_{\text{liquidus}}) / T_{\text{m,Ce}_2\text{Si}_2\text{O}_7} T_{\text{liquidus}}]$ should be a straight line with a slope equal to $(-\Delta H_{\text{m,Ce}_2\text{Si}_2\text{O}_7}^\circ / 2.303R)$. The plot of this line is given in Figure 4, from which we calculated $\Delta H_{\text{m,Ce}_2\text{Si}_2\text{O}_7}^\circ$ to be 36.81 ± 0.25 kJ/mol. This translates to a value for $\Delta S_{\text{m,Ce}_2\text{Si}_2\text{O}_7}^\circ$ of 17.86 J/mol-K at the melting point of 1788°C. No values were found in the literature for the enthalpy and entropy of melting of any of the lanthanide pyrosilicates to compare with these data.

Figure 3. Binary phase diagram of Al_2O_3 - $\text{Ce}_2\text{Si}_2\text{O}_7$ system



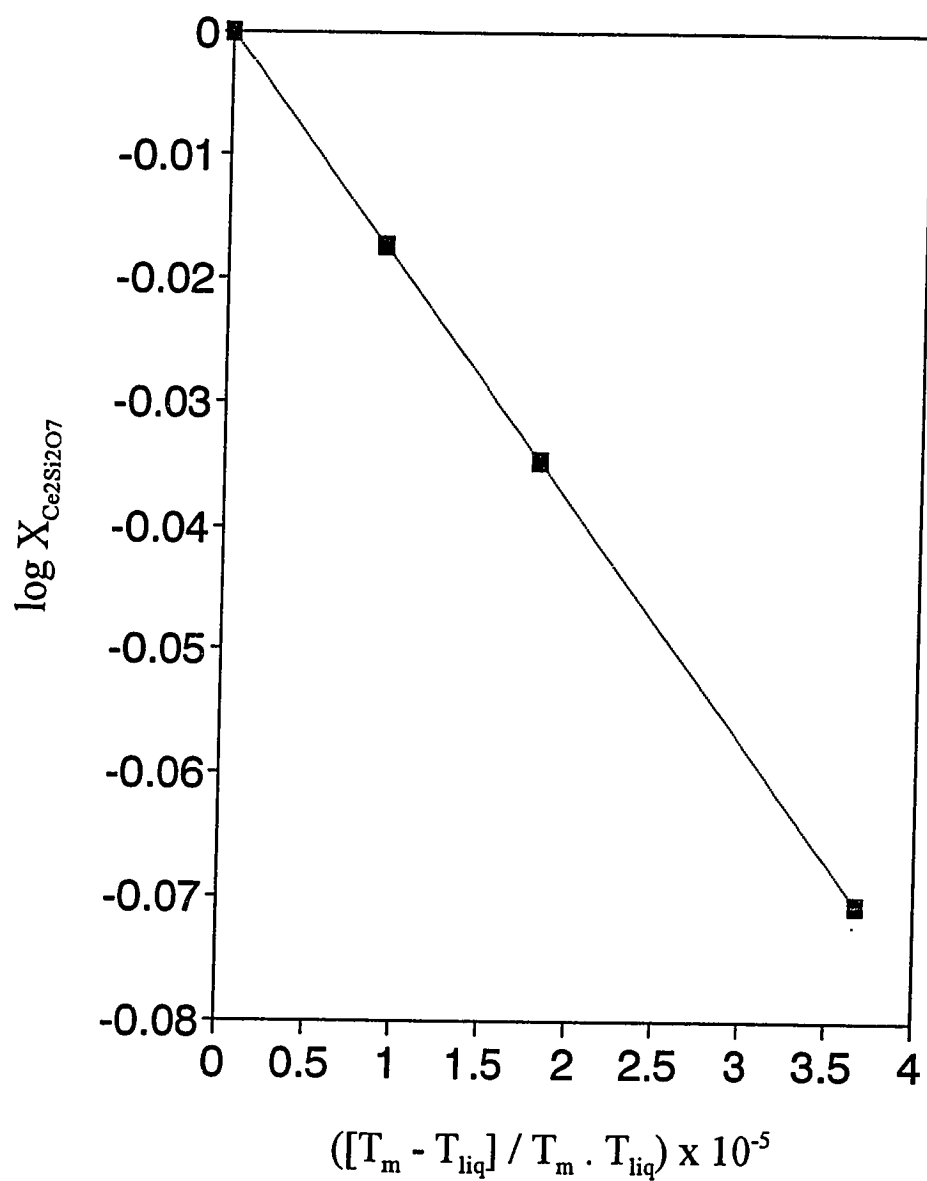


Figure 4. The heat of melting of $\text{Ce}_2\text{Si}_2\text{O}_7$, calculated from the slope of its liquidus line

CONCLUSIONS

1) It was found that cerium pyrosilicate, $\text{Ce}_2\text{Si}_2\text{O}_7$, like other light lanthanide pyrosilicates has two polymorphic forms. The high-temperature form is monoclinic and the low-temperature form is tetragonal. The low-temperature, tetragonal polymorph of $\text{Ce}_2\text{Si}_2\text{O}_7$ can be produced only by slowly cooling the high-temperature form if the high-temperature form had been prepared from pure binary oxides, CeO_2 and SiO_2 in an inert atmosphere. The polymorphic transformation occurs at $1274 \pm 5^\circ\text{C}$. The melting point of $\text{Ce}_2\text{Si}_2\text{O}_7$ was determined to be $1788 \pm 5^\circ\text{C}$ using DTA experiments.

2) The Al_2O_3 - $\text{Ce}_2\text{Si}_2\text{O}_7$ binary system is of the simple eutectic type. The eutectic occurs at $1375 \pm 5^\circ\text{C}$ and 51 mol% $\text{Ce}_2\text{Si}_2\text{O}_7$. The enthalpy of melting of the cerium pyrosilicate phase was calculated as 36.81 kJ/mol from the slope of the liquidus.

3) The microstructures in this binary system can be controlled by proper selection of heating and cooling rates and annealing times. The equilibrium phases formed and depicted here require a strict control over the inertness of the annealing atmosphere.

REFERENCES

- ¹ J. Felsche, "Polymorphism and Crystal Data of the Rare-Earth Disilicates of Type $\text{RE}_2\text{Si}_2\text{O}_7$," *J. Less-Common Met.*, **21**, 1-14 (1970).
- ² R. Heindl, N. Jonkierre and J.A. Lories, "Preparation and Luminescence Properties of Tetragonal Cerium Disilicate $\text{Ce}_2\text{Si}_2\text{O}_7$ and Its Terbium-Activated Derivative," *Proc. Rare Earth Res. Conf., 9th*, VA, USA, 1, 25-34, (1971).
- ³ H.A.M. van Hal and H.T. Hintzen, "Compound Formation in the Ce_2O_3 - SiO_2 System," *J. Alloys Compd.*, **179**, 77-85 (1992).
- ⁴ J. Felsche and W. Hirsiger, "The Polymorphs of the Rare-Earth Pyrosilicates $\text{RE}_2\text{Si}_2\text{O}_7$," *J. Less-Common Met.*, **18**, 131 (1969).
- ⁵ C. Calvo, "The Crystal Structure of $\alpha\text{-Ca}_2\text{P}_2\text{O}_7$," *Inorg. Chem.*, **7**, 1345-1351 (1968).
- ⁶ N.A. Toropov, I.F. Andreev, A.N. Sokolov and L.N. Sanzharevskaya, "Solid Solutions in the System $\text{Y}_2\text{Si}_2\text{O}_7$ - $\text{Ce}_2\text{Si}_2\text{O}_7$," *Izv. Akad. Nauk SSSR, Neorg. Mater.*, **6** [3], 519-523 (1970).

- ⁷ A.I. Leonov, "The Valence of Cerium in Synthetic and Natural Cerium Aluminates and Silicates, Part 2, Cerium Silicates," *Izv. Akad. Nauk SSSR, Ser. Khim.*, **12**, 2084-2089 (1963).
- ⁸ M.H. O'Brien and M. Akinc, "Role of Ceria in Enhancing the Resistance of Aluminosilicate Refractories to Attack by Molten Aluminum Alloy," *J. Am. Ceram. Soc.*, **72** [6], 896-904 (1989).
- ⁹ E.I. Galant and V.A. Tsekhomskii, "The Electron Conductivity of Cerium-containing Glasses," *Izv. Akad. Nauk SSSR, Neorg. Mater.*, **3** [10], 1953-1955 (1967).
- ¹⁰ A. Makishima, M. Kobayashi, T. Shimohira and T. Nagata, "Formation of Aluminosilicate Glasses Containing Rare-Earth Oxides," *J. Am. Ceram. Soc.*, **65**[12] C-210 (1982).
- ¹¹ E.M. Levin, C.R. Robbins and H.F. McMurdie, *Phase Diagrams for Ceramists*; Fig.356. Edited by M.K. Reser. American Ceramic Society, Columbus,OH, 1964.
- ¹² A. C. Tas and M.Akinc, "Cerium Oxygen Apatite ($\text{Ce}_{4.67}[\text{SiO}_4]_3\text{O}$) X-Ray Diffraction Pattern Revisited," *Powder Diffr.*, **7**, 219-222, 1992 .

APPENDIX 1. X-RAY DIFFRACTION PATTERN OF MONOCLINIC $\text{Ce}_2\text{Si}_2\text{O}_7$

X-ray Diffraction Pattern of Monoclinic $\text{Ce}_2\text{Si}_2\text{O}_7$ (Am.Ceram.Soc. Depository)

$a = 13.0803(6) \text{ \AA}$, $b = 8.7270(4) \text{ \AA}$, $c = 5.4054(5) \text{ \AA}$, $\beta = 90.134^\circ$, $Z = 4$, $V = 617.03(5) \text{ \AA}^3$
 Monoclinic, Space group : P21/n (14), $D_x = 4.83 \text{ gm/cm}^3$, Powder diffractometer, $\text{CuK}\alpha$,
 Peak-height intensities, External Si standard (NBS640a), Reflection conditions : 1) $0k0$:
 $k = 2n$, 2) $h0l$: $h+l = 2n$.

hkl	d_{calc}	d_{obs}	I/I_0
110	7.260	7.266	38
200	6.540	6.547	11
210	5.234	5.237	5
020	4.364	4.363	8
-111	4.340	4.341	3
111	4.331	4.331	5
310	3.900	3.902	1
211	3.754	3.757	4
220	3.630	3.630	2
021	3.395	3.396	100
-121	3.288	3.289	29
121	3.284	3.283	20
-311	3.168	3.167	10
311	3.158	3.156	6

(continued)

-320	3.084	3.085	24
410	3.062	3.063	4
-221	3.016	3.016	1
130	2.840	2.841	7
-411	2.669	2.669	9
411	2.660	2.659	11
420	2.617	2.617	5
112	2.531	2.532	3
-131	2.515	2.515	10
131	2.513	2.512	8
510	2.506	2.507	7
330	2.4198	2.4194	1
-212	2.4044	2.4050	2
212	2.3983	2.3990	2
-231	2.3867	2.3868	1
231	2.3837	2.3828	1
-421	2.3582	2.3580	2
-122	2.2643	2.2644	1
122	2.2617	2.2616	1
040	2.1817	2.1814	10
600	2.1800	2.1796	9
430	2.1735	2.1739	4

(continued)

-222	2.1700	2.1694	3
222	2.1655	2.1648	4
140	2.1520	2.1519	13
610	2.1150	2.1153	5
-521	2.0747	2.0737	2
521	2.0698	2.0692	1
-322	2.0355	2.0358	13
-412	2.0300	2.0300	21
041	2.0232	2.0240	4
-431	2.0184	2.0185	3
-141	1.9998	2.0000	2
141	1.9989	1.9984	2
-611	1.9722	1.9715	1
611	1.9671	1.9675	1
-132	1.9585	1.9591	1
132	1.9569	1.9560	1
340	1.9511	1.9510	2
-241	1.9336	1.9335	8
-232	1.8966	1.8972	4
232	1.8936	1.8934	4
-422	1.8829	1.8825	4
422	1.8770	1.8770	4

(continued)

-621	1.8365	1.8368	10
341	1.8342	1.8347	10
-531	1.8320	1.8320	8
531	1.8286	1.8288	6
440	1.8149	1.8153	3
-332	1.8048	1.8049	2
332	1.8009	1.8010	1
701	1.7639	1.7649	1
150	1.7301	1.7300	4
-441	1.7216	1.7217	4
441	1.7194	1.7188	3
042	1.6976	1.6972	3
-432	1.6959	1.6952	2
432	1.6916	1.6919	2
-142	1.6840	1.6842	4
142	1.6829	1.6825	1
-540	1.6755	1.6757	3
612	1.6626	1.6623	6
-151	1.6480	1.6481	2
151	1.6475	1.6470	2
-721	1.6387	1.6381	2
721	1.6354	1.6349	1

(continued)

-251	1.6103	1.6104	7
810	1.6071	1.6073	2
-541	1.6015	1.6011	1
541	1.5993	1.5995	1
-342	1.5833	1.5829	2
-532	1.5809	1.5804	1
-351	1.5528	1.5532	2
351	1.5515	1.5513	2
-640	1.5421	1.5420	3
820	1.5311	1.5312	1
731	1.5083	1.5083	1
442	1.5052	1.5049	1
-641	1.4840	1.4840	1
152	1.4568	1.4564	1
-722	1.4521	1.4520	2
160	1.4456	1.4455	1
910	1.4336	1.4336	1
-252	1.4314	1.4315	1
-542	1.4257	1.4257	1
542	1.4225	1.4228	1
260	1.4198	1.4198	3
740	1.4192	1.4190	1

(continued)

-901	1.4049	1.4045	1
901	1.4021	1.4018	2
-161	1.3967	1.3970	1
-911	1.3870	1.3872	1
911	1.3844	1.3846	1
360	1.3797	1.3799	1
-831	1.3794	1.3791	2
-741	1.3737	1.3735	5
-732	1.3609	1.3606	2
732	1.3570	1.3573	3
-452	1.3389	1.3388	1
642	1.3378	1.3375	1
361	1.3365	1.3361	1
460	1.3290	1.3287	2
-651	1.3219	1.3217	3
10 1 0	1.2936	1.2937	1
-461	1.2910	1.2908	2
-552	1.2802	1.2801	3
-262	1.2574	1.2572	2
-561	1.2380	1.2382	1
561	1.2369	1.2367	3
-922	1.2301	1.2301	3

(continued)

922	1.2264	1.2266	2
-10 2 1	1.2216	1.2213	1
10 2 1	1.2196	1.2197	1
-652	1.2178	1.2179	1
652	1.2155	1.2156	1
660	1.2099	1.2100	1
370	1.1987	1.1984	1
462	1.1918	1.1917	1
842	1.1762	1.1764	1
932	1.1700	1.1698	1
10 1 2	1.1651	1.1651	3

APPENDIX 2. X-RAY DIFFRACTION PATTERN OF TETRAGONAL $\text{Ce}_2\text{Si}_2\text{O}_7$

X-ray Diffraction Pattern of Tetragonal $\text{Ce}_2\text{Si}_2\text{O}_7$ (Am.Ceram.Soc. Depository)

$a = 6.7918(4) \text{ \AA}$, $c = 24.700(2) \text{ \AA}$, $V = 1139.38 \text{ \AA}^3$, $Z = 8$, $D_x = 5.227 \text{ gm/cm}^3$
 Tetragonal , Reflection conditions : 1) $00l : l=4n$
 Possible space group : $P4_1$, $F(30) = 31.(0.016212,61)$
 Powder Diffractometer, $\text{CuK}\alpha$, Ni-filter, Peak height intensities, External Si standard (NBS640a)

hkl	d_{obs}	d_{calc}	I/I_0
101	6.54	6.548	11
004	6.16	6.175	4
102	5.94	5.951	4
103	5.22	5.239	8
110	4.80	4.802	13
111	4.71	4.714	4
112	4.47	4.476	16
113	4.14	4.148	24
105	4.00	3.995	5
106	3.518	3.520	9
115	3.441	3.443	22
201	3.365	3.364	95
202	3.274	3.274	70
008	3.086	3.087	100
211	3.013	3.014	25
204	2.974	2.975	7
212	2.948	2.949	9
117	2.848	2.849	32
205	2.797	2.798	14
214	2.724	2.725	8
206	2.620	2.619	12

(continued)

215	2.586	2.587	9
207	2.444	2.447	4
221	2.389	2.390	13
222	2.356	2.357	3
223	2.303	2.305	3
208	2.284	2.284	8
301	2.255	2.254	9
218	2.164	2.165	7
310	2.149	2.148	12
209	2.135	2.134	11
304	2.125	2.125	18
312	2.115	2.116	10
313	2.074	2.078	3
0012	2.058	2.058	7
314	2.028	2.028	32
2010	1.998	1.997	11
227	1.985	1.985	12
1112	1.892	1.892	4
321	1.878	1.878	8
2011	1.873	1.873	8
322	1.862	1.862	5
229	1.806	1.807	12
2012	1.761	1.761	5
309	1.747	1.746	3
326	1.713	1.713	8
327	1.662	1.662	11
1114	1.656	1.656	8
411	1.644	1.643	5
3110	1.621	1.621	3
328	1.608	1.608	7
414	1.592	1.591	3

(continued)

406	1.571	1.570	3
415	1.563	1.563	7
3111	1.553	1.552	3
334	1.550	1.550	4
416	1.530	1.529	4
335	1.523	1.523	4
417	1.493	1.493	6
3112	1.486	1.486	4
425	1.452	1.452	3
2214	1.423	1.422	4
1017	1.421	1.420	3
4110	1.372	1.370	4
2215	1.358	1.358	4
501	1.356	1.356	4
502	1.350	1.350	6
3213	1.338	1.338	3
3214	1.288	1.288	4
3016	1.275	1.275	5
516	1.268	1.267	3
522	1.255	1.255	4
4113	1.245	1.245	4
3215	1.240	1.240	9
0020	1.235	1.235	3
5010	1.190	1.190	3
4115	1.165	1.165	4

PAPER III: PHASE RELATIONS IN THE SYSTEM Ce_2O_3 - $\text{Ce}_2\text{Si}_2\text{O}_7$ IN THE
TEMPERATURE RANGE 1150° TO 1970° C IN REDUCING AND
INERT ATMOSPHERES

Phase Relations in the System Ce_2O_3 - $\text{Ce}_2\text{Si}_2\text{O}_7$ in the Temperature Range 1150° to 1970°C in Reducing and Inert Atmospheres

Submitted by

A. Cuneyt Tas and Mufit Akinc

Department of Materials Science and Engineering

Iowa State University

Ames, Iowa 50011

This manuscript has been submitted for publication to the Journal of the American Ceramic Society.

ABSTRACT

The high temperature phase relations in the system Ce_2O_3 - $\text{Ce}_2\text{Si}_2\text{O}_7$ have been studied in the temperature range 1150° to 1970°C in inert and reducing atmospheres by conventional quenching and differential thermal analysis. Three eutectic reactions were found to occur at 1664°C and 27 mol% SiO_2 between Ce_2O_3 and Ce_2SiO_5 , at 1870°C and 54 mol% SiO_2 between Ce_2SiO_5 and $\text{Ce}_{4.67}(\text{SiO}_4)_3\text{O}$, and at 1762°C and 65 mol% SiO_2 between $\text{Ce}_{4.67}(\text{SiO}_4)_3\text{O}$ and $\text{Ce}_2\text{Si}_2\text{O}_7$. Microstructural characteristics of the eutectic reactions were observed. Cerium pyrosilicate exhibits a polymorphic transformation at 1274°C. The binary compounds of this system were all found to melt congruently. The enthalpy and entropy of melting of these binary compounds were calculated from the initial slopes of their experimentally determined liquidus lines.

INTRODUCTION

The present study is concerned with phase relations in the Ce_2O_3 - $\text{Ce}_2\text{Si}_2\text{O}_7$ system which is the 0 to 66.67 mol% SiO_2 section of the Ce_2O_3 - SiO_2 binary. The presence of three binary compounds, i.e., Ce_2SiO_5 ¹⁻⁷ (cerium oxyorthosilicate), $\text{Ce}_{4.67}(\text{SiO}_4)_3\text{O}$ ³⁻¹⁰ (cerium oxygen apatite) and $\text{Ce}_2\text{Si}_2\text{O}_7$ ^{1-7,11-14} (cerium pyrosilicate or disilicate) have been reported. $\text{Ce}_2\text{Si}_2\text{O}_7$ has been reported to have two polymorphs. The high temperature form has long been regarded^{1-5,7,11-13} to be the rare earth G-type "pseudo-orthorhombic" (with a monoclinic angle of 90°). It has recently been shown by us¹⁴ that the high temperature form is indeed monoclinic with a monoclinic angle of only 90.13° . The low temperature form^{7,12,14} has been reported to have a tetragonal unit cell. The extremely sluggish phase transition was found to occur at 1274°C ¹⁴.

Owing to the stable trivalent states of most of the rare earth elements, many of their oxides are found to exist as sesquioxides (RE_2O_3). However, since cerium assumes the 4+ state in air, its stable oxide is CeO_2 with a cubic fluorite structure. Heating CeO_2 in a "reducing" atmosphere at a temperature not less than 1400°C will reduce it to $\text{CeO}_{1.5}$. On the other hand, the complete conversion of CeO_2 to Ce_2O_3 in an "inert" atmosphere, such as vacuum or purified argon, requires temperatures in excess of 1700°C . At lower temperatures, the formation of a continuum of defect phases, usually designated as CeO_{2-x} , is observed in "inert" atmospheres. Hence, pure Ce_2O_3 , obtained in an inert atmosphere by

heating the cerium (IV) oxide, for instance, at 1850°C can only be brought down to room temperature by careful and rapid quenching. Slow or even moderate cooling rates cause the conversion of Ce_2O_3 partially or totally to CeO_{2-x} , depending on the rate of cooling employed. To complicate matters further, Sata and Yoshimura¹⁵ have reported that pure Ce_2O_3 formed in vacuum begins to "sublime" upon heating to above 1900°C. On the other hand, the melting point for Ce_2O_3 in dry hydrogen, was reported by the same authors to be $2210 \pm 10^\circ\text{C}$, without further mention of the problem of sublimation.

There have been no studies in the literature aimed at experimentally determining the melting points of Ce_2SiO_5 and $\text{Ce}_{4.67}(\text{SiO}_4)_3\text{O}$. The melting point of $\text{Ce}_2\text{Si}_2\text{O}_7$ was previously determined by us¹⁴ to be $1788 \pm 5^\circ\text{C}$ which is in relatively close agreement with the value of Toropov et al.¹³ ($1770 \pm 25^\circ\text{C}$).

There have been two versions of a phase diagram for the Ce_2O_3 - SiO_2 system given in the literature. The early one given by Leonov² in 1970 did not even include the cerium oxygen apatite phase ($\text{Ce}_{4.67}(\text{SiO}_4)_3\text{O}$). It indicated to the presence of a eutectic reaction occurring at 1700°C and at about 33 mol% SiO_2 between Ce_2O_3 (which was shown to melt at 2160°C) and Ce_2SiO_5 (which was shown to melt at 1870°C). The phase diagram also showed a polymorphic transformation for $\text{Ce}_2\text{Si}_2\text{O}_7$ at about 1200°C. The high temperature polymorph was shown to melt incongruently at above 1700°C. The uncertain nature of the liquid drawn between Ce_2SiO_5 and SiO_2 , and the absence of the $\text{Ce}_{4.67}(\text{SiO}_4)_3\text{O}$ phase in this diagram suggested that further study of this system was needed. The second construction for this

system was given by Kaufman et al⁶ in 1982. This diagram was calculated from available thermodynamic data and from lattice stability parameters of the terminal members, Ce_2O_3 and SiO_2 . This compilation indicated a eutectic between Ce_2O_3 and Ce_2SiO_5 at 1607°C ; however, it also claimed that Ce_2SiO_5 decomposed above 1647°C . This diagram also showed the compounds $\text{Ce}_{4.67}(\text{SiO}_4)_3\text{O}$ and $\text{Ce}_2\text{Si}_2\text{O}_7$ to melt congruently at 2172°C and 2242°C , respectively, but made no mention of a polymorphic transformation in $\text{Ce}_2\text{Si}_2\text{O}_7$.

In this work, compound formation, compound stability, and the phase relations at and above liquidus temperatures have been investigated to determine the phase diagram of the sub-binary Ce_2O_3 - $\text{Ce}_2\text{Si}_2\text{O}_7$ of the system Ce_2O_3 - SiO_2 .

EXPERIMENTAL PROCEDURE

(1) Materials and Sample Preparation

Compositions in the Ce_2O_3 - $\text{Ce}_2\text{Si}_2\text{O}_7$ system were prepared by mixing the appropriate amounts of the oxides CeO_2 and SiO_2 so as to achieve the desired Ce:Si ratios. CeO_2 transforms into Ce_2O_3 at temperatures above 1400°C when heated either in vacuum ($P_{\text{O}_2} \leq 6 \times 10^{-9}$ atm) or in an argon + 10% H_2 atmosphere. The starting oxides CeO_2 (99.87%, $0.7 \mu\text{m}$) and fumed SiO_2 (99.98%, $0.007 \mu\text{m}$), whose chemical analyses and surface areas were reported elsewhere¹⁴, were heated in air at 975°C for 12 hours prior to weighing mainly to ascertain the CeO_2 stoichiometry and to remove any adsorbed water layer on fumed SiO_2 . The stoichiometric amounts of the calcined oxides were mixed in pure ethanol in glass jars for about an hour with a mechanical stirrer. Following this, the jar contents were dispersed by 15 minutes of ultrasonification prior to overnight drying at 70°C . The recovered cakes were then calcined in air at 950°C for 12 hours as a precaution to remove hydrocarbon residues that might be present. The calcined mixtures were then lightly ground in an agate mortar for about 30 minutes.

Pellets, 1.0 cm diameter by 0.4 cm thick, were prepared by uniaxial dry pressing of approximately 2.5 grams of oxide mixtures of each composition at 20 MPa in a tungsten carbide-lined steel die followed by cold isostatic pressing in latex gloves at 200 MPa. The pressed samples were equilibrated at a predetermined temperature in a MoSi_2 quench furnace

within a vertical sillimanite reaction tube 120 cm long by 5 cm diameter . A slightly reducing atmosphere in the furnace tube was attained by a constant flow of a pre-purified mixture argon + 10% H₂ gas. The pellets were suspended in the hot zone of the furnace* with a molybdenum wire which is hooked to an envelope, which contained the pellets, made from 0.4 mm thick foils of molybdenum. The three pellets that were put into an envelope at one time were physically separated from each other by placing small molybdenum strips between them. The temperature in the furnace tube was controlled to within $\pm 6^{\circ}\text{C}$ in the temperature range 1150° to 1560°C by a B-type control thermocouple which feeds the programmable furnace temperature controller. The temperature in the hot zone was monitored with a B-type sample thermocouple located adjacent to the suspended sample envelopes. The sample thermocouple was calibrated after every 120 hours of heating above 1400°C against the melting points of Au (1064°C) and Pd (1554°C) under a moderate flow of argon. At the end of the specified equilibration times, the samples were quenched by dropping the envelope into a well-stirred, deionised water bath (which was brought to about 3°C by adding ice cubes into the water bath at the quenching time), covered with a thin layer of vacuum pump oil, which also served to seal the bottom end of the furnace tube during the course of the experiment.

* Model 3320, ATS Inc., PA, USA

(2) Phase and Microstructural Analyses

For phase analyses, every quenched sample was ground to a mean particle size of about 7 μm and examined by XRD in the 5-85° 2 Θ range using a Cu-tube powder diffractometer[†] with a maximum scanning rate of 0.4° 2 Θ /min. The X-ray data collected by the diffractometer computer were later analysed in 1° 2 Θ intervals by separate peak detection and profile fitting software packages for weak reflections and peak overlaps for every sample. Least squares cell refinement and lattice parameter determinations were performed by the Appleman and Evans routine¹⁶. To determine the resolving power of the X-ray diffractometer, that we used for the characterisation of the crystalline phases of this system, small quantities (1 - 3 mol%) of pure, pre-fired and equilibrated compounds were added to each other (i.e., 1-3 mol% compound A + 99-97 mol% compound B) at room temperature and thoroughly mixed. We presupposed that to be able to ascertain the presence of a minor phase in the mixture, the three strongest reflections from that phase should be detected in the XRD trace of the mixture. The selected mixtures were 1 mol% Ce₂O₃-99 mol% Ce₂SiO₅ (=0.8 wt% Ce₂O₃), 3 mol% Ce₂SiO₅-97 mol% Ce_{4.67}(SiO₄)₃O (=1.2 wt% Ce₂SiO₅), and 1 mol% Ce_{4.67}(SiO₄)₃O-99 mol% Ce₂Si₂O₇ (=2.1 wt% Ce_{4.67}(SiO₄)₃O). After the XRD analyses of these samples, at the maximum scanning rate of this study in the same 2 Θ range, the intensities of the strongest

[†] XDS 2000, Scintag, Inc., CA, USA

reflections of the three minor phases were found to be 12, 4, and 9, respectively. This information used as a guide for the detection of minor phases by XRD in the samples of the rest of this study. Elemental silicon (NBS640a) was used as an external standard.

Microstructural analyses were carried out by SEM* and reflected light microscopy on polished or as is surfaces of the samples. The chemical compositions of microstructural features observed in SEM images of polished samples were determined by EDXS* using pure Ce_2O_3 , $\text{Ce}_{4.67}(\text{SiO}_4)_3\text{O}$ and $\text{Ce}_2\text{Si}_2\text{O}_7$ as standards, and the information obtained were believed to be accurate to within ± 4 atomic percent. Analyses of phase distribution and phase amounts were carried out on polished surfaces with the X-ray mapping and automated image analysis attachments to the SEM to give the elemental distribution among the microstructural features and the areal fractions of specific phases on polished surfaces which were used especially in ascertaining the positions of the liquid in the binary phase diagram.

(3) Equilibration Experiments

The minimum equilibration times during preliminary experiments were 100 hours at 1150°C and 50 hours at 1550°C in argon + 10% H_2 . After 50 hours of heating, for instance at 1550°C, the samples were quenched, ground, examined by XRD for phase analysis,

* JSM-6100, JEOL, Inc., MA, USA

* Model Delta-5, Kevex Corp., CA, USA

re-pelletised, and heated for an additional 45-50 hours followed by quenching and phase analysis. The same procedure was repeated for other temperatures as well. The minimum time required for a certain composition to reach equilibrium at a certain temperature was deduced when XRD traces showed no detectable changes in kinds and amounts of the phases present.

The equilibration runs above 1550°C were carried out in a vacuum furnace[†] with a tungsten mesh heater which has a maximum temperature capability of 2050°C at a partial pressure of oxygen of $\leq 6 \times 10^{-9}$ atm. The samples were suspended in the hot zone in molybdenum crucibles which were also visible through a fused quartz window during the runs. The crucibles were tightly crimped to significantly reduce the evaporation of the liquid phases formed. The temperature of the vacuum furnace was controlled by a C-type thermocouple. Sample temperatures were monitored by an IR-pyrometer, calibrated frequently against the melting point of Pt (1772°C), aimed directly at the samples. At the end of the equilibration treatment, the samples were furnace quenched to ambient temperature by shutting off the furnace power, typically providing cooling rates in excess of 600°C/min in the temperature range 1950° - 1150°C.

[†] Centorr Associates, Inc., NH, USA

(4) Differential Thermal Analyses

DTA experiments were carried out to monitor phase transitions in this system. The DTA runs were performed in the vacuum furnace with a custom built DTA module equipped with a C-type differential thermocouple assembly and a capped molybdenum sample block. The circular sample block contained two 1 cm diameter by 1 cm deep cavities (one for sample and the other for the reference) drilled symmetrically about the center of the block. The thermocouple tips reached these cavities from the top through the holes in the block cap. Al_2O_3 (99.96%) was used as the reference material. Samples (not less than 380 mg) were placed in molybdenum crucibles, which fit snugly into the cavities in the sample block, made from molybdenum foils by pressing and crimping them to the shape of the cavities. The electrical output of the thermocouples were sent to two (one for the sample temperature and the other for the temperature difference between the sample and the reference cells) high sensitivity millivoltmeters connected to a PC to acquire the data in a time (sec), temperature ($^{\circ}\text{C}$) and temperature difference (μV) string. The thermocouples of the DTA module were calibrated after every 20 hours of operation above 1675°C against the melting points of pure Au (1064°C), Li_2SiO_3 (1204°C), Pd (1554°C), and Pt (1772°C). For the determination of liquidus points in the binary, samples were first equilibrated at 1550°C in argon + 10% H_2 for a prolonged time and then water-quenched to room temperature. These samples, after grinding to a fine powder, were used in DTA runs with a heating rate of 10 - 15 $^{\circ}\text{C}/\text{min}$ in the

low temperature range (1150 - 1550°C) followed by slower heating rates, typically 4-5 °C / min, to a final temperature of 1935 °C. The DTA samples were furnace quenched to room temperature to facilitate phase analysis of the recovered material by XRD and SEM , as described above. The thermal events indicated by DTA for specific temperature - composition points were then confirmed in equilibration experiments by heating portions of the same samples (equilibrated but not yet tested with DTA) to temperatures 10° above and 10° below the temperature read from the DTA traces followed by quenching and phase analysis.

RESULTS AND DISCUSSION

(1) Stability and the Melting Points of the Compounds

The three previously reported binary compounds, i.e., Ce_2SiO_5 , $\text{Ce}_{4.67}(\text{SiO}_4)_3\text{O}$, and $\text{Ce}_2\text{Si}_2\text{O}_7$, of this system have successfully been synthesized as single phase substances in this work. It has been found that in flowing purified argon it was almost impossible to form Ce_2SiO_5 even at 1550°C for a heating time of 180 hours (followed by quenching). The other two were easily formed in an argon atmosphere at 1550°C in less than 7 hours. The addition of 10% H_2 to argon allowed us to synthesize Ce_2SiO_5 at 1550°C in about 12 hours. There has been found to be no difference in the lattice parameters of samples of $\text{Ce}_{4.67}(\text{SiO}_4)_3\text{O}$, monoclinic $\text{Ce}_2\text{Si}_2\text{O}_7$, and tetragonal $\text{Ce}_2\text{Si}_2\text{O}_7$ prepared separately in pure argon and argon+10% H_2 . Pure CeO_2 , when heated in an argon + 10% H_2 atmosphere, was found to transform completely into Ce_2O_3 in 200 hours at 1150°C , 185 hours at 1250°C , 170 hours at 1350°C , 100 hours at 1450°C , and 70 hours at 1550°C . It should be noted that these times were not the minimum required durations for this reduction to go to completion, they just represent the times selected by us for equilibration, in other words, the actual times could be significantly lower than those. We also encountered the same problem reported by Sata and Yoshimura¹⁵ that Ce_2O_3 heated above 1875°C sublimed completely before melting in vacuum.

Ce_2SiO_5 was found to be stable in the temperature range of this study, i.e., 1150° to 1970°C. A small piece of pure Ce_2SiO_5 , with several sharp edges, was suspended by a molybdenum wire in the vacuum furnace which was visible through the viewing port. The IR-pyrometer, calibrated just prior to this run, was focused on the sample. The sample was heated with a heating rate of 4°C/min. The melting behaviour of the chunk was continuously observed through the pyrometer, and at $1970 \pm 30^\circ\text{C}$ the sharp edges of the samples began to round up. At this point, the sample was quenched by shutting off the power to the furnace. The recovered sample showed a tiny skin of black liquid formed around the sample, although the bulk of the sample was still showing the crystalline Ce_2SiO_5 . This fact contradicts the calculated phase diagram of Kaufman et al.⁶ which predicted Ce_2SiO_5 to decompose into cerium oxygen apatite and liquid at temperatures above 1647°C, but agrees with that of Leonov² in terms of being stable up to the melting point. We, therefore, assumed the above temperature, with the indicated degree of uncertainty, as the melting point of Ce_2SiO_5 .

The melting point of $\text{Ce}_{4.67}(\text{SiO}_4)_3\text{O}$ was determined to be at $1950 \pm 30^\circ\text{C}$ in a similar fashion. The small chunk did again form a black, viscous liquid on the outside which did not crystallise upon quenching as was the case with Ce_2SiO_5 . This temperature was noted to be 220° lower than that reported by Kaufman et al.⁶ in their calculated phase diagram.

The melting point of monoclinic, high temperature form of $\text{Ce}_2\text{Si}_2\text{O}_7$ was previously found by us¹⁴ to be at $1788 \pm 5^\circ\text{C}$ by repeated DTA experiments. Since our DTA module has had Al_2O_3 insulation tubes on its thermocouple wires, we did decide not to push it to the vicinity

of 2000°C for the determination of the melting points of Ce_2SiO_5 and $\text{Ce}_{4.67}(\text{SiO}_4)_3\text{O}$.

However, the DTA traces for these two compounds obtained between 1200° and 1930°C (4°C/min) did not show any thermal events. Table I shows the pertinent crystallographic and density (measured by using Archimedes principle) data for the compounds of the Ce_2O_3 - $\text{Ce}_2\text{Si}_2\text{O}_7$ system.

(2) Phase Relations between Ce_2O_3 and Ce_2SiO_5

The compositions investigated in the equilibration experiments in this portion of the system are denoted in Table II as SILI 9.5 (9.5 mol% SiO_2 , balance Ce_2O_3) through SILI 50. The four different compositions (SILI 9.5, 18, 26, and 40) fired in a purified argon + 10% H_2 atmosphere at five different temperatures (1150, 1250, 1350, 1450, and 1550°C) all yielded, after being quenched to room temperature, solid state phase mixtures of Ce_2O_3 and Ce_2SiO_5 . No solid solubility was found between the two phases nor any reaction between the phases and the molybdenum crucibles used. From the XRD patterns of the final samples of this portion of the system, we were able to distinguish 15 to 16 reflections of Ce_2O_3 in addition to more than 90 reflections of Ce_2SiO_5 . The colours of the quenched samples in this composition range did display a smooth variation from mustard (Ce_2O_3 -rich) to dark green (moderate Ce_2O_3) and finally to light blue (Ce_2SiO_5 -rich).

Table I. Crystallographic and Density Data of the Binary Compounds

Compound	Lattice Parameters	Space Group	Cell Volume	Z	D_{XRD}	D_{Meas}	Ref.
Ce_2O_3 (Hexagonal)	$a=3.891$, $c=6.063$	P321(150)	79.51	1	6.85	6.80	TS & 17
Ce_2SiO_5 (Monoclinic)	$a=9.278$, $b=7.382$, $c=6.956$ $\beta=108.33^\circ$	P12 ₁ /c1(14)	452.26	4	5.70	5.64	TS & 7
$Ce_{4.67}(SiO_4)_3O$ (Hexagonal)	$a=9.658$, $c=7.119$	P6 ₃ /m(176)	575.07	2	5.47	5.40	TS & 10
$Ce_2Si_2O_7$ (Tetragonal)	$a=6.792$, $c=24.700$	P4 ₁ (76)	1139.38	8	5.23	5.19	TS & 14
$Ce_2Si_2O_7$ (Monoclinic)	$a=8.727$, $b=13.080$, $c=5.405$ $\beta=90.13^\circ$	P21/n(14)	617.11	4	4.83	4.78	TS & 14

Units : Lattice parameters = Å, Cell volumes = Å³, D = gm/cm³, Z = Formula units per cell. Hermann - Mauguin numbers are given in parantheses following the space group denoters. TS = this study.

Table II. Results of Equilibration Runs in the System Ce_2O_3 - $\text{Ce}_2\text{Si}_2\text{O}_7$

Composition	Temperature ($^{\circ}\text{C}$)	Time (h)	Phases Observed	Atm.
SILI 9.5 ^a	1150	200	$\text{Ce}_2\text{O}_3 + \text{Ce}_2\text{SiO}_5$	(G)
SILI 9.5	1450	100	$\text{Ce}_2\text{O}_3 + \text{Ce}_2\text{SiO}_5$	(G)
SILI 9.5	1550	70	$\text{Ce}_2\text{O}_3 + \text{Ce}_2\text{SiO}_5$	(G)
SILI 9.5	1700	6	$\text{Ce}_2\text{O}_3 + \text{Liquid}$	(V)
SILI 9.5	1750	4	$\text{Ce}_2\text{O}_3 + \text{Liquid}$	(V)
SILI 9.5	1850	0.8	$\text{Ce}_2\text{O}_3 + \text{Liquid}$	(V)
SILI 18	1150	200	$\text{Ce}_2\text{O}_3 + \text{Ce}_2\text{SiO}_5$	(G)
SILI 18	1250	190	$\text{Ce}_2\text{O}_3 + \text{Ce}_2\text{SiO}_5$	(G)
SILI 18	1450	100	$\text{Ce}_2\text{O}_3 + \text{Ce}_2\text{SiO}_5$	(G)
SILI 18	1550	70	$\text{Ce}_2\text{O}_3 + \text{Ce}_2\text{SiO}_5$	(G)
SILI 18	1700	6	$\text{Ce}_2\text{O}_3 + \text{Liquid}$	(V)
SILI 18	1760	4	$\text{Ce}_2\text{O}_3 + \text{Liquid}$	(V)
SILI 26	1150	200	$\text{Ce}_2\text{O}_3 + \text{Ce}_2\text{SiO}_5$	(G)
SILI 26	1350	200	$\text{Ce}_2\text{O}_3 + \text{Ce}_2\text{SiO}_5$	(G)
SILI 26	1450	100	$\text{Ce}_2\text{O}_3 + \text{Ce}_2\text{SiO}_5$	(G)
SILI 26	1550	70	$\text{Ce}_2\text{O}_3 + \text{Ce}_2\text{SiO}_5$	(G)
SILI 26	1760	4	Liquid	(V)
SILI 33	1715	3.5	Liquid + Ce_2SiO_5	(V)
SILI 40	1450	100	$\text{Ce}_2\text{O}_3 + \text{Ce}_2\text{SiO}_5$	(G)
SILI 40	1550	70	$\text{Ce}_2\text{O}_3 + \text{Ce}_2\text{SiO}_5$	(G)
SILI 40	1715	3.5	Liquid + Ce_2SiO_5	(V)
SILI 40	1815	1.5	Liquid + Ce_2SiO_5	(V)
SILI 50	1170	200	Ce_2SiO_5	(G)
SILI 50	1450	100	Ce_2SiO_5	(G)
SILI 50	1550	70	Ce_2SiO_5	(G)
SILI 50	1715	12	Ce_2SiO_5	(V)
SILI 50	1820	4.5	Ce_2SiO_5	(V)
SILI 50	~ 1970	0.1	Liquid	(V)

Table II. (continued)

Composition	Temp. (°C)	Time (h)	Phases observed	Atm.
SILI 53	1150	200	$\text{Ce}_2\text{SiO}_5 + \text{Ce}_{4.67}(\text{SiO}_4)_3\text{O}$	(G)
SILI 53	1250	185	$\text{Ce}_2\text{SiO}_5 + \text{Ce}_{4.67}(\text{SiO}_4)_3\text{O}$	(G)
SILI 53	1450	100	$\text{Ce}_2\text{SiO}_5 + \text{Ce}_{4.67}(\text{SiO}_4)_3\text{O}$	(G)
SILI 53	1550	70	$\text{Ce}_2\text{SiO}_5 + \text{Ce}_{4.67}(\text{SiO}_4)_3\text{O}$	(G)
SILI 53	1790	8	$\text{Ce}_2\text{SiO}_5 + \text{Ce}_{4.67}(\text{SiO}_4)_3\text{O}$	(V)
SILI 53	1850	4.5	$\text{Ce}_2\text{SiO}_5 + \text{Ce}_{4.67}(\text{SiO}_4)_3\text{O}$	(V)
SILI 53	1930	0.8	Liquid	(V)
SILI 53.5	1920	0.8	$\text{Ce}_2\text{SiO}_5 + \text{Liquid}$	(V)
SILI 54	1920	0.8	Liquid	(V)
SILI 54.5	1920	0.8	Liquid + $\text{Ce}_{4.67}(\text{SiO}_4)_3\text{O}$	(V)
SILI 55	1450	100	$\text{Ce}_2\text{SiO}_5 + \text{Ce}_{4.67}(\text{SiO}_4)_3\text{O}$	(G)
SILI 55	1550	70	$\text{Ce}_2\text{SiO}_5 + \text{Ce}_{4.67}(\text{SiO}_4)_3\text{O}$	(G)
SILI 55	1920	0.8	Liquid + $\text{Ce}_{4.67}(\text{SiO}_4)_3\text{O}$	(V)
SILI 56.2	1170	200	$\text{Ce}_{4.67}(\text{SiO}_4)_3\text{O}$	(G)
SILI 56.2	1350	145	$\text{Ce}_{4.67}(\text{SiO}_4)_3\text{O}$	(G)
SILI 56.2	1550	6	$\text{Ce}_{4.67}(\text{SiO}_4)_3\text{O}$	(G)
SILI 56.2	1715	4	$\text{Ce}_{4.67}(\text{SiO}_4)_3\text{O}$	(V)
SILI 56.2	1820	2	$\text{Ce}_{4.67}(\text{SiO}_4)_3\text{O}$	(V)
SILI 56.2	1950	0.1	Liquid	(V)
SILI 59	1250	250	$\text{Ce}_{4.67}(\text{SiO}_4)_3\text{O} + \text{T-Ce}_2\text{Si}_2\text{O}_7$	(G)
SILI 59	1450	100	$\text{Ce}_{4.67}(\text{SiO}_4)_3\text{O} + \text{M-Ce}_2\text{Si}_2\text{O}_7$	(G)
SILI 59	1550	70	$\text{Ce}_{4.67}(\text{SiO}_4)_3\text{O} + \text{M-Ce}_2\text{Si}_2\text{O}_7$	(G)
SILI 59	1685	12	$\text{Ce}_{4.67}(\text{SiO}_4)_3\text{O} + \text{M-Ce}_2\text{Si}_2\text{O}_7$	(V)
SILI 59	1840	2	$\text{Ce}_{4.67}(\text{SiO}_4)_3\text{O} + \text{Liquid}$	(V)
SILI 62	1150	250	$\text{Ce}_{4.67}(\text{SiO}_4)_3\text{O} + \text{T-Ce}_2\text{Si}_2\text{O}_7$	(G)
SILI 62	1450	100	$\text{Ce}_{4.67}(\text{SiO}_4)_3\text{O} + \text{M-Ce}_2\text{Si}_2\text{O}_7$	(G)
SILI 62	1550	70	$\text{Ce}_{4.67}(\text{SiO}_4)_3\text{O} + \text{M-Ce}_2\text{Si}_2\text{O}_7$	(G)
SILI 62	1800	2	$\text{Ce}_{4.67}(\text{SiO}_4)_3\text{O} + \text{Liquid}$	(V)
SILI 65	1150	250	$\text{Ce}_{4.67}(\text{SiO}_4)_3\text{O} + \text{T-Ce}_2\text{Si}_2\text{O}_7$	(G)
SILI 65	1250	250	$\text{Ce}_{4.67}(\text{SiO}_4)_3\text{O} + \text{T-Ce}_2\text{Si}_2\text{O}_7$	(G)

Table II. (continued)

Composition	Temp. (°C)	Time (h)	Phases observed	Atm.
SILI 65	1350	200	Ce _{4.67} (SiO ₄) ₃ O+M-Ce ₂ Si ₂ O ₇	(G)
SILI 65	1450	100	Ce _{4.67} (SiO ₄) ₃ O+M-Ce ₂ Si ₂ O ₇	(G)
SILI 65	1550	70	Ce _{4.67} (SiO ₄) ₃ O+M-Ce ₂ Si ₂ O ₇	(G)
SILI 65	1770	2	Liquid	(V)
SILI 66	1770	4	M-Ce ₂ Si ₂ O ₇ + Liquid	(V)
SILI 66.7	1150	200	T-Ce ₂ Si ₂ O ₇	(G)
SILI 66.7	1250	200	T-Ce ₂ Si ₂ O ₇	(G)
SILI 66.7	1350	100	M-Ce ₂ Si ₂ O ₇	(G)
SILI 66.7	1450	100	M-Ce ₂ Si ₂ O ₇	(G)
SILI 66.7	1550	8	M-Ce ₂ Si ₂ O ₇	(G)
SILI 66.7	1790	0.1	Liquid	

^a **SILI 9.5** : 9.5 mol% SiO₂ - 90.5 mol% Ce₂O₃, (G) = Argon + 10% H₂ gas,
(V) = Vacuum (P_{TOT.} ≤ 2.5×10⁻⁸ atm)

The DTA runs (8°C/min: RT-1500°C; 4°C/min: 1500-1930°C), with about 400 mg portions of the equilibrated and quenched samples of the above compositions, indicated a significant endothermic event at 1664 ± 5°C as shown in Figure 1. This temperature was the temperature of first liquid formation in this system, i.e., the eutectic temperature. The sample of SILI 9.5 showed some degree of sublimation (being rich in Ce₂O₃) above 1900°C when heated in an open DTA crucible. The sublimed material condensed on the sample block cap. The XRD of this mustard coloured material showed that it was Ce₂O₃. Repeating the same run in a tightly crimped crucible eliminated the sublimation significantly. While the compositions

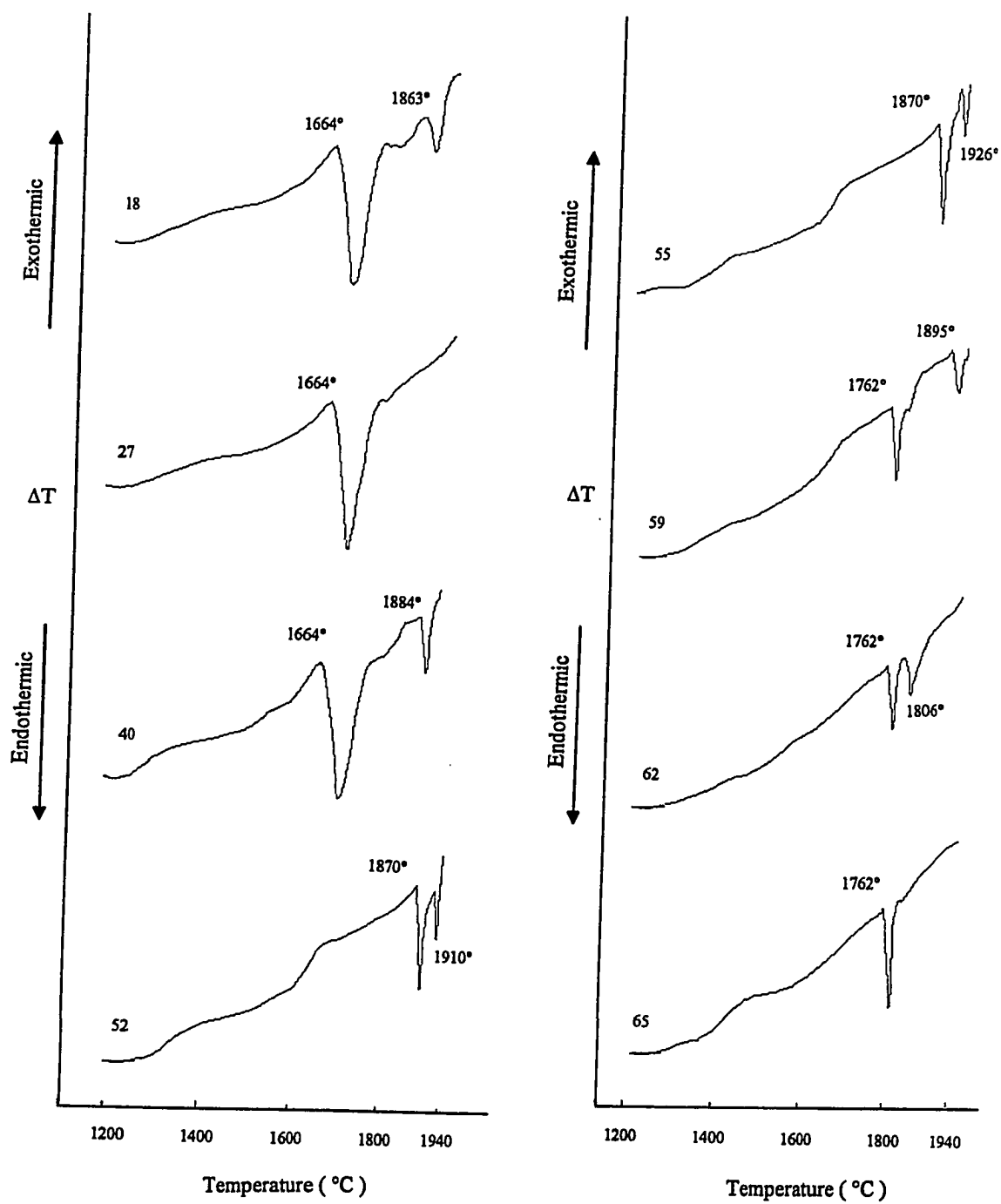


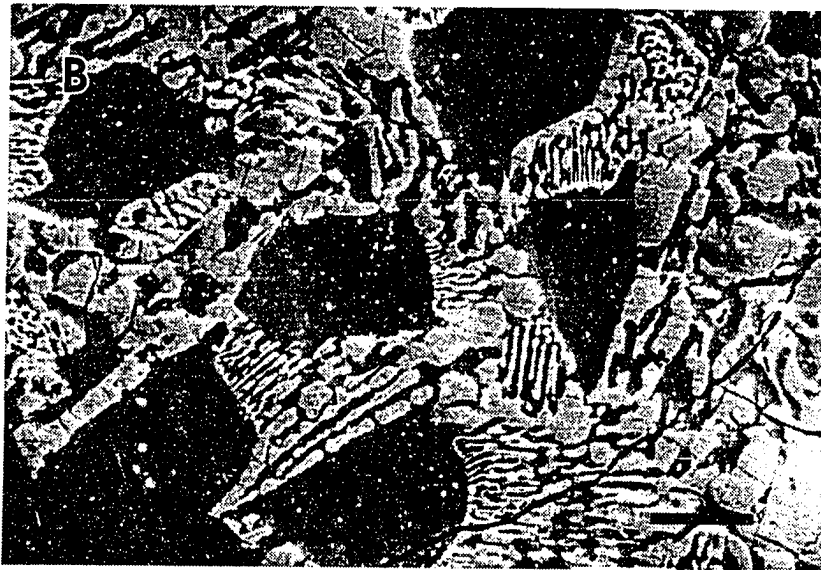
Figure 1. DTA traces of some of the compositions studied in the $\text{Ce}_2\text{O}_3 - \text{Ce}_2\text{Si}_2\text{O}_7$ system

SILI 9.5 and SILI 26 did not display another event in the whole heating range, an endothermic peak appeared for the SILI 18 sample at 1863°C. This was the liquidus temperature for that composition. The corresponding liquidus temperature for the SILI 40 composition was observed at 1884°C. Microscopic and XRD analyses of these furnace quenched (from 1930°C) DTA samples showed large Ce_2O_3 grains in a eutectic matrix in the SILI 18 sample, whereas the SILI 40 sample displayed chunky Ce_2SiO_5 crystals in a eutectic matrix. An unpolished surface of such a SILI 40 given in Figure 2a shows the Ce_2SiO_5 crystals embedded in the solidified liquid. Figure 2b displays a lightly polished section of the same sample which now depicts the eutectic nature of the surrounding phase. The extensive cracks through the eutectic structure, due to thermally induced stresses, were clearly visible in this micrograph. Microstructure of the lightly polished SILI 18 sample (from the above mentioned DTA run) is given in Figure 2c which shows the Ce_2O_3 grains in a eutectic matrix. The XRD trace of this sample shows the reflections of both Ce_2O_3 and Ce_2SiO_5 .

To determine the liquidus lines and the composition of the eutectic, the samples with compositions SILI 20, 22, 25, 27, 28, 30, and 35 were prepared, equilibrated in argon + 10% H_2 at 1550°C for 70 hours followed by quenching. The DTA's were taken under similar conditions to those of above. The liquidus points were identified by relatively small endothermic events in their DTA traces. The beginning temperatures of these small endothermic events were read as follows; 1809°C for SILI 20, 1769°C for SILI 22, 1679°C for SILI 25, 1700°C for SILI 30, and 1790°C for SILI 35. The DTA traces for the samples of compositions SILI 27 and SILI 28 did produce only one endothermic peak corresponding to

Figure 2. SEM micrographs of samples in the Ce_2O_3 - $\text{Ce}_2\text{Si}_2\text{O}_7$ system

- (A) Unpolished surface of a 40 mol% SiO_2 sample quenched from 1930°C . Large Ce_2SiO_5 grains are seen embedded in a eutectic matrix (BAR = 10 μm)
- (B) Polished surface of the sample of (A) (BAR = 10 μm)
- (C) 18 mol% SiO_2 sample quenched from 1930°C . Eutectic matrix surrounds the large Ce_2O_3 grains (BAR = 10 μm)
- (D) 27 mol% SiO_2 sample (eutectic composition between Ce_2O_3 and Ce_2SiO_5) quenched from 1600°C followed by equilibration at 1700°C (BAR = 10 μm)
- (E) Same sample at a higher magnification (BAR = 1 μm)
- (F) 54 mol% SiO_2 sample (eutectic composition between Ce_2SiO_5 and $\text{Ce}_{4.67}[\text{SiO}_4]_3\text{O}$) quenched from 1800°C followed by equilibration at 1930°C (BAR = 10 μm)



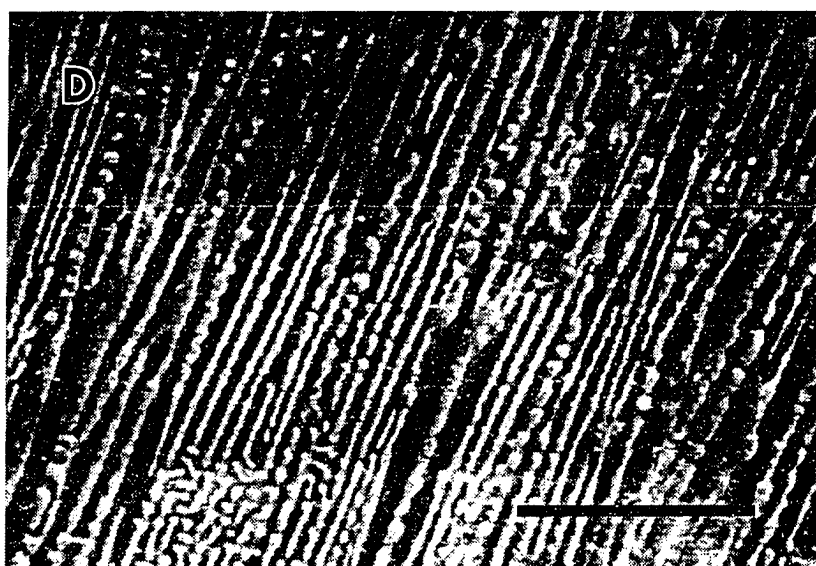
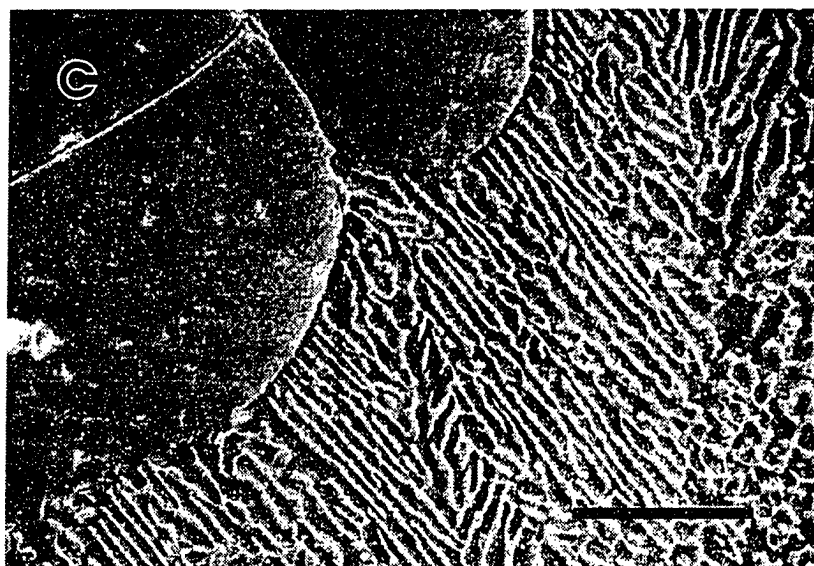


Figure 2. Continued

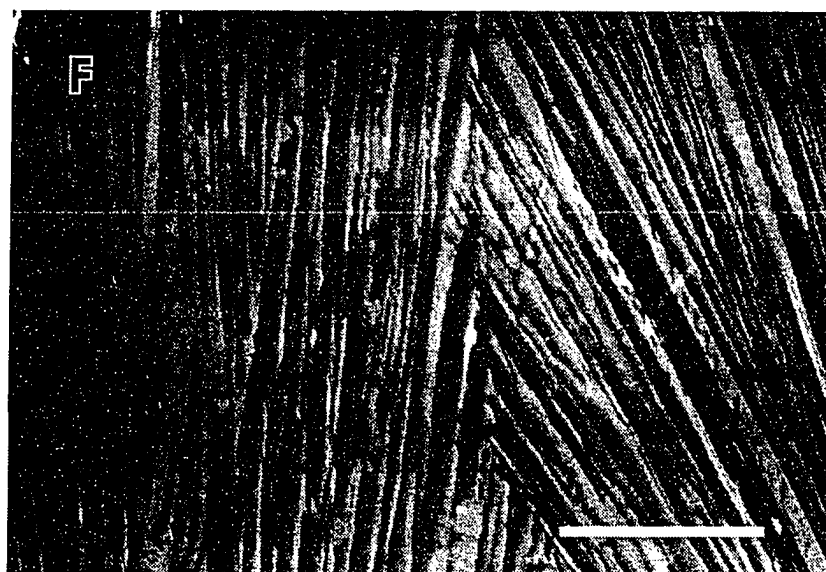
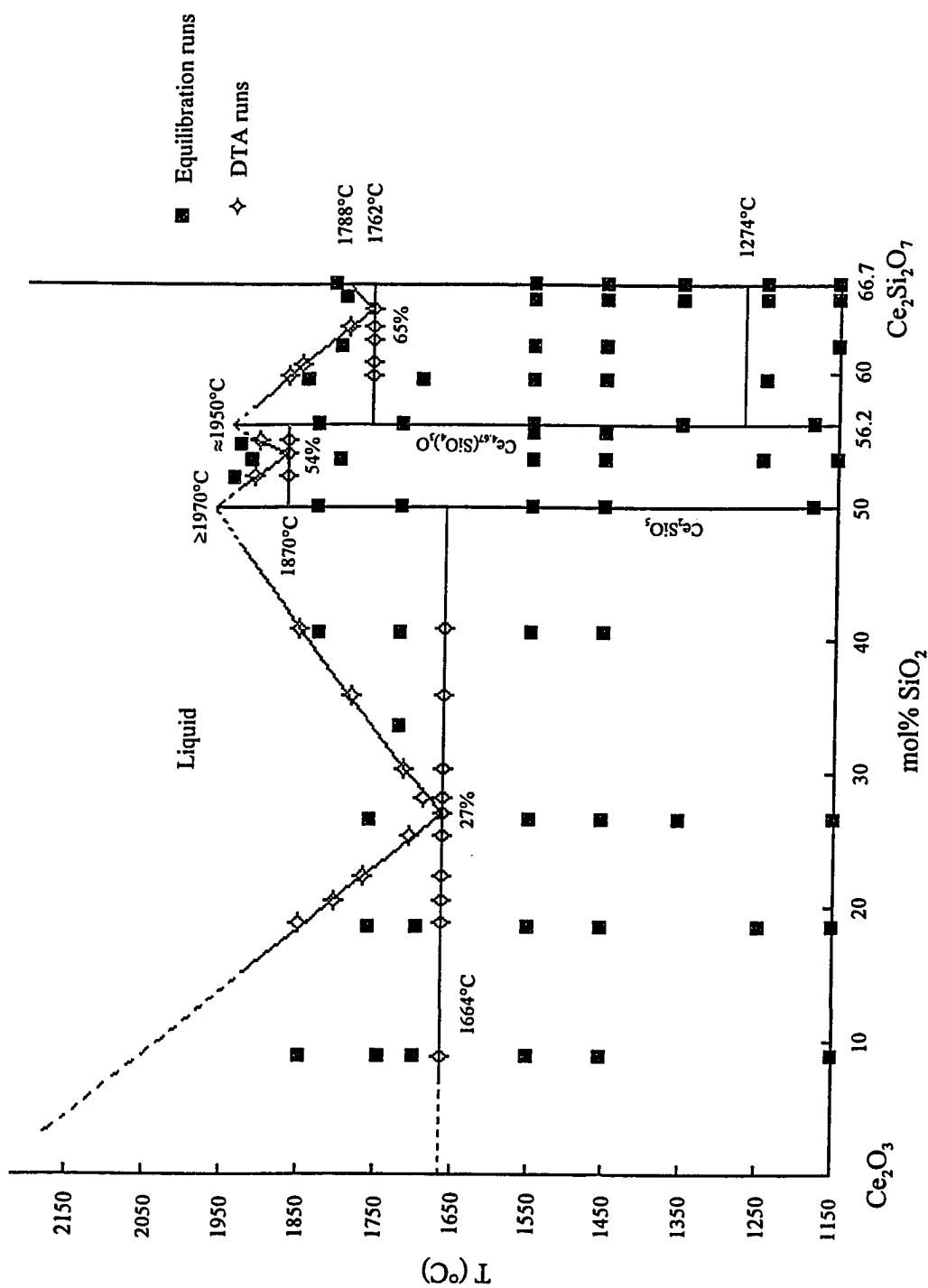


Figure 2. Continued

the eutectic temperature (see Figure 1). We were not able to detect a difference in the temperature of the beginning of the endothermic event in these two samples. Therefore, we assumed the eutectic composition to be at 27 ± 1 mol% SiO_2 . To observe the eutectic microstructure that would occur between Ce_2O_3 and Ce_2SiO_5 , we heated a SILI 27 sample to 1700°C , and held it at that temperature for 4 hours followed by cooling to 1600°C with $3^\circ\text{C}/\text{min}$. The sample was furnace quenched under vacuum to ambient from 1600°C . Figures 2d and 2e show the eutectic microstructure consisting of submicron sized lamellae with the bright fibrils of Ce_2O_3 . It should be noted that the microstructure was found to be free of cracks possibly due to the relatively slow cooling rate employed in this experiment. The information gathered from this portion of the system Ce_2O_3 - $\text{Ce}_2\text{Si}_2\text{O}_7$ has been plotted into the phase diagram suggested in Figure 3. We have put dashed lines for the portions of the liquidus which were extending above 1930°C in this diagram because the uncertainty in the temperature measurement exceeded 30°C above that temperature. The extension of the Ce_2O_3 liquidus of Figure 3 intersects the temperature axis at about 2260°C which could be assumed to be in reasonable agreement with the melting point of Ce_2O_3 reported by Sata and Yoshimura¹⁵ as $2210 \pm 10^\circ\text{C}$.

Figure 3. Binary phase diagram of Ce_2O_3 - $\text{Ce}_2\text{Si}_2\text{O}_7$ system



(3) Phase Relations between Ce_2SiO_5 and $Ce_{4.67}(SiO_4)_3O$

The compositions investigated to determine the phase relations between these two compounds have been labeled as SILI 50 through SILI 56.2 (corresponding to the composition of cerium oxygen apatite) in Table II. The heat treatment in an argon + 10% H_2 atmosphere in the temperature range 1150° to 1550°C for the times listed in Table II followed by ice-water quenching have produced solid state phase mixtures of Ce_2SiO_5 and $Ce_{4.67}(SiO_4)_3O$, excluding the samples of compositions SILI 50 and SILI 56.2. Partial decomposition of Ce_2SiO_5 to $Ce_{4.67}(SiO_4)_3O$, reported by Van Hal and Hintzen⁷, at 1200°C, could be resulting from "slow cooling" to room temperature after heating for two hours in a H_2 - N_2 atmosphere. The ice-water quenched samples of this study did not show such a partial decomposition. Two separate samples having the composition SILI 53, which lies at about midway between the two compounds, have also been equilibrated at 1790°C for 8 hours and at 1850°C for 4.5 hours in vacuum ($P_{O_2} \leq 6 \times 10^{-9}$ atm at all times during the heat treatments) followed by furnace quenching to room temperature. These two samples also did not form a liquid phase. In the XRD traces of the above samples, we were able to detect 52-53 separate reflections of $Ce_{4.67}(SiO_4)_3O$ in addition to more than 90 reflections of Ce_2SiO_5 in the 5-85° 2θ range conforming to the lattice parameters given in Table I for these compounds. The typical scan rates employed to obtain this level of resolution in XRD traces were about 0.15-0.20 ° 2θ /min. We did not see any signs of solid solution forming between these two compounds. The colours displayed by the quenched samples varied from pale mustard (Ce_2SiO_5 -rich

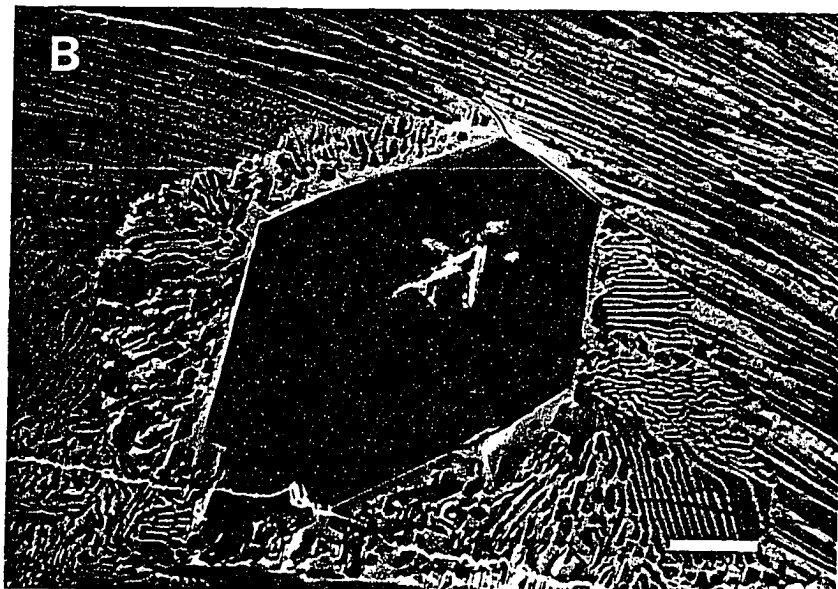
samples) to dark mustard ($\text{Ce}_{4.67}(\text{SiO}_4)_3\text{O}$ -rich samples) while the colours assuming darker tones with increasing temperatures.

The two DTA traces shown in Figure 1 for the samples of SILI 52 and 55, recorded under similar conditions described in the previous section, both showed at $1870 \pm 25^\circ\text{C}$ the beginning of a significant endothermic event. Two minor endothermic peaks observed at $1910 \pm 30^\circ\text{C}$ and $1926 \pm 30^\circ\text{C}$, respectively. In order to investigate the nature of these events, we heated four samples with the compositions SILI 53, 53.5, 54, and 54.5 to a possible liquid formation temperature, i.e., 1920 to 1930 $^\circ\text{C}$, under vacuum followed by cooling to 1800 $^\circ\text{C}$ with 3 $^\circ\text{C}/\text{min}$ and then furnace quenching to room temperature. The resultant phases were listed in Table II. Combining these results, we deduced that the first liquid forms at 1870 $^\circ\text{C}$ between Ce_2SiO_5 and $\text{Ce}_{4.67}(\text{SiO}_4)_3\text{O}$. The eutectic composition was found to be at 54 mol% SiO_2 . The Ce_2SiO_5 -liquidus passes through the points {1970 $^\circ\text{C}$, 50%}, {1910 $^\circ\text{C}$, 52%}, and {1870 $^\circ\text{C}$, 54%}. On the other hand, the liquidus of $\text{Ce}_{4.67}(\text{SiO}_4)_3\text{O}$ could be defined by the points {1870 $^\circ\text{C}$, 54%}, {1926 $^\circ\text{C}$, 55%}, and {1950 $^\circ\text{C}$, 56.2%}. The equilibrated sample of SILI 54 produced the eutectic microstructure shown in Figure 2f. The XRD trace of this sample had the reflections of both oxyorthosilicate and apatite phases. The microstructure of the sample of composition SILI 53.5 heated to 1920 $^\circ\text{C}$ contained relatively thick strands of Ce_2SiO_5 crossing the eutectic mixture of Ce_2SiO_5 and $\text{Ce}_{4.67}(\text{SiO}_4)_3\text{O}$ which is given in Figure 4a. The rather scarce but well defined hexagonal crystals of $\text{Ce}_{4.67}(\text{SiO}_4)_3\text{O}$ in a eutectic mixture were the major characteristics of the microstructure of the SILI 54.5 sample heated to 1920 $^\circ\text{C}$ which is depicted in Figure 4b. The black, glassy-looking samples of the above were

Figure 4. SEM micrographs of samples in the Ce_2O_3 - $\text{Ce}_2\text{Si}_2\text{O}_7$ system

- (A)** 53.5 mol% SiO_2 sample showing the strands of $\text{Ce}_2\text{Si}_2\text{O}_7$ over a eutectic matrix which was quenched from 1800°C after heating at 1920°C
- (B)** 54.5 mol% SiO_2 . Large hexagonal crystals of $\text{Ce}_{4.67}[\text{SiO}_4]_3\text{O}$ distributed in a eutectic matrix having the same thermal history with the sample of (A)
- (C)** 59 mol% SiO_2 . Hexagonal crystals of $\text{Ce}_{4.67}[\text{SiO}_4]_3\text{O}$ formed above the eutectic temperature. Quenched from 1730°C after being heated at 1840°C
- (D) & (E)** 65 mol% SiO_2 . Microstructure of the eutectic reaction occurring between the binary compounds $\text{Ce}_{4.67}[\text{SiO}_4]_3\text{O}$ and $\text{Ce}_2\text{Si}_2\text{O}_7$. Quenched from 1730°C after the equilibration heating at 1770°C
- (F)** 66 mol% SiO_2 . Long streaks of the high-temperature monoclinic form of $\text{Ce}_2\text{Si}_2\text{O}_7$ crossing the eutectic matrix. Quenched from 1730°C following the equilibration at 1770°C

BAR LENGTHS = 10 μm



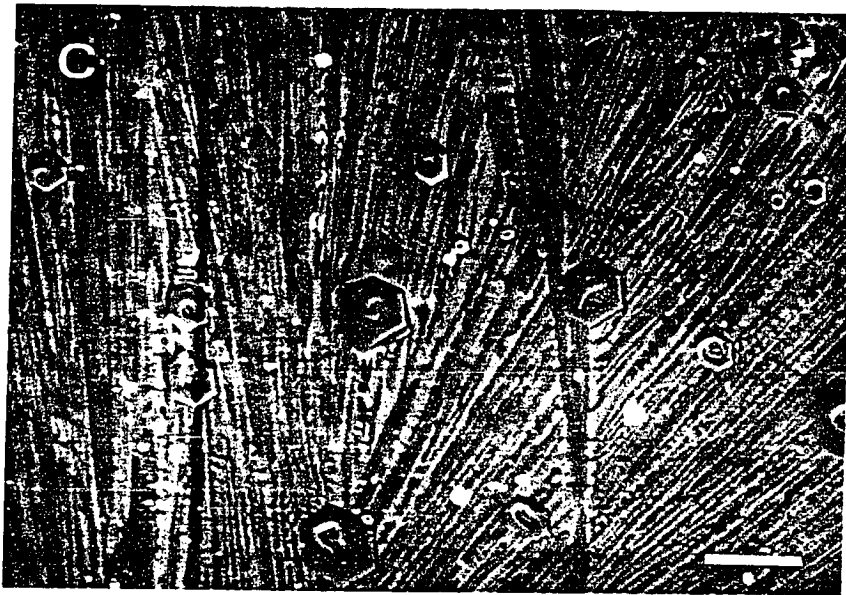


Figure 4. Continued

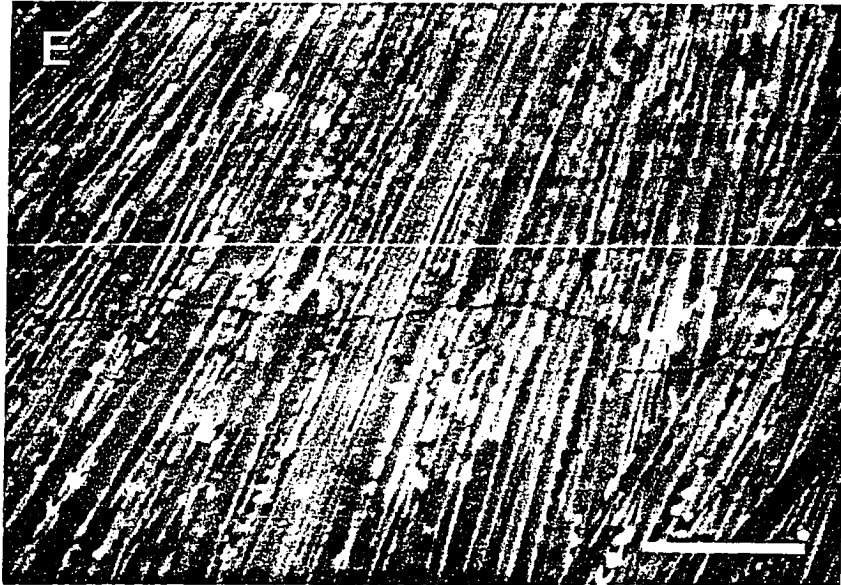


Figure 4. Continued

extremely brittle and our repeated attempts to polish them have all failed resulting in all-over-shattered samples. Hence, in order not to destroy the formed microstructures, micrographs were taken from the "as is" surfaces of these samples.

(4) Phase Relations between $Ce_{4.67}(SiO_4)_3O$ and $Ce_2Si_2O_7$

Some of the compositions studied in this portion of the system Ce_2O_3 - $Ce_2Si_2O_7$ have been tabulated in Table II denoted with SILI 56.2 through SILI 66.7 . It has been known^{7,14} that $Ce_2Si_2O_7$ exhibited a polymorphic transformation at 1274°C. The high-temperature form has been shown¹⁴ to have a monoclinic unit cell (see Table I) which has long been misrepresented^{7,11} with an orthorhombic crystal structure having a monoclinic space group. The low-temperature polymorph is known^{7,12,14} to have a tetragonal unit cell. The equilibration heatings of samples, in argon + 10% H_2 followed by quenching, in this composition range have all confirmed one more time the presence of these two polymorphs of $Ce_2Si_2O_7$. Although the monoclinic $Ce_2Si_2O_7$ was formed and identified easily in the samples heated to above 1300°C, the tetragonal low-temperature form required, for the completion of this sluggish transformation, slower cooling rates (typically in the order of 3 to 4°C/hour) to be employed from above 1300°C to below the transformation temperature of 1274° C. The samples of the equilibration heatings in the temperature range 1150° to 1550°C produced XRD patterns of two crystalline phase mixtures of either $Ce_{4.67}(SiO_4)_3O$ and M- $Ce_2Si_2O_7$

($T \geq 1350^\circ\text{C}$) or $\text{Ce}_{4.67}(\text{SiO}_4)_3\text{O}$ and $\text{T-Ce}_2\text{Si}_2\text{O}_7$ ($T \leq 1250^\circ\text{C}$). The colours of the equilibrated samples have varied from mustard to ivory with the increasing amounts of $\text{Ce}_2\text{Si}_2\text{O}_7$. The formed liquid phases between these two compounds were again black like the rest of the liquid phases of this system.

The sample DTA (obtained under similar conditions as described above) traces given in Figure 1 for the compositions 59, 62 and 65 mol% SiO_2 have all indicated to the presence of a major endothermic event at $1762 \pm 10^\circ\text{C}$ whereas the samples of 59 and 62 mol% showed two minor endothermic peaks at 1895° and 1806°C , respectively. Further DTA traces of samples of 60.5 and 63.5 mol% SiO_2 have shown small secondary endothermic peaks at 1850° and 1782°C , respectively, besides the primary event occurring at 1762°C again. The suggested $\text{Ce}_{4.67}(\text{SiO}_4)_3\text{O}$ - liquidus (Fig. 3) passes through the points $\{1950^\circ, 56.25\%\}$, $\{1895^\circ, 59\%\}$, $\{1850^\circ, 60.5\%\}$, $\{1806^\circ, 62\%\}$, $\{1782^\circ, 63.5\%\}$, and $\{1762^\circ, 65\%\}$. On the other hand, $\text{Ce}_2\text{Si}_2\text{O}_7$ - liquidus lie on the points $\{1788^\circ, 66.7\%\}$ and $\{1762^\circ, 65\%\}$. The eutectic reaction was found to occur between $\text{Ce}_{4.67}(\text{SiO}_4)_3\text{O}$ and $\text{Ce}_2\text{Si}_2\text{O}_7$ at 1762°C and 65 ± 0.5 mol% SiO_2 .

The microstructure of a SILI 59 sample heated to about 1840°C ($4^\circ\text{C}/\text{min}$) in vacuum, and then cooled to 1730°C after being held at the high temperature for 2 hours showed the hexagonal crystals of $\text{Ce}_{4.67}(\text{SiO}_4)_3\text{O}$ dispersed in a eutectic matrix which is depicted in Figure 4c. The micrographs of Figure 4d and 4e displays the characteristic eutectic microstructure between these two compounds which were taken from a sample of composition SILI 65 heated to 1770°C in vacuum and cooled to 1730°C (followed by furnace quenching) after a

soaking time of 2 hours. A sample of composition SILI 66 heated to 1770°C in vacuum and cooled to 1730°C after a soaking time of 4 hours displayed rather long and darker streaks of $\text{Ce}_2\text{Si}_2\text{O}_7$ over a eutectic matrix in its microstructure which is reproduced in Figure 4f. The XRD traces of this sample showed more than 50 reflections of $\text{Ce}_{4.67}(\text{SiO}_4)_3\text{O}$ and about 125 reflections of monoclinic $\text{Ce}_2\text{Si}_2\text{O}_7$ in the 5-85° 2Θ range collected with a scanning rate of 0.1° $2\Theta/\text{min}$.

(5) Enthalpy of Melting Calculations

Assuming ideal mixing in the liquid phase and complete immiscibility of Ce_2O_3 in solid Ce_2SiO_5 , the enthalpy of melting of Ce_2SiO_5 can be calculated from the experimentally determined liquidus line, using the freezing point depression of Ce_2SiO_5 by the addition of Ce_2O_3 , according to :

$$\log X_A = - \frac{\Delta H_{m,A}}{R} \left[\frac{(T_{m,A} - T_L)}{T_{m,A} \cdot T_L} \right] \quad (1),$$

where $A = \text{Ce}_2\text{SiO}_5$.

Therefore, a plot of $\log X_{\text{Ce}_2\text{SiO}_5}$ (liquidus) against the term $[(T_{m,\text{Ce}_2\text{SiO}_5} - T_{\text{liquidus}}) / T_{m,\text{Ce}_2\text{SiO}_5} \cdot T_{\text{liquidus}}]$ should be a straight line with a slope equal to $(-\Delta H_{m,\text{Ce}_2\text{SiO}_5}^{\circ} / 2.303R)$. The plot of this line is given in Figure 5 from which we calculated $\Delta H_{m,\text{Ce}_2\text{SiO}_5}^{\circ}$ to be 102.3 ± 6 kJ/mole. This translates to a value for $\Delta S_{m,\text{Ce}_2\text{SiO}_5}^{\circ}$ of 46.5 ± 2 J/mole-K at the melting point of 1970°C.

Repeating the calculations for $\text{Ce}_{4.67}(\text{SiO}_4)_3\text{O}$ liquidus (56.2 to 65 mol% SiO_2) and $\text{Ce}_2\text{Si}_2\text{O}_7$ liquidus, we estimated the $\Delta H_{\text{m,Ce}_{4.67}(\text{SiO}_4)_3\text{O}}^\circ$ to be 222.5 ± 13 kJ/mole and the $\Delta H_{\text{m,Ce}_2\text{Si}_2\text{O}_7}^\circ$ to be 39.0 ± 3 kJ/mole. The straight lines produced from equation (1) for the liquidi of these two phases were also plotted in Figure 5. The corresponding entropies for these two phases were found to be $\Delta S_{\text{m,Ce}_{4.67}(\text{SiO}_4)_3\text{O}}^\circ = 100.1 \pm 6$ J/mole-K at the melting point of 1950°C and $\Delta S_{\text{m,Ce}_2\text{Si}_2\text{O}_7}^\circ = 19.0 \pm 2$ J/mole-K at the melting point of 1788°C . Although no values were found in the literature for the enthalpy and entropy of melting of Ce_2SiO_5 and $\text{Ce}_{4.67}(\text{SiO}_4)_3\text{O}$ to compare with, the enthalpy of melting calculated in this system for $\text{Ce}_2\text{Si}_2\text{O}_7$, as 39 ± 3 kJ/mole agrees well with the enthalpy of melting reported¹⁴ (36.8 kJ/mole) for the same phase in a study of the phase diagram of Al_2O_3 - $\text{Ce}_2\text{Si}_2\text{O}_7$ system.

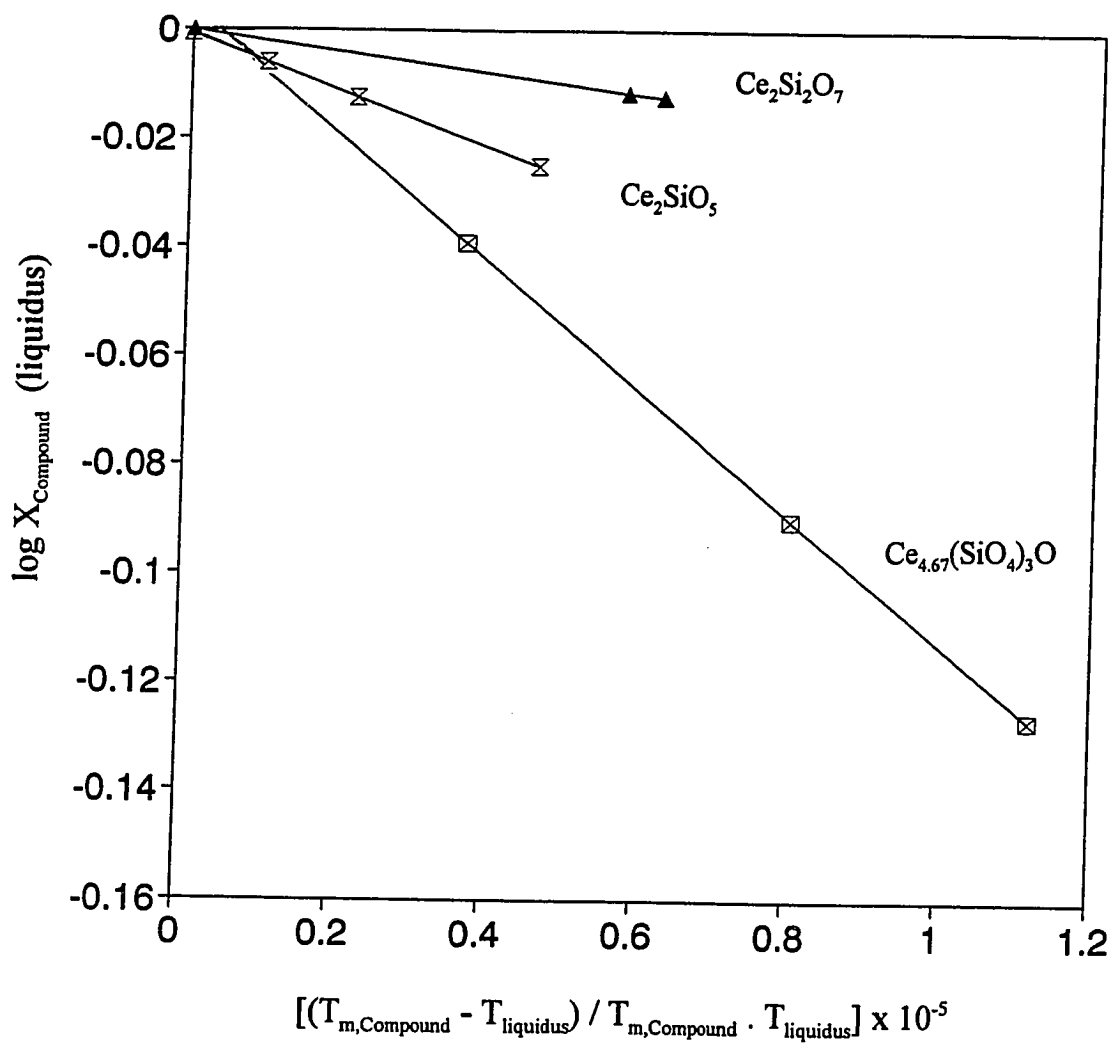


Figure 5. The heat of melting of the three binary compounds calculated from the initial slopes their liquidus lines. The slopes of the individual lines are equal to $[-\Delta H_{\text{m, compound}}^{\circ} / 2.303R]$

CONCLUSIONS

The high temperature phase relations have been investigated in the Ce_2O_3 - $\text{Ce}_2\text{Si}_2\text{O}_7$ section of Ce_2O_3 - SiO_2 binary between 1150° and 1970°C. Three eutectics have been identified for this system. The first eutectic reaction occurs at $1664 \pm 5^\circ\text{C}$ and 27 mol% SiO_2 between Ce_2O_3 and Ce_2SiO_5 . The binary compound Ce_2SiO_5 melts congruently at $1970 \pm 30^\circ\text{C}$. The second eutectic reaction of the Ce_2O_3 - $\text{Ce}_2\text{Si}_2\text{O}_7$ system occurs at $1870 \pm 25^\circ\text{C}$ and 54 mol% SiO_2 between Ce_2SiO_5 and $\text{Ce}_{4.67}(\text{SiO}_4)_3\text{O}$. The binary compound $\text{Ce}_{4.67}(\text{SiO}_4)_3\text{O}$ melts congruently at $1950 \pm 30^\circ\text{C}$. The third eutectic is found to be at $1762 \pm 10^\circ\text{C}$ and 65 mol% SiO_2 between $\text{Ce}_{4.67}(\text{SiO}_4)_3\text{O}$ and $\text{Ce}_2\text{Si}_2\text{O}_7$. $\text{Ce}_2\text{Si}_2\text{O}_7$ exhibits a polymorphic transformation at 1274°C between a tetragonal low-temperature form and a monoclinic high-temperature form before melting congruently at $1788 \pm 5^\circ\text{C}$. Microstructural characteristics of these eutectic reactions are documented. No solid solubility has been detected between the phases of this system. The enthalpies and entropies of melting of the three binary compounds are calculated from the initial slopes of the corresponding liquidus lines. Finally, a binary phase diagram is suggested, for the first time, for the Ce_2O_3 - $\text{Ce}_2\text{Si}_2\text{O}_7$ system which accounts for the three binary compounds Ce_2SiO_5 , $\text{Ce}_{4.67}(\text{SiO}_4)_3\text{O}$, and $\text{Ce}_2\text{Si}_2\text{O}_7$.

REFERENCES

- ¹ A.I. Leonov, "The Valence of Cerium in Synthetic and Natural Cerium Aluminates and Silicates, Part 2, Cerium Silicates," *Izv. Akad. Nauk SSSR, Ser. Khim.*, **12**, 2084-2089 (1963).
- ² A.I. Leonov and E.K. Koehler, "Les Oxydes de Cerium dans les Reactions en Phase Solide," *Rare Earth Elements, Book 1*, Proc. of Int. Conf. of the National Center of Scientific Research, France, 193-207 (1970).
- ³ J. Felsche, "The Crystal Chemistry of the Rare Earth Silicates," *Structure and Bonding*, **13**, 99-197 (1973).
- ⁴ K.B. Buang, "The Magnesium, Cerium and Zirconium Sialons," *Ph.D. Thesis*, University of Newcastle Upon Tyne, (1979).
- ⁵ I.A. Bondar, "Rare-Earth Silicates," *Ceramics International*, **8**, 83-89 (1982).
- ⁶ L. Kaufman, F. Hayes and D. Birnie, "Calculation of Quasibinary and Quasiternary Oxynitride Systems," *High Temperatures-High Pressures*, **14**, 619-631 (1982).

- ⁷ H.A.M. van Hal and H.T. Hintzen, "Compound Formation in the Ce_2O_3 - SiO_2 System," *Journal of Alloys and Compounds*, **179**, 77-85 (1992).
- ⁸ J. Felsche, "Rare Earth Silicates with the Apatite Structure," *Journal of Solid State Chemistry*, **5**, 266-275 (1972).
- ⁹ E.L. Belokoneva, T.L. Petrova, M.A. Simonov and N.V. Belov, "Crystal Structure of Synthetic TR Analogs of Apatite $\text{Dy}_{4.67}[\text{GeO}_4]_3\text{O}$ and $\text{Ce}_{4.67}[\text{SiO}_4]_3\text{O}$," *Soviet Physics-Crystallography*, **17**, 429-431 (1972).
- ¹⁰ A.C. Tas and M. Akinc, "Cerium Oxygen Apatite ($\text{Ce}_{4.67}[\text{SiO}_4]_3\text{O}$) X-Ray Diffraction Pattern Revisited," *Powder Diffraction*, **7**, 219-222 (1992).
- ¹¹ J. Felsche, "Polymorphism and Crystal Data of the Rare-Earth Disilicates of Type $\text{RE}_2\text{Si}_2\text{O}_7$," *J. of Less Comm. Metals*, **21**, 1-14 (1970).
- ¹² R. Heindl, N. Jonkierre and J.A. Loriers, "Preparation and Luminescence Properties of Tetragonal Cerium Disilicate $\text{Ce}_2\text{Si}_2\text{O}_7$ and Its Terbium-Activated Derivative," *Proc. of the 9th Rare Earth Research Conference*, VA, USA, **1**, 25-34, Oct.10-14, (1971).

- ¹³ N.A. Toropov, I.F. Andreev, A.N. Sokolov and L.N. Sanzharevskaya, "Solid Solutions in the System $\text{Y}_2\text{Si}_2\text{O}_7\text{-Ce}_2\text{Si}_2\text{O}_7$," *Izv. Akad. Nauk SSSR, Neorg. Mater.*, **6**, 519-523 (1970).
- ¹⁴ A.C. Tas and M. Akinc, "Phase Relations in the System $\text{Al}_2\text{O}_3\text{-Ce}_2\text{Si}_2\text{O}_7$ in the Temperature Range 900° to 1925°C in Inert Atmosphere," *J. Am. Ceram. Soc.*, (To be published).
- ¹⁵ T. Sata and M. Yoshimura, "Some Material Properties of Cerium Sesquioxide," *J. Ceram. Assoc. Japan*, **76**, 30-36 (1968).
- ¹⁶ D.E. Appleman and H.T. Evans, *U.S. Geological Survey, Computer Contribution No. 20*, U.S. National Technical Information Service, Document **PB-216188**, (1973).
- ¹⁷ F. McCarthy, *JCPDS PDF No. 23-1048* (Ce_2O_3) (1971).

PAPER IV: PHASE RELATIONS AND STRUCTURES IN THE SYSTEM Ce_2O_3 - Al_2O_3 IN INERT AND REDUCING ATMOSPHERES

Phase Relations and Structures in the System Ce_2O_3 - Al_2O_3 in Inert and Reducing Atmospheres

Submitted by

A. Cunezt Tas and Mufit Akinc

Department of Materials Science and Engineering

Iowa State University

Ames, Iowa 50011

This manuscript has been submitted for publication to the Journal of the American Ceramic Society.

ABSTRACT

The 1:1 compound, CeAlO_3 , in the system Ce_2O_3 - Al_2O_3 has been synthesized from the oxides and shown to have a perovskite-like tetragonal unit cell with the lattice parameters $a = 3.763$ and $c = 3.792 \text{ \AA}$. A new XRD pattern is suggested for CeAlO_3 . This compound is shown to be stable upto 1950°C . The 1:11 compound, $\text{CeAl}_{11}\text{O}_{18}$, has also been synthesized and shown to possess a magnetoplumbite-like hexagonal unit cell with the lattice parameters $a = 5.558$ and $c = 22.012 \text{ \AA}$. An XRD pattern is suggested for $\text{CeAl}_{11}\text{O}_{18}$ for the first time. The evolution of eutectic-like microstructures were observed and reported in the Ce_2O_3 -rich side of this binary system.

INTRODUCTION

One of the two previously reported compounds of the Ce_2O_3 - Al_2O_3 system, cerium monoaluminate (CeAlO_3), was first synthesized from the oxides by Zachariasen¹ at 1600° C in a helium atmosphere. The crystal structure of the compound was reported to be perovskite-like, tetragonal pseudo-cubic with $a = 3.760 \pm 0.004 \text{ \AA}$ and $c = 3.787 \pm 0.004 \text{ \AA}$. Keith and Roy² later confirmed the presence of this compound at 1:1 molar ratio in this system. They used $\text{Ce}_2(\text{C}_2\text{O}_4)_3 \cdot 9\text{H}_2\text{O}$ and Al_2O_3 as the starting materials, and observed the splitting in the (111) reflection which would indicate to a hexagonal (rhombohedral) symmetry, in contrary to Zachariasen¹. Roth³ observed the formation of CeAlO_3 at 1600°C in about 1 hour in helium in the perovskite structure but this time with a rhombohedral symmetry ($a = 3.766 \text{ \AA}$, $\alpha = 90.2^\circ$). Leonov⁴ reported the formation of bright green-coloured, cubic ($a = 3.77 \text{ \AA}$) CeAlO_3 in inert or slightly reducing atmospheres at elevated temperatures having prepared the compound from 99.85 % CeO_2 and hydrated aluminum oxide. It was also noted that CeAlO_3 would completely decompose to CeO_2 and Al_2O_3 in air at 800° C in 1 hour. The binary phase diagram given by Leonov et al.⁵ for the Ce_2O_3 - Al_2O_3 system showed two polymorphic transformations. The first one noted to occur at 90°C (of unidentified nature) and the second one was reported to be a rhombic - to - cubic transition which took place at $980 \pm 20 \text{ }^\circ\text{C}$. Kim⁶ indexed this compound, synthesized from $\text{Ce}(\text{C}_2\text{O}_4)_3 \cdot x\text{H}_2\text{O}$ and alumina in vacuum at 1600° C, on the basis of a hexagonal cell of rhombohedral symmetry (JCPDS PDF 21-0175) with the lattice constants of $a = 5.35 \text{ \AA}$ and $c = 13.02 \text{ \AA}$. He reported the x-ray

density as 6.62 gm/cm^3 . Geller and Raccach⁷ estimated the rhombohedral-to-cubic transition for CeAlO_3 , if there is any, to occur at about 960°C by extrapolating the data they obtained for the transition temperatures of the La (522°C), Pr (1370°C), and Nd (1747°C) aluminates. Scott⁸ predicted, by Raman spectroscopy, the same temperatures as 1047°C and 1367°C for Pr and Nd aluminates, respectively. Mizuno et al.⁹ reported the cerium monoaluminate to be cubic at $T \geq 150^\circ\text{C}$ in inert atmosphere (JCPDS PDF 28-0260) with a lattice constant of 3.767 \AA . They also claimed that the rhombohedral polymorph could be synthesized at temperatures less than 100°C . More recently, Steinberg et al.¹⁰ prepared CeAlO_3 in a flowing hydrogen atmosphere at 1000°C . The structure of the slowly cooled product was found to be pseudo-cubic, tetragonal with the lattice parameters $a = 3.760 \pm 0.004 \text{ \AA}$ and $c = 3.787 \pm 0.004 \text{ \AA}$. The XRD pattern of the tetragonal structure, to our knowledge, has never been published and has not been included in the JCPDS files.

The second compound, cerium hexaaluminate ($\text{Ce}_2\text{O}_3 \cdot 11\text{Al}_2\text{O}_3$), has been included in the first phase diagram for this system suggested by Leonov et al.⁵ and it has been reported to melt incongruently in a reducing atmosphere at about 1950°C whereas being stable down to room temperature upon cooling. In the more recent phase diagram suggested by Mizuno et al.⁹ for this system, the hexaaluminate was drawn in with a dashed line owing to the difficulty in preparing it as a single phase compound which was shown to melt incongruently at 1890°C in a reducing atmosphere. It was reported to have a hexagonal structure with the lattice constants $a = 5.543 \text{ \AA}$ and $c = 21.979 \text{ \AA}$ and that the sample contained CeAlO_3 and $\alpha\text{-Al}_2\text{O}_3$ as minor phases. This compound has been labeled as $\text{Ce-}\beta\text{-Al}_2\text{O}_3$ in this phase

diagram mainly due to the compositional similarity with Na- β' -Al₂O₃ (Na₂O.11Al₂O₃). The synthesis and characterisation of cerium hexaaluminate, in its pure form, has been attempted, to our knowledge, only in the above two studies in literature. In both of these, this compound was assumed to have a β -alumina structure. A similar type of compound (LaAl₁₁O₁₈) was reported^{11,12} to be present in the La₂O₃-Al₂O₃ system. It has been realised¹³⁻¹⁸ that the addition of one divalent cation, such as Mg²⁺, Mn²⁺, Co²⁺, Ni²⁺ etc., to the above formula unit would produce a series of new compounds, LaMAl₁₁O₁₉, with structures quite similar to that of the magnetoplumbite (PbFe₁₂O₁₉) phase encountered in PbO-Fe₂O₃ system. It so appeared that the divalent M ions selected to be used as dopants should be chosen among the MO oxides that were able to form spinel type (MAl₂O₄) phases with α -alumina¹⁸. According to this scheme¹⁵, Al³⁺ substitutes Fe³⁺, La³⁺ (or Ce³⁺) substitutes Pb²⁺, and the divalent cation takes the place of one Fe³⁺ to conserve the electrical neutrality and the extra oxygen required would be brought in by the divalent element. The magnetoplumbite and Na- β' -alumina structures were both comprised of spinel blocks formed by the close-packing of Al and O atoms. The only significant difference between the two could be found in the two mirror planes ($z = 0.25$ and 0.75) present in their roughly similar unit cells. Each mirror plane in the β -alumina structure contains one large cation (Na⁺) and one oxygen^{19,20}. Figure 1 displays half of the unit cells of the two structures drawn according to the atomic coordinates reported by Gasperin et al.¹⁷ for LaMnAl₁₁O₁₉ and those reported by Felsche²⁰ for NaAl₁₁O₁₇. The non-close-packed mirror planes join together the stable spinel blocks. Moreover, the sites of the large cation and one oxygen in these planes are not fully occupied which leads to a

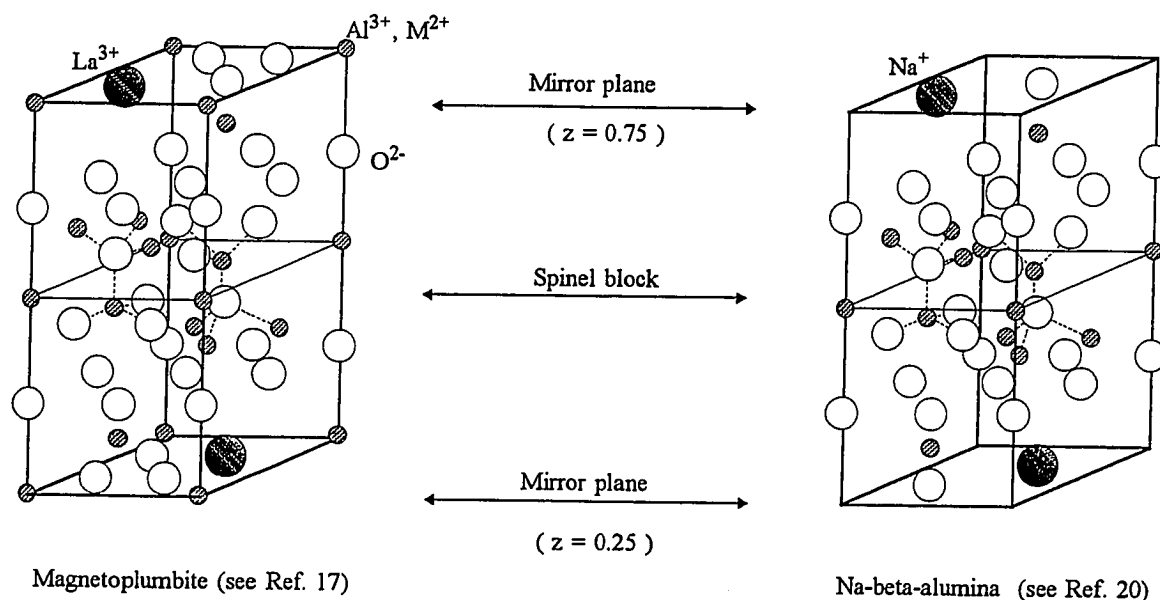


Figure 1. Half unit cells of magnetoplumbite and sodium beta-alumina structures

disorder in the mirror planes caused by a possible indeterminacy in the position of the large ion. On the other hand, the mirror planes of the magnetoplumbite structure contain one large cation (La^{3+} or Ce^{3+}), and three oxygens lying within the plane and finally four aluminums located at the cell edges intersected by the mirror planes¹⁸. The mirror planes of the magnetoplumbite-like structure were found¹⁷, for $\text{LaMAI}_{11}\text{O}_{19}$ -type compounds, to be disordered; the single, fully occupied, ideal site $(2/3, 1/3, 1/4)$ for the large cation splitted into two partially occupied, close sites in the plane. This gave the large cation of such

structures a rather large volume in which it could move in a diffuse manner. The packing of the spinel blocks are virtually the same in both structures. The added divalent ions (M^{2+}), for $LaMAl_{11}O_{19}$ -type compounds, were commonly found to localize themselves among the tetrahedrally coordinated Al sites within the spinel blocks¹⁷ of the structure rather than achieving a statistical distribution over all the available Al sites. Hence, prior to this study, the previous literature has shown that the lanthanide-hexaaluminates, excluding that of cerium, exhibited structures similar to that of magnetoplumbite rather than that of Na- β' -alumina. Moreover, there have been no attempts to suggest an XRD pattern for the pure compound $Ce_2O_3 \cdot 11Al_2O_3$, although the JCPDS files did contain an entry for the divalent cation-doped version, $CeMgAl_{11}O_{19}$, of the magnetoplumbite-type (JCPDS PDF 26-0872)²¹.

The present study focuses on the structural characterisation of $CeAlO_3$ and $CeAl_{11}O_{18}$ with powder x-ray diffraction and the high temperature phase equilibria in Ce_2O_3 - Al_2O_3 system in reducing ($Ar + 10\%H_2$), inert (Ar) and vacuum atmospheres.

EXPERIMENTAL PROCEDURE

Compositions in the Ce_2O_3 - Al_2O_3 system were prepared by mixing the appropriate amounts of the starting oxides, CeO_2 (99.87%, 0.7 μm , Cerac, Inc.) and Al_2O_3 (99.96%, 0.5 μm , Reynolds, Inc.) in ethanol in glass jars for about an hour followed by 15 minutes of ultrasonification. The contents of the jars were dried overnight at 70°C in air. The recovered cakes were then calcined in air at 950°C for 12 hours mainly to remove the carbonaceous residues, if there were any. The calcined mixtures were then lightly ground in an agate mortar for about 30 minutes. The details of the green pellet preparation, equilibration heatings (in reducing, inert and vacuum atmospheres), quench practices and DTA analyses employed were reported elsewhere²².

The phase analysis of every equilibrated, quenched, and ground to a mean particle size of 7 μm sample was performed by XRD in the 5-160° 2 θ range using a Cu-tube powder diffractometer[†] operated at 45kV and 30 mA with a maximum scanning rate of 0.7° 2 θ /min. Least squares cell refinement, indexing, and lattice constant determinations were performed by Appleman and Evans²³ and Treor²⁴ routines. Elemental silicon (NBS 640a) was used as an external standard.

[†] XDS 2000, Scintag, Inc., USA.

Microstructural analyses were carried out by SEM [♦] on polished or as is surfaces of the fired pellets. The chemical compositions of the microstructural features observed in SEM images of the polished samples were examined with EDXS [†] using single phase CeAlO₃ as standard and the information thus obtained were believed to be accurate to within ± 3 atomic percent.

[♦] JSM-6100, JEOL, MA, USA [†] Model Delta-5, Kevex, Inc., CA, USA.

RESULTS AND DISCUSSION

Compositions of $\text{Ce}_2\text{O}_3 : \text{Al}_2\text{O}_3$ stoichiometry were heated either in flowing purified argon ($\text{O} + \text{H}_2\text{O} \leq 50$ ppm), argon + 10% H_2 or vacuum ($P_{\text{O}_2} \leq 6 \times 10^{-9}$ atm) at the maximum temperatures ranging from 1450° to 1950°C for periods of 50 to 1 hour, respectively. The equilibration heat treatments carried out in this study are tabulated in Table I. All of the thermal treatments of samples of this stoichiometry constantly produced a single phase (without any free Ce_2O_3 and $\alpha\text{-Al}_2\text{O}_3$ remaining) substance with a typical XRD pattern given in Table II (American Ceramic Society Data Depository Service). The pattern shown in this table was obtained from a sample heated at 1550°C for 50 hours followed by slow cooling (15°C/hour) to room temperature (21-23°C) in the furnace under a flow of argon + 10% H_2 gas. The structure has been determined to be tetragonal with lattice constants $a = 3.763$ Å and $c = 3.792$ Å. We, therefore, do not agree with either of the previously published JCPDS file cards (21-0175, Hexagonal and 28-0260, Cubic) for CeAlO_3 . However, our lattice constants agree well with those published by Zachariasen¹ (1949) and by Steinberg et al.¹⁰ (1985). The splitting of the peaks and the proper observation of those were thought to be the most important factors in the correct resolution of such a structure. Figure 2 shows a portion of the peak analysis performed for the data of the above XRD pattern. In order this structure to be regarded as cubic, the splitting of the peaks displayed in Figures 2a, 2b, 2d, 2e, and 2f should certainly be absent. Similarly, the peak splitting observed in Figures 2a and 2d, and the 004 : 400 splitting shown in the pattern given in Table II should be absent to index this structure on

Table I. Results of Equilibration Runs in the System Ce_2O_3 - Al_2O_3

Composition	Temp.(°C)	Time (h)	Atmosphere	Cooling	Phases Observed
CeAlO_3	1450	50	A	Q	Tetr. CeAlO_3
CeAlO_3	1550	40	A	Q	Tetr. CeAlO_3
CeAlO_3	1450	50	A+10H	Q	Tetr. CeAlO_3
CeAlO_3	1550	40	A+10H	Q	Tetr. CeAlO_3
CeAlO_3	1650	20	V	F.Q	Tetr. CeAlO_3
CeAlO_3	1750	10	V	F.Q	Tetr. CeAlO_3
CeAlO_3	1850	3	V	F.Q	Tetr. CeAlO_3
CeAlO_3	1950	1	V	F.Q	Tetr. CeAlO_3
CeAlO_3	1550	50	A+10H	FC15	Tetr. CeAlO_3
CeAlO_3	1550	50	A	FC15	Tetr. CeAlO_3
CeAlO_3	1650	25	V	FC15	Tetr. CeAlO_3
$\text{Ce}_2\text{O}_3 \cdot 11\text{Al}_2\text{O}_3$	1550	30	A	Q	$\text{Ce}_2\text{O}_3 \cdot 11\text{Al}_2\text{O}_3 + \text{Al}_2\text{O}_3 + \text{CeAlO}_3$
$\text{Ce}_2\text{O}_3 \cdot 11\text{Al}_2\text{O}_3$	1550	30	A+10H	Q	"
$\text{Ce}_2\text{O}_3 \cdot 11\text{Al}_2\text{O}_3$	1775	12	V	F.Q	"
$\text{Ce}_2\text{O}_3 \cdot 11\text{Al}_2\text{O}_3$	1880	2	V	F.Q	$\text{Ce}_2\text{O}_3 \cdot 11\text{Al}_2\text{O}_3 + \text{Al}_2\text{O}_3$
$\text{Ce}_2\text{O}_3 \cdot 11\text{Al}_2\text{O}_3$	1880	2	V	FC10	"
$\text{Ce}_2\text{O}_3 \cdot 11\text{Al}_2\text{O}_3$	1915	0.1	V	F.Q	Liquid + Al_2O_3
$\text{Ce}_2\text{O}_3 \cdot 11\text{Al}_2\text{O}_3$	1915	0.1	V	FC10	$\text{Ce}_2\text{O}_3 \cdot 11\text{Al}_2\text{O}_3 + \text{trace Al}_2\text{O}_3$
12 mol% Ce_2O_3 - 88 mol% Al_2O_3	1700	12	V	F.Q	$\text{Ce}_2\text{O}_3 \cdot 11\text{Al}_2\text{O}_3 + \text{CeAlO}_3$

Table I. (cont.)

Composition	Temp.	Time	Atmosphere	Cooling	Phases observed
12 Ce ₂ O ₃ - 88 Al ₂ O ₃	1820	8	V	F.Q	Liquid + Ce ₂ O ₃ .11Al ₂ O ₃
74 Ce ₂ O ₃ - 26 Al ₂ O ₃	1875	4	V	F.Q	CeAlO ₃ + Ce ₂ O ₃ + CeO _{2-x}
79 Ce ₂ O ₃ - 21 Al ₂ O ₃	1940	3	V	F.Q	"
83 Ce ₂ O ₃ - 17 Al ₂ O ₃	1940	3	V	F.Q	"

A = Argon, A+10H = Argon + 10% H₂, V = Vacuum, Q = Water quench, F.Q = Furnace quench, FC10 = 10°C/m to RT, FC15 = 15°C/h to RT

the basis of a hexagonal cell with rhombohedral symmetry. The rhombohedral symmetry also requires the tetragonal 111 reflection, as we observed in Figure 2c, to split into 202 and 006 reflections of the hexagonal (rhombohedral) system.

Our repeated attempts to observe the polymorphic transformation that was previously reported ^{7,9} to occur at 960°C or 100°C with differential thermal analysis have all failed. The DTA traces (4°C/min) all registered the undisturbed background from room temperature to 1950° C. Nevertheless, the enthalpy of such a transformation, if there really was one, might be too low to detect by DTA. We found that slow cooling (15°C/h) a CeAlO₃ sample following the equilibration at 1550°C (Ar+10% H₂) or 1650°C (Vacuum) to 500° C (holding there for

Table II . X-ray Diffraction Pattern of Tetragonal CeAlO₃

hkl	d_{calc}	d_{obs}	I/I₀
001	3.7919	3.790	30
100	3.7629	3.762	58
101	2.6710	2.6706	100
110	2.6608	2.6610	55
111	2.1781	2.1781	54
002	1.8959	1.8957	17
200	1.8815	1.8816	41
102	1.6932	1.6931	10
201	1.6854	1.6847	16
112	1.5441	1.5444	18
211	1.5382	1.5383	36
202	1.3355	1.3357	12
220	1.3304	1.3303	8
212	1.2586	1.2587	6
221	1.2554	1.2553	6
103	1.1982	1.1984	7
301	1.1909	1.1908	11
113	1.1417	1.1418	3
311	1.1354	1.1354	8
222	1.0890	1.0891	5

Table II. (continued)

hkl	d _{calc}	d _{obs}	I/I ₀
203	1.0492	1.0492	1
302	1.0461	1.0461	2
320	1.0437	1.0437	2
213	1.0107	1.0107	5
312	1.0079	1.0079	7
321	1.0062	1.0063	7
004	0.9480	0.9479	1
400	0.9407	0.9408	2
104	0.9193	0.9192	1
223	0.9164	0.9164	2
322	0.9143	0.9143	3
401	0.9130	0.9130	3

Tetragonal, $a = 3.7630(1) \text{ \AA}$, $c = 3.7919(2) \text{ \AA}$, $V = 53.694(3) \text{ \AA}^3$

Space group = $P4^*$, $Z = 1$, $D_x = 6.651 \text{ gm/cm}^3$, $D_{\text{meas}} = 6.55 \text{ gm/cm}^3$

X-ray Powder Diffractometer, $\text{CuK}\alpha$, External silicon standard (NBS640a)

Scan rate : $0.6^\circ 2\theta / \text{min}$, SS/FOM : $F(32) = 133 (0.0067, 36)$

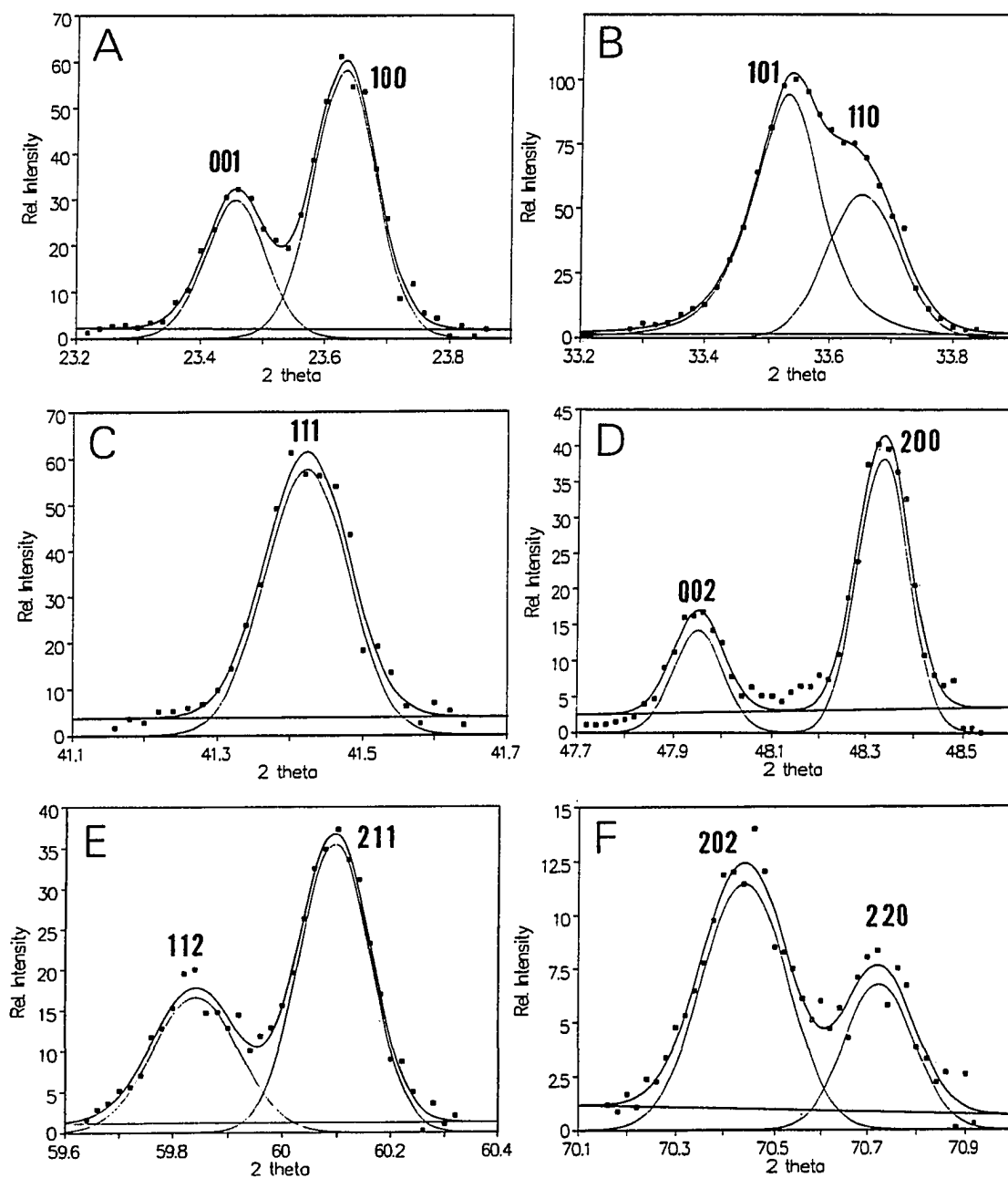


Figure 2. Splitting of the XRD peaks in tetragonal CeAlO_3 ($a = 3.763 \text{ \AA}$, $c = 3.792 \text{ \AA}$)

24 hours) and then to room temperature (21-23°C) followed by 1 to 2 hour holding in the furnace did also not produce any changes at all in the suggested XRD pattern which would be indicative of a polymorphic transformation. One question that still remains is the possibility of the presence of an extremely sluggish transition that might occur below 100°C. On the other hand, it needs to be noted that the purity of the starting materials might play a much more important role, in high temperature phase equilibria and structural chemistry, than it was once thought. For instance, it may well not be a coincidence for the two different group of researchers (Keith & Roy-1954, and Kim-1968) to use the same starting material, i.e., cerous oxalate; $\text{Ce}(\text{C}_2\text{O}_4)_3 \cdot n\text{H}_2\text{O}$, in the preparation of CeAlO_3 and to produce the rhombohedral "polymorph". Is the presence of carbon in the structure causing this rhombic symmetry? It might still be a possibility, which needs to be investigated, that the carbon would not "burn out" until the temperature reaches 960 - 980°C. As an other possibility, to our knowledge, LaAlO_3 does not have a reported "cubic" polymorph. In our laboratory we also were not able to produce a tetragonal or cubic form of LaAlO_3 . Our quenched samples (from above 1550°C) of LaAlO_3 always showed the (202 : 2.190 Å) - (006 : 2.184 Å) splitting which was a prerequisite for the rhombohedral symmetry to set in and be identified. Therefore, considering the fact that the significant presence of La_2O_3 as an impurity in cerium oxides was not so uncommon one or two decades ago, the rhombohedral LaAlO_3 which might form at very small quantities might have acted as a seed which would then impose the CeAlO_3 structure to acquire the rhombic symmetry of LaAlO_3 .

Small portions of equilibrated, single phase CeAlO_3 samples were heated in Pt envelopes in a flowing air atmosphere at 250°C (5 days) and 1000°C (12 hours) to test the stability of the compound. The XRD analysis showed that CeAlO_3 was still perfectly intact at 250°C , however, in the 1000°C sample, only traces of CeAlO_3 could be detected among the major phases of CeO_2 and $\alpha\text{-Al}_2\text{O}_3$. The same tetragonal XRD pattern, as that given in Table II, observed in the sample heated in air at 250°C for 5 days has excluded, once again, for us the possibility of identifying the previously reported ⁶, low-temperature rhombohedral "polymorph".

If one considers the perovskite-like lattice of CeAlO_3 as composed of Al^{3+} ions being at the octahedral interstices (cell corners, $\text{CN}=6$), O^{2-} ions at the edge centers, and finally the large Ce^{3+} being at the body center ($\text{CN}=12$), then it would be noticed that the (111) planes of this structure will be the highest atomic density regions allowing the close-packing of ceriums and oxygens. The close-packed (111) faces of such a cell would then be expected to display the hexagonal symmetry characterised by the presence of trigonal axes while being the most thermodynamically stable faces especially during anomalous grain growth. As it was very recently discussed by Drofenik ²⁵ for the BaTiO_3 perovskite, predominant (111) faces displaying the trigonal axes might be the surface habit during the grain growth stage of densification process. We have observed such microstructures in studying CeAlO_3 . Figure 3a shows the SEM micrograph of the fracture surface of a CeAlO_3 pellet equilibrated in argon at 1550°C for 35 hours followed by water quenching. The extensive grain growth and well developed (111) faces are clearly visible especially in the upper right hand corner of this

Figure 3. SEM micrographs of CeAlO_3 samples

- (A) 1550°C, Argon, 35 hours, quenched (BAR = 1 μm)
- (B) 1650°C, Vacuum, 15 hours, fce. quenched (BAR = 1 μm)
- (C) 1950°C, Vacuum, 1 hour, fce. quenched (BAR = 10 μm)



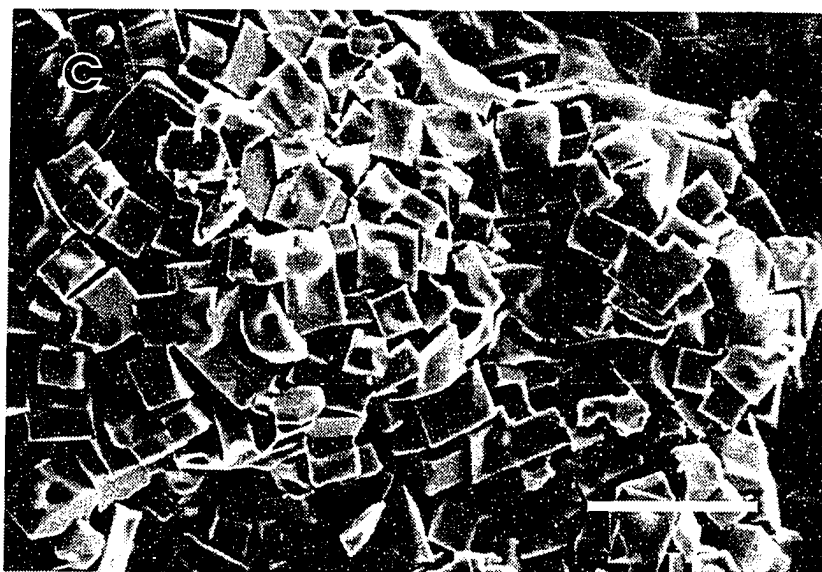


Figure 3. Continued

micrograph. This sample produced the typical "tetragonal" XRD pattern of Table II. The micrograph of Figure 3b was taken from the fracture surface of a CeAlO_3 sample equilibrated at 1650°C for 15 hours in vacuum followed by furnace quenching (by shutting off of the main power; 600°C/min cooling from 1650° to 1000°C) to room temperature. A (111) face is visible at the center which is surrounded by microfacets and steps. The sample still produces the characteristic tetragonal XRD pattern indicating one more time that the real symmetry of a crystal does not necessarily depend upon the symmetrical shape and size of its apparent faces. Figure 3c shows the as is surface of a CeAlO_3 pellet heated at 1950°C for 1 hour in vacuum followed by furnace quenching to room temperature. In this sample, it was almost impossible to find a region of the fracture surface which shows the (111) faces. Apparently,

recrystallisation has occurred and the whole surface has been covered with cuboids and tetragons. The XRD pattern of this sample still conforms to that given in Table II.

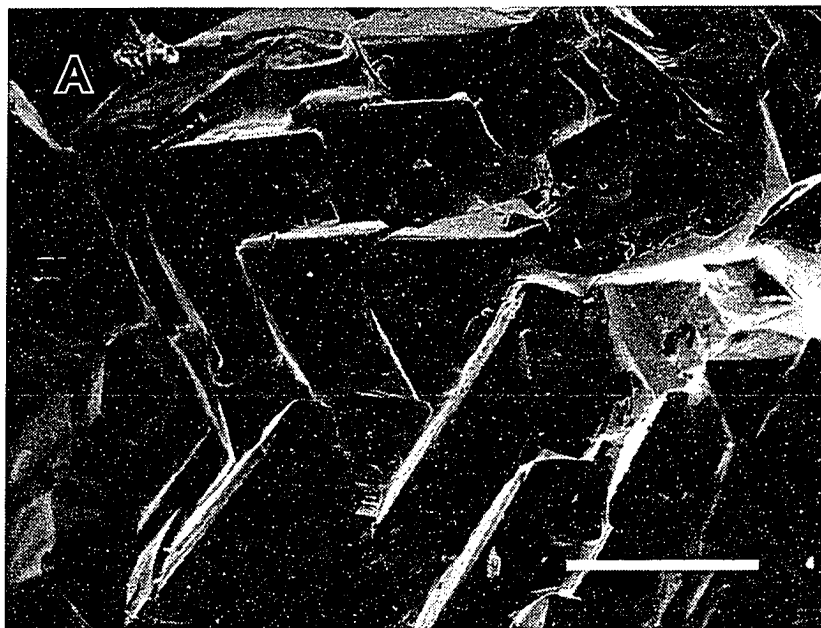
We synthesized the binary compound $\text{Ce}_2\text{O}_3 \cdot 11\text{Al}_2\text{O}_3$ from the starting oxides CeO_2 and Al_2O_3 by heating the samples either in argon, argon + 10% H_2 or in vacuum at temperatures above 1550°C . The resultant product was never pure, it always contained some $\alpha\text{-Al}_2\text{O}_3$ as a minor phase whose quantity decreased significantly with increasing temperature upto 1880°C . At lower temperatures, such as 1550°C , the samples also contained small amounts of tetragonal CeAlO_3 . Cerium hexaaluminate was found to be an incongruently melting compound as was predicted by Mizuno et al.⁹. To determine the first liquid formation temperature, a small piece of a pre-equilibrated cerium hexaaluminate sample, with several sharp edges, was suspended by a molybdenum wire in the vacuum furnace which was visible through a viewing port. An IR-pyrometer, calibrated just prior to this run against the melting point of Pt, was focused on the sample. The sample was heated with a heating rate of $3^\circ\text{C}/\text{min}$. The melting behaviour of the chunk was continuously monitored through the pyrometer, and at $1915 \pm 25^\circ\text{C}$ the sharp edges of the sample began to round up. The chunk, at this point, began to flow and then fell as a drop onto a molybdenum foil placed just below the wire. Following a 5 minutes of hold at this state, the sample was furnace quenched to room temperature. We assumed this temperature (i.e., the peritectic temperature) as the incongruent melting temperature of this compound. This reading agrees well with the temperature reported for the same event by Mizuno et al.⁹. The final sample of this experiment showed, in its XRD analysis, $\alpha\text{-Al}_2\text{O}_3$ as the only crystalline phase present.

Figures 4a and 4b depict the surface morphology of this sample showing darker trigonal alumina crystals surrounded by lighter, cerium-containing once-liquid phase. Repeating the same experiment, but this time using a slow cooling from 1915°C to room temperature, yielded the most pure hexaaluminate sample we obtained in this study. Traces of α - Al_2O_3 still found in that sample would be indicative of incomplete resorption.

We suggest an XRD pattern for cerium hexaaluminate, $\text{CeAl}_{11}\text{O}_{18}$, in Table III (American Ceramic Society Data Depository Service). This pattern is obtained from a sample first heated at 1550°C for 30 hours, water quenched, ground, repelletised, and then heated at 1550°C for another 30 hours in a flowing argon + 10% H_2 atmosphere, followed by quenching. The sample still contained some α - Al_2O_3 that could easily be detected from the pattern and very small amounts of CeAlO_3 , which could only be detected in the pattern only after a Rietveld analysis. The peaks of these minor phases are excluded from the pattern given in the above table. Figures 4c and 4d show the details of the fracture surfaces of this sample. Plate-like, large grains of $\text{CeAl}_{11}\text{O}_{18}$ had always been the characteristic microstructural features of our hexaaluminate samples in this study. The EDXS analyses carried out on the flat surfaces of the grains of this sample (by using pure, single phase CeAlO_3 as a standard) gave us the mean weight percentages of the three elements present as follows; Ce:19.0%, Al:40.8%, and O:40.2%. When compared with the theoretical percentages (Ce:19.33%, Al:40.94%, O:39.73) that were calculated from $\text{CeAl}_{11}\text{O}_{18}$, within the limits of error of EDXS analysis, these may be regarded as a good match.

Figure 4. SEM micrographs of samples of $\text{CeAl}_{11}\text{O}_{18}$ composition

- (A) & (B) Backscattered electron images. $3^\circ\text{C}/\text{min}$ to 1915°C , 5 min, fce.
quenched to RT. Darker trigonal α -alumina crystals surrounded by lighter
cerium-containing once-liquid phase (BARS = $100\ \mu\text{m}$)
- (C) 1550°C , 30 hours, quenched, ground, repelletised, 1550°C , 30 hours,
quenched (BAR = $10\ \mu\text{m}$)
- (D) Same sample in (C) (BAR = $1\ \mu\text{m}$)



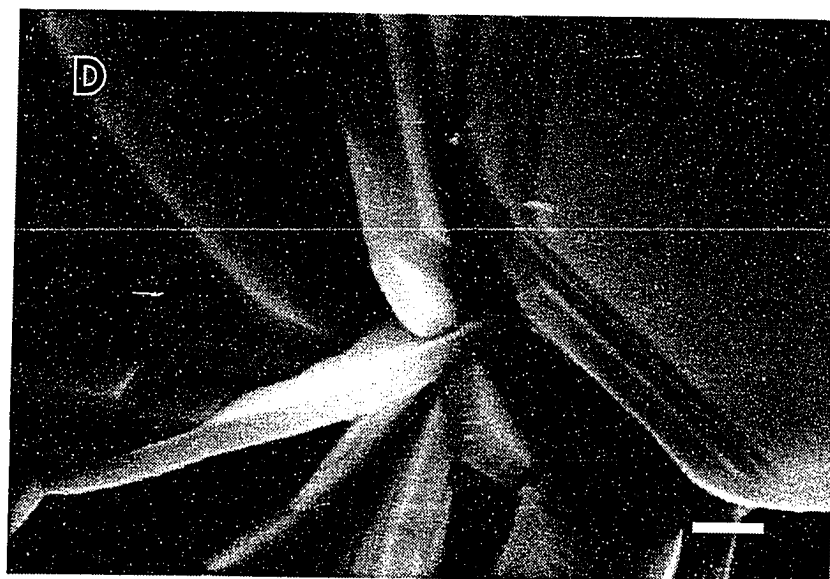


Figure 4. Continued

Table III. XRD Pattern of Cerium Hexaaluminate, $\text{CeAl}_{11}\text{O}_{18}$

hkl	d_{calc}	d_{obs}	I/I_0
002	11.006	11.0	28
004	5.503	5.50	8
100	4.814	4.82	2
101	4.702	4.702	23
102	4.410	4.409	22
103	4.024	4.023	7
006	3.668	3.667	31
104	3.623	3.623	8
105	3.249	3.248	7
110	2.779	2.779	29
008	2.752	2.751	25
112	2.694	2.694	8
107	2.632	2.632	100
114	2.481	2.480	58
200	2.407	2.406	4
201	2.392	2.391	2
202	2.351	2.351	2
203	2.287	2.287	20
0 0 10	2.201	2.202	27
109	2.180	2.180	8
205	2.112	2.112	42
206	2.012	2.012	33
118	1.955	1.955	2
1 0 11	1.848	1.848	10
0 0 12	1.834	1.834	1
211	1.813	1.813	2
213	1.766	1.766	1
1 1 10	1.726	1.725	4

Table III. (cont.)

hkl	d_{calc}	d_{obs}	I/I_0
209	1.715	1.715	9
215	1.681	1.682	1
2 0 10	1.624	1.624	1
302	1.588	1.588	1
217	1.575	1.574	18
2 0 11	1.539	1.539	38
1 1 12	1.531	1.531	5
218	1.518	1.517	2
305	1.508	1.508	1
1 0 14	1.495	1.494	2
306	1.470	1.470	1
2 0 12	1.459	1.459	2
1 0 15	1.404	1.404	4
2 1 10	1.402	1.402	3
220	1.390	1.390	19
2 0 13	1.385	1.385	4
0 0 16	1.376	1.376	2
1 1 14	1.368	1.369	1
2 1 11	1.346	1.346	2
310	1.335	1.335	1
1 0 16	1.323	1.323	1
2 0 14	1.316	1.316	11
226	1.2994	1.2995	1
3 0 10	1.2966	1.2967	1
2 0 15	1.2529	1.2532	1
228	1.2403	1.2404	3
2 1 13	1.2395	1.2395	3
1 1 16	1.2329	1.2329	3
317	1.2289	1.2289	3
402	1.1962	1.1964	1

Table III. (cont.)

hkl	d_{calc}	d_{obs}	I/I_0
2 0 16	1.1944	1.1945	2
2 1 14	1.1896	1.1893	2
1 0 18	1.1852	1.1852	3
404	1.1756	1.1757	1
2 2 10	1.1750	1.1750	1
405	1.1608	1.1609	2
3 1 10	1.1415	1.1417	2
1 1 18	1.1193	1.1193	4
3 1 11	1.1106	1.1104	1
2 2 12	1.1076	1.1076	1
0 0 20	1.1006	1.1006	4
2 1 16	1.0973	1.0972	1
2 0 18	1.0902	1.0902	1
3 0 15	1.0829	1.0830	1
409	1.0798	1.0800	1
326	1.0574	1.0573	1
4 0 10	1.0559	1.0558	1
410	1.0504	1.0506	1
327	1.0419	1.0419	4
4 0 11	1.0313	1.0314	4
1 0 21	1.0242	1.0241	2
3 1 14	1.0177	1.0175	1
2 1 18	1.0149	1.0148	1
4 0 12	1.0062	1.0061	1
417	0.9963	0.9965	1
3 1 15	0.9875	0.9875	1
4 0 13	0.9809	0.9809	1
1 0 22	0.9796	0.9795	1
2 2 16	0.9776	0.9778	1
3 0 18	0.9726	0.9727	2

Table III. (cont.)

hkl	d_{calc}	d_{obs}	I/I_0
3 2 11	0.9668	0.9667	1
501	0.9618	0.9617	1
3 1 16	0.9581	0.9581	1
4 0 14	0.9556	0.9556	2
503	0.9545	0.9544	1
504	0.9483	0.9483	1
2 1 20	0.9417	0.9418	1
3 0 19	0.9393	0.9393	1
4 1 11	0.9300	0.9300	1
330	0.9263	0.9263	1
2 0 22	0.9239	0.9240	1
507	0.9205	0.9206	1
2 2 18	0.9180	0.9181	1
334	0.9135	0.9135	1
2 1 21	0.9082	0.9083	2
3 1 18	0.9018	0.9018	2
509	0.8958	0.8956	1
425	0.8908	0.8908	1
2 0 23	0.8893	0.8894	1
426	0.8829	0.8828	2
1 0 25	0.8661	0.8660	1
2 2 20	0.8628	0.8628	3
513	0.8586	0.8585	2
2 0 24	0.8570	0.8569	1
429	0.8526	0.8527	1
0 0 26	0.8466	0.8466	1
516	0.8415	0.8415	1
3 2 17	0.8402	0.8403	1
5 0 13	0.8369	0.8370	1
4 0 19	0.8346	0.8347	2

Table III. (cont.)

hkl	d_{calc}	d_{obs}	I/I_0
517	0.8336	0.8336	2
4 2 11	0.8281	0.8282	3
3 3 12	0.8269	0.8269	6
518	0.8248	0.8247	2
3 0 23	0.8219	0.8220	1
5 0 14	0.8210	0.8211	1
3 2 18	0.8196	0.8196	1
4 1 17	0.8157	0.8158	1
4 0 20	0.8121	0.8122	1
2 2 22	0.8120	0.8120	1
1 1 26	0.8099	0.8098	1
5 0 15	0.8049	0.8050	1
1 0 27	0.8038	0.8038	1
600	0.8022	0.8023	3
601	0.8017	0.8016	2
3 1 22	0.8006	0.8006	1
2 0 26	0.7986	0.7986	2
4 1 18	0.7968	0.7969	2
604	0.7939	0.7939	1
2 1 25	0.7925	0.7926	1
432	0.7893	0.7894	1
5 0 16	0.7888	0.7886	1
4 2 14	0.7874	0.7874	2
433	0.7868	0.7868	2
0 0 28	0.7861	0.7862	1
606	0.7837	0.7836	1

Hexagonal, $a = 5.55812(8) \text{ \AA}$, $c = 22.0121(4) \text{ \AA}$, $V = 588.91(2) \text{ \AA}^3$

Space group : $P6_3/mmc$ (194), $Z = 2$, $D_x = 4.087 \text{ gm/cm}^3$

X-Ray Powder Diffractometer, $\text{CuK}\alpha$, External silicon standard (NBS640a)

Scan rate : $0.125^\circ 2\theta/\text{min}$, SS/FOM : $F(30) = 104 (0.0055, 52)$

The determination of the crystal structure among the two likely candidates; magnetoplumbite and β' -alumina, while working with a powder sample rather than a single crystal of cerium hexaaluminate, had been a difficult question to answer. However, we have chosen to suggest a relatively simple and rough answer to this problem in Figure 5. We have generated two synthetic powder patterns by using the refined atomic coordinates of the single crystal, $\text{LaAl}_{11}\text{O}_{18}$ (defective magnetoplumbite) phase from the Gasperin et al.¹⁷ study and by using the atomic coordinates of single crystal, $\text{Na}_2\text{O} \cdot 11\text{Al}_2\text{O}_3$ (β' -alumina) reported by Felsche²⁰. We placed the generated magnetoplumbite pattern above and the β' -alumina pattern below the raw data file of our sample in Figure 5. The comparison of the intensities between the two generated patterns and our experimental pattern would help to make a rough decision between the two candidates, even though the outcome might have a significant degree of doubt attached to it. In the 10 to 30° 2 θ range, our raw data contained the (012) reflection of $\alpha\text{-Al}_2\text{O}_3$, at 25.6° 2 θ . After disregarding this peak, the intensities of the remaining 9 peaks of this range of our data were found to match more strongly with those of magnetoplumbite than β' -alumina. In the 30 to 50° 2 θ range, this comparison becomes more difficult. However, in the 50 to 80° 2 θ range, our intensity data favour mostly the magnetoplumbite structure. Therefore, based solely on this analysis, it would be more reasonable to assume the structure of $\text{CeAl}_{11}\text{O}_{18}$ to resemble to the magnetoplumbite-like structure of $\text{LaAl}_{11}\text{O}_{18}$ than that of $\text{NaAl}_{11}\text{O}_{17}$. The assessment of the degree of disorder and the extent of site splitting in the mirror planes of the $\text{CeAl}_{11}\text{O}_{18}$ structure which might cause the possible variations in the phase stoichiometry, as well as the exact determination of the

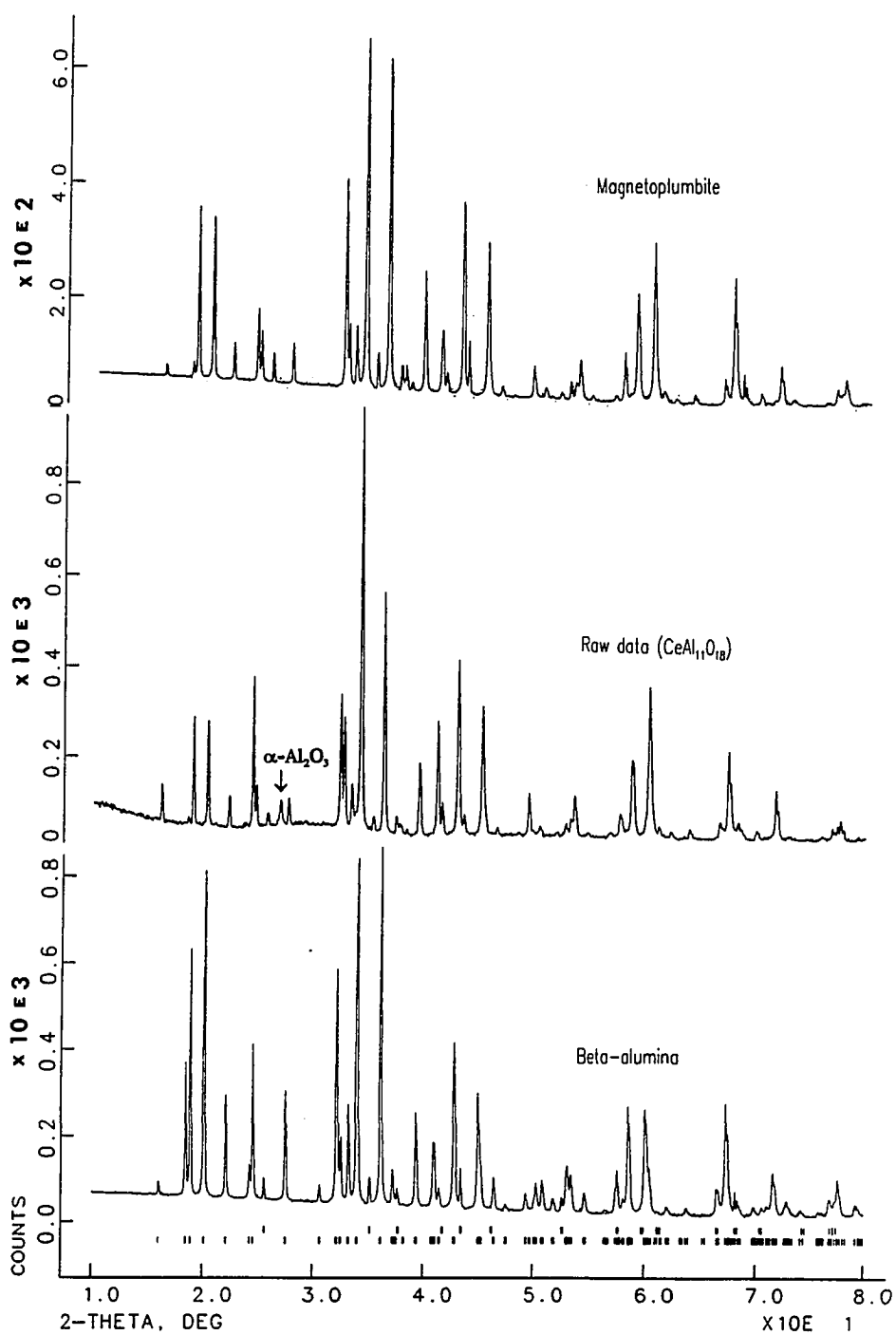


Figure 5. Comparison of the generated XRD patterns for magnetoplumbite and Na- β '-alumina with the experimental XRD pattern of $\text{CeAl}_{11}\text{O}_{18}$

structure type, will have to await the single crystal x-ray diffraction or powder neutron diffraction experiments.

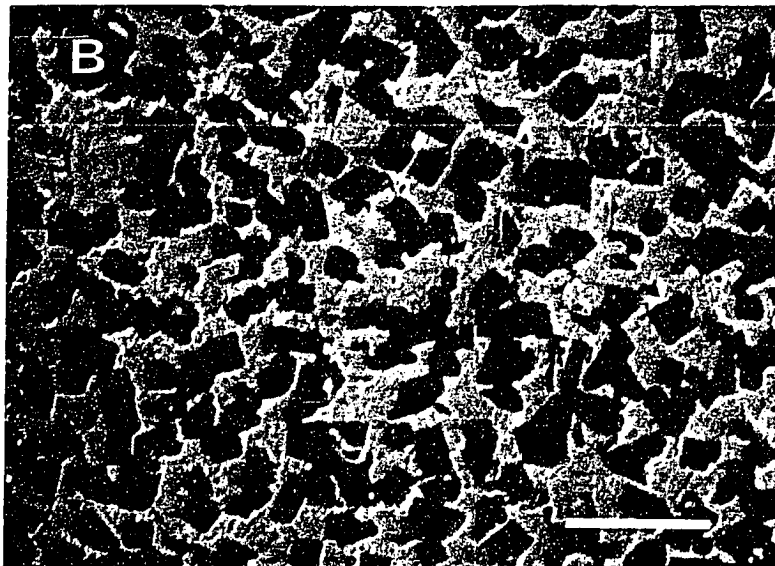
We have confirmed that the eutectic reaction between $\text{CeAl}_{11}\text{O}_{18}$ and CeAlO_3 occurred at $1785 \pm 15^\circ\text{C}$ as it was predicted by Mizuno et al.⁹. The equilibration heat treatments for a sample of composition 12 mol% Ce_2O_3 - 88 mol% Al_2O_3 at 1700° and 1820°C produced a solid state phase mixture of $\text{CeAl}_{11}\text{O}_{18}$ and CeAlO_3 , and a mixture of $\text{CeAl}_{11}\text{O}_{18}$ and liquid, respectively, upon furnace quenching, as predicted by the available phase diagram. DTA runs for the same composition indicated a single endothermic event at 1785°C corresponding to the first liquid formation. Heating one of these samples to 1820°C , holding for 6 hours at that temperature, and slowly cooling ($5^\circ\text{C}/\text{min}$) to 1100°C caused the eutectic matrix to crystallise surrounding the elongated $\text{CeAl}_{11}\text{O}_{18}$ crystals. A sample micrograph of this structure is given in Figure 6a. The XRD pattern of this sample showed the presence of two crystalline phases, CeAlO_3 and $\text{CeAl}_{11}\text{O}_{18}$.

We could not synthesize the R-compound which was reported to form at 79 mol% Ce_2O_3 and decompose at temperatures below 1850°C by Mizuno et al.⁹. One probable reason for this might be the inadequate quenching rates we had in the vacuum furnace which would not be rapid enough to prevent the decomposition of this compound. We were only able to furnace quench (i.e., the natural cooling of the furnace itself upon turning off of the power) our samples, although Mizuno et al.⁹ reported that they were able to water quench their samples from temperatures in excess of 1900°C . Heating a 74 mol% Ce_2O_3 - 26 mol% Al_2O_3 sample (pre-equilibrated at 1550°C for 24 hours, followed by water quenching, grinding, and

Figure 6. SEM micrographs of samples in the Ce_2O_3 - Al_2O_3 system

- (A) 12 mol% Ce_2O_3 - 88 mol% Al_2O_3 sample heated at 1820°C for 6 hours. Slow cooling to 1100°C caused the eutectic matrix to crystallise. Long grains of $\text{CeAl}_{11}\text{O}_{18}$ are dispersed throughout
- (B) 74 mol% Ce_2O_3 - 26 mol% Al_2O_3 . 1875°C, 4 hours, furnace quenched. Darker phase is CeAlO_3 . The brighter grains represent a mixture of Ce_2O_3 and CeO_{2-x}
- (C) 83 mol% Ce_2O_3 - 17 mol% Al_2O_3 sample. 1940°C, 3 hours, furnace quenched. Eutectic microstructure

BAR LENGTHS = 10 μm



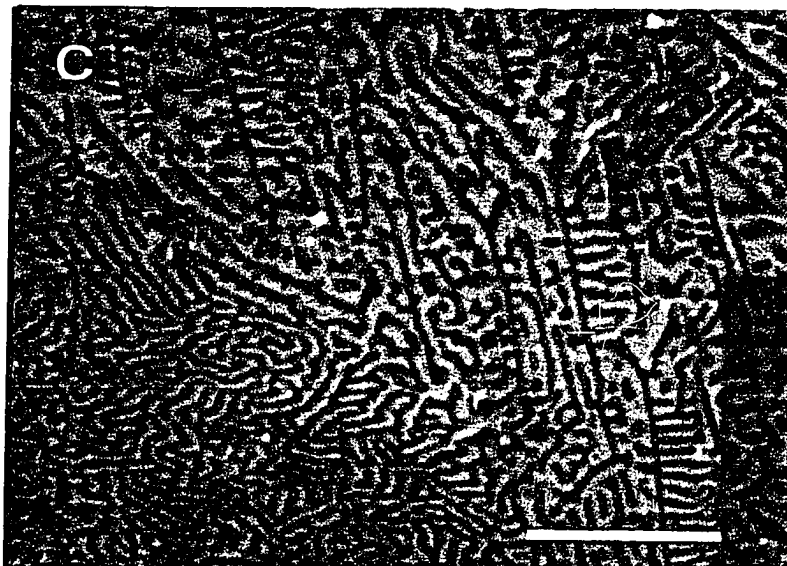


Figure 6. Continued

re-pelletising) to 1875°C and furnace quenching produced a solid state phase mixture of CeAlO_3 and $[\text{Ce}_2\text{O}_3 + \text{CeO}_{2-x}]$ as shown in Figure 6b. The dark phase was CeAlO_3 in this picture. The other two compositions we studied in the Ce_2O_3 -rich region of this system produced rather unique microstructures as displayed in Figure 6c. Upon heating the 79 mol% and 83 mol% Ce_2O_3 samples to 1940°C, followed by furnace quenching, the liquid was formed, and during cooling the submicron spaced, eutectic-like matrix evolved. At this point we just choose to report the microstructures observed even though they may not represent the equilibrium conditions for this portion of the binary. The lighter phase in Figure 6c was the crystalline mixture $[\text{Ce}_2\text{O}_3 + \text{CeO}_{2-x}]$ whereas the darker phase was CeAlO_3 .

Although our attempts to synthesize the orthorhombic R-compound ⁹ have failed, we still detected the traces of an orthorhombic phase embedded in the backgrounds of the XRD patterns of the above three samples. The extremely low intensities of that phase, with the tentative lattice constants $a = 19.28 \text{ \AA}$, $b = 12.35 \text{ \AA}$, and $c = 6.37 \text{ \AA}$, did not warrant us at this point to give an accurate listing of the individual reflections. It is to be noted that the R-compound reported by Mizuno et al.⁹ in the Ce_2O_3 - Al_2O_3 system had the quite different lattice constants; $a = 9.538 \text{ \AA}$, $b = 5.850 \text{ \AA}$, and $c = 15.205 \text{ \AA}$.

CONCLUSIONS

The two binary compounds, CeAlO_3 and $\text{CeAl}_{11}\text{O}_{18}$, of the system Ce_2O_3 - Al_2O_3 have been synthesized from the oxides CeO_2 and Al_2O_3 . It has been found that the conditions of formation of these two compounds were not affected by the atmospheres used in this study, namely, argon, argon + 10% H_2 , and vacuum. CeAlO_3 was shown to be stable in a perovskite-like tetragonal structure, with the lattice constants $a = 3.763 \text{ \AA}$ and $c = 3.792 \text{ \AA}$, in the atmospheres used in this study from room temperature to 1950°C . A new XRD pattern was suggested for CeAlO_3 .

$\text{CeAl}_{11}\text{O}_{18}$ was synthesized from the oxides and was shown to be an incongruently melting compound confirming the findings of the previous researchers. It decomposed into $\alpha\text{-Al}_2\text{O}_3$ and a liquid phase at $1915 \pm 25^\circ\text{C}$ upon heating. An XRD pattern is suggested for the first time for the hexagonal compound $\text{CeAl}_{11}\text{O}_{18}$, with the lattice constants $a = 5.558 \text{ \AA}$ and $c = 22.012 \text{ \AA}$.

The eutectic reaction between $\text{CeAl}_{11}\text{O}_{18}$ and CeAlO_3 was confirmed to occur at $1785 \pm 15^\circ\text{C}$ as reported by Mizuno et al.⁹. Although it was almost impossible for us to form the single phase $\text{CeAl}_{11}\text{O}_{18}$ in the solid state, we were able to form the crystals of this compound, in the presence of a liquid phase, at a composition of 12 mol% Ce_2O_3 (without any unreacted $\alpha\text{-Al}_2\text{O}_3$), within a eutectic matrix of $\text{CeAl}_{11}\text{O}_{18}$ and CeAlO_3 .

Eutectic-like microstructures, with sub-micron sized lamellae, were observed, for the first time in any $\text{RE}_2\text{O}_3\text{-REAlO}_3$ system, in the Ce_2O_3 -rich (74-83 mol%) side of the $\text{Ce}_2\text{O}_3\text{-Al}_2\text{O}_3$ binary.

ACKNOWLEDGEMENTS

This work is in part supported by the McKnight Foundation, Iowa State University, and Middle East Technical University of Ankara, Turkey. Authors express their appreciation for the financial support.

REFERENCES

- ¹ W.H. Zachariasen, "Crystal Chemical Studies of the 5f-Series of Elements. XII. New Compounds Representing Known Structure Types," *Acta Cryst.*, **2**, 388-390 (1949).
- ² M.L. Keith and R. Roy, "Structural Relations Among Double Oxides of Trivalent Elements," *The Am. Miner.*, **39**, 1-23 (1954).
- ³ R.S. Roth, "Classification of Perovskite and Other ABO_3 - type Compounds," *J. Res. NBS*, **58**, 75 (1957).
- ⁴ A.I. Leonov, "The Valence of Cerium in Synthetic and Natural Cerium Aluminates and Silicates. Part 1. Compounds of the Perovskite Group," *Izv. Akad. Nauk SSSR, Otd. Khim. Nauk*, **1**, 8-13 (1963).
- ⁵ A.I. Leonov, A.V. Andreeva, V.E. Shvaiko-Shvaikovskii and E.K. Keler, "High - Temperature Chemistry of Cerium in the Systems Ce_2O_3 - Al_2O_3 , Cr_2O_3 , Ga_2O_3 ," *Izv. Akad. Nauk SSSR, Neorg. Mater.*, **2**, 517-523 (1966).
- ⁶ Y.S. Kim, "Crystallographic Study of Cerium Aluminate ($CeAlO_3$)," *Acta Cryst.*, **B24**, 295-296 (1968).

- ⁷ S. Geller and P.M. Raccach, "Phase Transitions in Perovskitelike Compounds of the Rare Earths," *Physical Review B*, **2**, 1167-1172 (1970).
- ⁸ J.F. Scott, "Raman Study of Trigonal-Cubic Phase Transitions in Rare-Earth Aluminates," *Phys. Rev.*, **183**, 823-825 (1969).
- ⁹ M. Mizuno, T. Yamada and T. Noguchi, "Phase Diagram of the System Al_2O_3 - Ce_2O_3 at High Temperature," *Yogyo-Kyokai-Shi*, **83**, 90-95 (1975).
- ¹⁰ N. Kaufherr, L. Mendelovici and M. Steinberg, "The Preparation of Cerium(III) Aluminate at Lower Temperatures: IR, X-ray and Electron Spin Resonance Study," *J. Less Comm. Met.*, **107**, 281-289 (1985).
- ¹¹ M. Mizuno, T. Yamada and T. Noguchi, "Phase Diagram of the System Al_2O_3 - La_2O_3 at High Temperatures," *Yogyo-Kyokai-Shi*, **82**, 630-636 (1974).
- ¹² R.C. Ropp and G.G. Libowitz, "The Nature of the Alumina-Rich Phase in the System La_2O_3 - Al_2O_3 ," *J. Am. Ceram. Soc.*, **61**, 473-475 (1978).

- ¹³ J.M.P.J. Verstegen, J.L. Sommerdijk and J.G. Verriet, "Cerium and Terbium Luminescence in $\text{LaMgAl}_{11}\text{O}_{19}$," *J. Lumin.*, **6**, 425-431 (1973).
- ¹⁴ J.M.P.J. Verstegen, "A Survey of a Group of Phosphors, Based on Hexagonal Aluminate and Gallate Host Lattices," *J. Electrochem. Soc.*, **121**, 1623-1627 (1974).
- ¹⁵ A. Kahn, A.M. Lejus, M. Madsac, J. Thery, D. Vivien and J.C. Bernier, "Preparation, Structure, Optical, and Magnetic Properties of Lanthanide Aluminate Single Crystals ($\text{LnMAI}_{11}\text{O}_{19}$)," *J. Appl. Phys.*, **52**, 6864-6869 (1981).
- ¹⁶ F. Laville and A.M. Lejus, "Crystal Growth and Characterisation of $\text{LaMAI}_{11}\text{O}_{19}$ Lanthanum Aluminates," *J. Cryst. Growth*, **63**, 426-428 (1983).
- ¹⁷ M. Gasperin, M.C. Saine, A. Kahn, F. Laville and A.M. Lejus, "Influence of M^{2+} Ions Substitution on the Structure of Lanthanum Hexaaluminates with Magnetoplumbite Structure," *J. Sol. State Chem.*, **54**, 61-69 (1984).
- ¹⁸ X.H. Wang, A.M. Lejus, D. Vivien and R. Collongues, "Synthesis and Characterisation of Lanthanum Aluminum Oxynitrides with Magnetoplumbite like Structure," *Mat. Res. Bull.*, **23**, 43-49 (1988).

- ¹⁹ C.A. Beevers and M.A.S. Ross, "The Crystal Structure of "Beta Alumina" $\text{Na}_2\text{O} \cdot 11\text{Al}_2\text{O}_3$," *Z. Kristallogr.*, **97**, 59-66 (1937).
- ²⁰ J. Felsche, "The Alkali Problem in the Crystal Structure of Beta Alumina," *Z. Kristallogr.*, **127**, 94-100 (1968).
- ²¹ J.M.P.J. Verstegen, *JCPDS PDF 26-0872*, Philips, Eindhoven, Netherlands.
- ²² A.C. Tas and M. Akinc, "Phase Relations in the System Ce_2O_3 - $\text{Ce}_2\text{Si}_2\text{O}_7$ in the Temperature Range 1150° to 1970°C in Reducing and Inert Atmospheres," *J. Am. Ceram. Soc.*, Accepted for publication.
- ²³ D.E. Appleman and H.T. Evans, *U.S. Geological Survey, Computer Contribution No. 20*, U.S. National Technical Information Service, Document **PB-216188**, (1973).
- ²⁴ P.E. Werner, "Trial and Error Program for Indexing of Unknown Powder Patterns, TREOR," University of Stockholm, Stockholm, Sweden, (1984).
- ²⁵ M. Drofenik, "Origin of the Grain Growth Anomaly in Donor-Doped Barium Titanate," *J. Am. Ceram. Soc.*, **76**, 123-128 (1993).

PAPER V: STRUCTURAL INVESTIGATION OF PURE AND N-DOPED
CERIUM OXYGEN APATITE ($\text{Ce}_{4.67}[\text{SiO}_4]_3\text{O}$) BY NEUTRON
DIFFRACTION

**Structural Investigation of Pure and N-doped Cerium Oxygen Apatite ($\text{Ce}_{4.67}[\text{SiO}_4]_3\text{O}$)
by Neutron Diffraction**

Submitted by

A. Cuneyt Tas, Victor G. Young, Jr. and Mufit Akinc

Departments of Chemistry and Materials Science and Engineering

Iowa State University

Ames, Iowa 50011

This manuscript has been submitted for publication in the Journal of the American Ceramic Society.

ABSTRACT

The site occupancy of nitrogen atoms were studied in a sample of 4800 ppm N-containing cerium oxygen apatite with neutron diffraction. The atomic parameters and occupancy factors for different oxygen sites of the apatite lattice were refined by Rietveld analysis. Cerium oxygen apatite was confirmed to have a space group of $P6_3/m$. The so-called "free" oxygen sites (0,0,1/4 and 0,0,3/4) were found to be the most likely sites for nitrogen substitution rather than the silicon-bonded sites.

INTRODUCTION

The apatite-type compound, $\text{Ce}_{4.67}[\text{SiO}_4]_3\text{O}$, has recently been shown¹ to be able to absorb nitrogen in its crystal structure (hexagonal, $a = 9.657 \text{ \AA}$, $c = 7.118 \text{ \AA}$) when it was prepared from nitrogen containing starting materials (such as Si_3N_4) or even after heating in nitrogen bearing gas atmospheres. The presence of small amounts of nitrogen in the structure could be identified with XRD by a significant increase in the unit cell volume, as compared to the pure form of the compound, mainly provided by a larger increase in the c-axis dimension of the cell^{1,2}.

Considering all atomic sites per unit cell, the structure of cerium oxygen apatite might best be described³ by the formula $^{\text{IX}}(\text{Ce}_{3.33} \square_{0.67}) ^{\text{VII}}(\text{Ce}_6)[^{\text{IV}}\text{Si}^{\text{IV}}\text{O}_4]_6 ^{\text{III}}\text{O}_2$. One possibility regarding the nature of nitrogen substitution for oxygen in this structure is the replacement of 3-coordinated "free" (i.e., not-bonded to the silicons of tetrahedra) oxygens, which are found at the 0,0,1/4 and 0,0,3/4 positions on the 6_3 axis, with nitrogen. Such a substitution would require more and more ceriums to occupy the cation vacancies in the 9-coordinated sites up to a maximum of 14100 ppm of nitrogen present in the material, leading to a formula for a defect-free and nitrogen-bearing cerium apatite as $\text{Ce}_{10}[\text{SiO}_4]_6\text{N}_2$. Using powder x-ray diffraction, chemical analysis and weight loss data, in a cerium apatite sample containing about 16600 ppm nitrogen, Gaude⁴ proposed the substitution of oxygen with nitrogen to take place in the distorted silicate tetrahedra according to the formula : $\text{Ce}_{10}[\text{SiO}_{3.61}\text{N}_{0.39}]_6\text{O}_{1.83}\square_{0.17}$ leading to the formation of vacancies in the 3-coordinated oxygen sites. Gaude⁴ also reported

the collapse of the hexagonal apatite structure in samples containing 21700 and 24400 ppm according to the XRD data.

The purpose of the present study was to investigate the site occupancy of nitrogen atoms with neutron diffraction, which would be more sensitive in distinguishing nitrogen from oxygen as compared to x-rays, in cerium apatite samples doped with ppm-level nitrogen.

EXPERIMENTAL PROCEDURE

To facilitate the conduct of a comparative study on the possible effects of nitrogen presence on the crystal structure of cerium apatite, pure and 7050 ppm nitrogen (in the unfired powder mixture) containing samples have been prepared. The pure sample was synthesized by combining appropriate quantities of CeO_2 (99.87% pure, Cerac) and fumed SiO_2 (99.98% pure, Sigma) in ethanol in an agate mortar and then wet mixing (in ethanol) in plastic jars with alumina balls for 24 hours followed by overnight drying at 80°C . The nitrogen doped sample was prepared by mixing the appropriate quantities of CeO_2 , fumed SiO_2 , and Si_3N_4 (>98% pure, Shin-Etsu) in a similar manner. Powders were first pressed uniaxially into pellets in a tungsten carbide-lined steel die at about 20 MPa and then cold isostatically pressed in latex bags at 200 MPa. Pellets were heated in platinum crucibles in a vertical Al_2O_3 tube furnace at 1560°C in a prepurified ($\text{O}_2 < 50$ ppm) flowing argon ("pure" sample) or nitrogen ("N-doped" sample) atmosphere for 6 hours ("pure") or 40 hours ("N-doped"), followed by quenching in water. The laser source mass spectroscopy analysis of a typical, heated "pure" cerium oxygen apatite sample has previously been reported¹. The inert gas fusion analysis carried out for the determination of nitrogen level revealed the presence of only about 4800 ± 500 ppm nitrogen in the heated doped sample. The density measurements (via Archimedes method) of both the "pure" and "doped" samples yielded $5.52 \pm 0.06 \text{ gm/cm}^3$ which well conformed to the XRD density calculated (5.47 gm/cm^3) for the samples of cerium oxygen apatite stoichiometry described by the above mentioned formula. The neutron diffraction

experiments of the powder samples were performed on the HIPD instrument at the Los Alamos Neutron Scattering Center. Rietveld analyses of the two samples were processed with GSAS⁵ on a DEC-Station 5000 computer.

RESULTS AND DISCUSSION

The main structural features of the "pure" sample are displayed in Figure 1. This structure was refined to a residual $R = 5.3\%$. The atomic parameters corresponding to cell dimensions $a = 9.652(2) \text{ \AA}$ and $c = 7.112(1) \text{ \AA}$ are listed in Table 1. The unit cell did have the centrosymmetric $P6_3/m$ space group. The parameters given in Table 1 only slightly differed from those given by Belokoneva et al.⁶ for $\text{Ce}_{4.67}[\text{SiO}_4]_3\text{O}$ with the cell dimensions $a = 9.736 \text{ \AA}$ and $c = 7.116 \text{ \AA}$. There was no reasonable explanation for the mismatch seen in the value of the a dimension, except for the possible variations in the purity of the samples and the method of evaluating the experimental data. The atomic distances and angles observed in the structure of pure sample were tabulated in Table 2. Cerium ions at the Ce(1) positions are surrounded by 9 oxygens which are all silicon-bonded. The refined value of the occupancy factor (i.e., $0.84(2)$) for those ceriums showed that Ce(1) sites were occupied only by about $3 \frac{1}{3} \text{ Ce}^{3+}$ cations out of a possible of 4. Therefore, $2/3$ vacant sites per cell would be statistically distributed on these lattice sites. This finding makes it possible for us to assume the above-mentioned defect formula for this compound. The average of the Ce(1)-O distances in the 9-coordinated polyhedra was found to be $2.609(5) \text{ \AA}$ in this sample. The other distinct cerium positions, Ce(2), were surrounded by 7 oxygens; 6 of those silicon - bonded, the other being the "free" oxygen, O(4). In these 7-pointed polyhedra of ceriums, 4 of the 6 silicon-bonded oxygens were those that occupied the O(3)-sites. The ceriums found at these

**Figure 1. Crystal structure of pure cerium oxygen apatite ($\text{Ce}_{4.67}[\text{SiO}_4]_3\text{O}$) based
on the atomic coordinates listed in Table I**

2

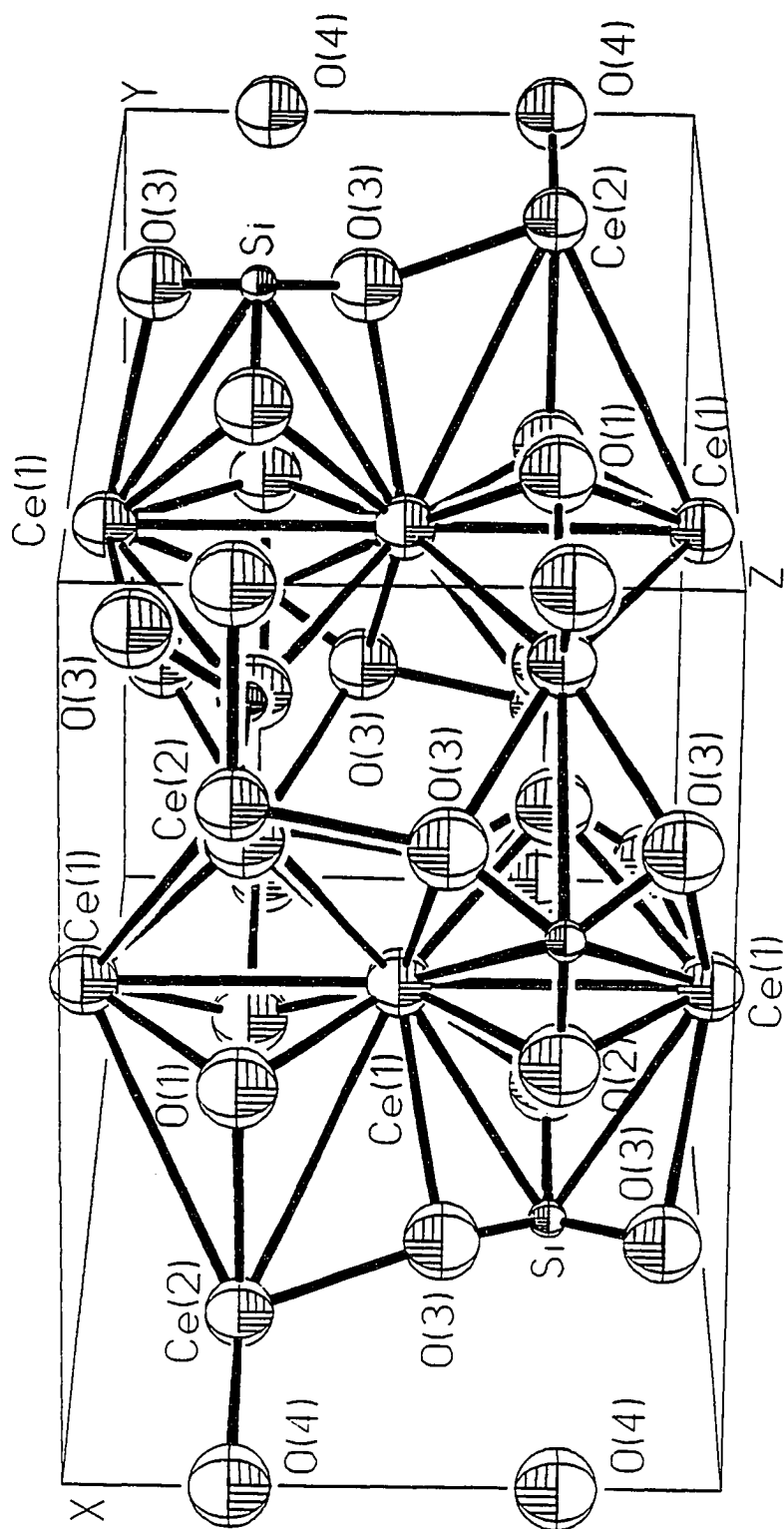


Table 1. Atomic Parameters of Pure $\text{Ce}_{4.67}[\text{SiO}_4]_3\text{O}$

Atom	Occ. factor	x	y	z	U_{iso}
Ce (1)	0.84(2)	0.6667	0.3333	0.0001(9)	0.9 (2)
Ce (2)	1	0.9880(6)	0.2297(5)	0.2500	0.7 (1)
Si	1	0.3726(5)	0.4025(5)	0.2500	0.02 (7)
O (1)	1	0.4850(5)	0.3230(4)	0.2500	1.9 (1)
O (2)	1	0.4726(5)	0.5968(4)	0.2500	1.49 (9)
O (3)	1	0.2548(4)	0.3448(4)	0.0685(3)	2.12 (8)
O (4)	1	0.0000	0.0000	0.2500	3.5 (2)

sites (three of which surround one O(4) on the 6_z axis) exhibited a significantly short distance of 2.28 Å to the "free" oxygens which are at the 0,0,1/4 and 0,0,3/4 positions which was even less than the sum of the ionic radii. This behaviour, as previously reported by Felsche³ for Gd-oxygen apatite, represents the strong polarizing forces exerted by the rare earth cation on the oxygen which is not silicon bonded. The average Ce(2) - O distance in the 7-coordinated polyhedra was 2.506(6) Å. Taking the average oxygen radius as 1.38 Å, the effective Ce^{3+} ionic radii would be 1.23 and 1.13 Å for the 9- and 7-coordinated polyhedra, respectively. From these, one could calculate the mean value of the Ce^{3+} ionic radius in the apatite structure as 1.177 Å. An exactly similar analysis carried out by Felsche³, for the gadolinium

Table 2. Interatomic Distances and Angles in Pure $\text{Ce}_{4.67}[\text{SiO}_4]_3\text{O}$

Vector	Length (Å)	Angle	Degrees
Ce(1)-Ce(1)	3.556(13)	Ce(1)-Ce(1)-O(1)	136.2(1)
Ce(1)-Si	3.282(5)	Ce(1)-Ce(1)-O(2)	135.0(1)
Ce(1)-O(1)	2.464(5)	O(1)-Ce(1)-O(1)	73.7(2)
Ce(1)-O(2)	2.516(5)	O(1)-Ce(1)-O(2)	153.7(1)
Ce(1)-O(3)	2.848(3)	O(2)-Ce(1)-O(2)	75.6(2)
Ce(2)-Ce(2)	3.944(7)	O(2)-Ce(2)-O(3)	70.5(2)
Ce(2)-Si	3.220(6)	O(2)-Ce(2)-O(4)	150.3(2)
Ce(2)-Si	3.322(6)	O(3)-Ce(2)-O(3)	135.4(2)
Ce(2)-O(1)	2.733(6)	O(3)-Ce(2)-O(4)	83.9(1)
Ce(2)-O(2)	2.492(6)	O(1)-Si-O(2)	113.4(3)
Ce(2)-O(3)	2.437(3)	O(1)-Si-O(3)	111.0(2)
Ce(2)-O(3)	2.583(5)	O(2)-Si-O(3)	107.8(2)
Ce(2)-O(4)	2.277(4)	O(3)-Si-O(3)	105.4(3)
Si-O(1)	1.612(5)	Ce(1)-O(1)-Si	128.0(1)
Si-O(2)	1.625(6)	Ce(2)-O(2)-Si	123.8(3)
Si-O(3)	1.623(4)	Ce(1)-O(2)-Si	102.7(2)
		Ce(2)-O(3)-Si	142.1(2)
		Ce(2)-O(4)-Ce(2)	120.0(0)

counterpart of this compound, generated the effective ionic radii of 1.15 and 1.02 Å in both types of polyhedra, and a mean value of Gd^{3+} ionic radius as 1.08 Å in the structure. This decrease in ionic radius (from Ce to Gd) should be regarded as a perfect example for the "lanthanide contraction" observed in the lanthanide series of elements. Felsche³ predicted the ionic radius of Ce^{3+} in the apatite structure as 1.17 Å from a plot of apatite cell volumes (for the other lanthanide oxygen apatites) versus the cube of ionic radii of the lanthanides. This early prediction has also been experimentally confirmed by this study.

The initial amount of nitrogen (in the form of Si_3N_4) we added to the powder mixture of the "doped" sample corresponded to about 7050 ppm elemental nitrogen in the compound, assuming all of the nitrogen end up substituting oxygens at the O(4)-sites. This amount and type of nitrogen incorporation in the apatite structure would then be denoted by the following formula; $\text{Ce}_{9.667}[\text{SiO}_4]_6\text{O}_{1.00}\text{N}_{1.00}$. If we had added 14100 ppm nitrogen, this formula would have changed to $\text{Ce}_{10}[\text{SiO}_4]_6\text{N}_2$. However, the chemical analysis we performed on the final, heat treated sample indicated the presence of only 4800 ppm elemental nitrogen in the doped compound. This amount of nitrogen would lead to a formula as $\text{Ce}_{9.553}[\text{SiO}_4]_6\text{O}_{1.341}\text{N}_{0.659}$. The site occupancy of the O(4) positions (by nitrogen) calculated from this formula would then correspond to about 33%.

Apparently, we have lost about 32 wt% of nitrogen, that has been present in the initial powder mixture, during the heating stage to synthesize the compound. One possible explanation for the loss of nitrogen at high temperatures might be the formation of gaseous N_2 during solid state reaction of the individual Si_3N_4 particles with CeO_2 and SiO_2 . Another

possibility could be the presence of significant amounts of SiO_2 in Si_3N_4 that might have adversely affected the initial assumed N levels in the powder mixtures. The relatively low atmospheric pressures exerted by the flowing (100 ml/min) N_2 gas in our tube furnace did clearly not suffice to compensate for the apparent nitrogen losses as one would expect from using higher pressures. Another drawback of our experimental technique might be pointed out as our use of CeO_2 rather than Ce_2O_3 in the initial powder mixture. CeO_2 would evolve gaseous O_2 during its transformation to Ce_2O_3 at temperatures above 1400° C in inert atmospheres. This O_2 to be supplied by CeO_2 might then cause, especially at the particle-to-particle interfaces as a surface phenomenon, the initial silicon nitride phase to convert into a family of silicon-oxynitride phases whose compositions would be determined mainly by factors such as the distance from the interface which supplies the oxygen, the magnitude of P_{O_2} in the vicinity of the particles, the temperature and, of course, the time in which such adverse conditions had persisted. The last factor, time, would mainly be controlled by the rate of flushing off of unsought O_2 by the flowing nitrogen atmosphere. Every step of the conversion of silicon nitride to silicon oxynitride would accompany a certain amount of gaseous nitrogen evolution, which would then only be expected to be replaced back by the nitrogen atmosphere.

As opposed to the pure, oxygen apatite sample we used for neutron diffraction studies, the N-doped sample had significant quantities of CeO_{2-x} and monoclinic, high-temperature form of $\text{Ce}_2\text{Si}_2\text{O}_7$ in it which were then needed to be accounted for and excluded in the structural refinements of the major apatite phase. As we have shown recently ⁷, in a study of

the high temperature phase relations in the system Ce_2O_3 - $\text{Ce}_2\text{Si}_2\text{O}_7$, cerium oxygen apatite phase is stable as a line compound in the temperature range 1200° to its melting point 1950°C in inert atmospheres such as purified argon and vacuum, or in reducing atmospheres like argon + 10% H_2 . Although we did not study its behaviour specifically in nitrogen atmospheres, we still would not expect it to decompose into CeO_{2-x} and $\text{Ce}_2\text{Si}_2\text{O}_7$ in pure nitrogen at 1560°C. We have shown that there were no solid solubility between $\text{Ce}_2\text{Si}_2\text{O}_7$ and $\text{Ce}_{9.33}[\text{SiO}_4]_6\text{O}_2$. The only possibility that remains to explain the observation of these minor phases in this sample is that the CeO_{2-x} phase appears to be unreacted and also tended to be isolated in distinct CeO_{2-x} -rich pockets all over the sample pellet. As a consequence of that, some SiO_2 -rich regions (as compared to the line compound stoichiometry of the apatite phase) have developed which would then shift the overall composition of those from apatite towards $\text{Ce}_2\text{Si}_2\text{O}_7$. The presence of these two minor phases in the N-doped sample could be regarded as a unique adverse condition that might still affect the accuracy of the structural refinement presented below.

Being the major question that needs to be answered, the determination of the site(s) that would be preferred by nitrogen in substituting for oxygen was the main concern of this part of the study. We have based the Rietveld refinement of the N-doped sample on the atomic coordinates that were obtained in the first part for the "pure" sample of cerium oxygen apatite. The tetrahedral oxygen sites that were silicon-bonded (i.e., O(1) and O(3)) as well as the "free" oxygen site (O(4)) were refined to a residual $R = 4.3\%$. In each of these refinements nitrogen was placed in those sites as if it was sharing the same site with oxygen. These did not

Table 3. Atomic Parameters of 4800 ppm N-doped $\text{Ce}_{4.67}[\text{SiO}_4]_3\text{O}$

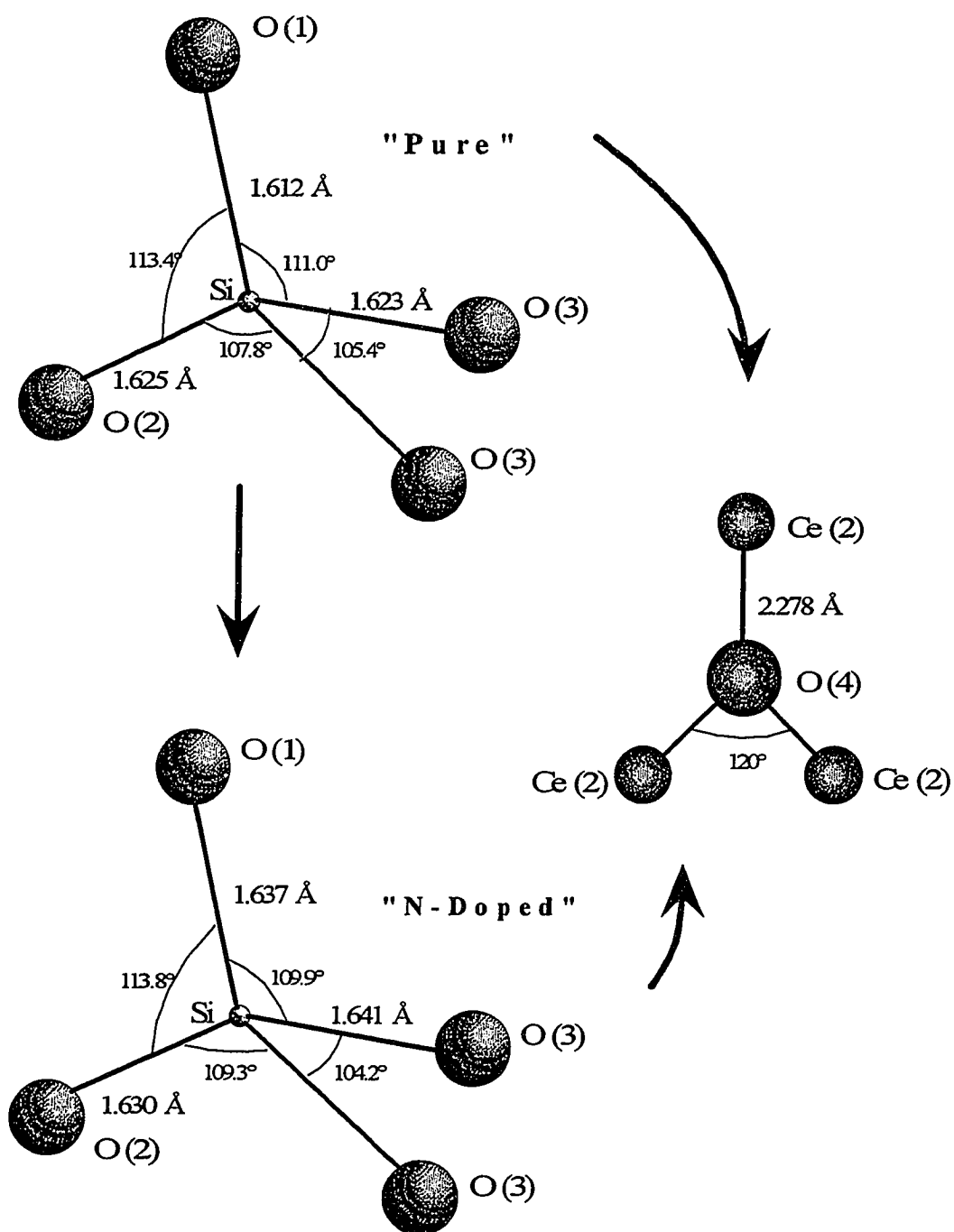
Atom	Occ. factor	x	y	z	U_{iso}
Ce(1)	0.85(2)	0.6667	0.3333	0.0007(19)	3.3 (3)
Ce(2)	1	0.9871(9)	0.2287(8)	0.2500	1.5 (1)
Si	1	0.3731(8)	0.4017(9)	0.2500	1.2 (1)
O(1)	1	0.4850(9)	0.3186(8)	0.2500	3.3 (2)
O(2)	1	0.4744(9)	0.5965(7)	0.2500	2.9 (2)
O(3)	1	0.2526(7)	0.3392(6)	0.0681(6)	3.5 (1)
O(4)	0.61(12)	0.0000	0.0000	0.2500	5.6 (7)
N(4)	0.39	0.0000	0.0000	0.2500	5.6 (7)

result in any significant changes in the atomic coordinates of the structure. The new lattice constants were found to be $a = 9.6585(3) \text{ \AA}$ and $c = 7.1139(4) \text{ \AA}$. They showed a very slight but definite increase in both axes when compared to those of the pure sample. The atomic parameters of the doped sample, while the nitrogen being placed at the O(4) site, are shown in Table 3. The occupancy factor of Ce(1) sites (0.85(2)) is in good agreement with the one predicted by the formula; $\text{Ce}_{9.553}[\text{SiO}_4]_6\text{O}_{1.341}\text{N}_{0.659}$ as 0.88. The occupancy factor refined as 0.39 for the nitrogens sharing the O(4)-sites with oxygen was predicted by the above formula as 0.33. On the other hand, when we put the nitrogens into O(3)-sites and O(1)-sites

separately, the occupancy factors for nitrogen were found to be 0.23 and 0.10, respectively, which were much less than that of predicted by the chemical formula. The temperature factors were found to be 4.3 and 3.7 when the nitrogens were put into O(3) and O(1) sites together with oxygens, respectively.

The response of the interatomic distances and angles to the introduction of 4800 ppm N into the lattice were displayed in Figure 2. Although the slight changes observed in the interatomic distances between the central silicon and four oxygens occupying three different sites may be regarded as insignificant, one could still detect the presence of a geometrical rearrangement and the tendency of the atoms toward the ideal symmetry of a perfect tetrahedra (i.e., equal interatomic distances and angles of 109.28°) in going from "pure" to "N-doped" sample. We believe that the motivation for this movement was mainly the elimination of vacancies at the Ce(1) sites (caused by N substitution in the oxygen sites of the lattice). It would have been quite interesting to see what would happen to the tetrahedra upon the complete elimination of vacancies, i.e., for a sample of $\text{Ce}_{10}[\text{SiO}_4]_6\text{N}_2$. As a further observation, the interatomic distances and angles displayed in Fig. 2 for the "N-doped" sample were virtually the same, after each refinement cycle, for all three candidate sites we examined for N, namely, the O(1)-, O(3)- and O(4)-sites. This means that the presence of N in the lattice does not directly affect the tetrahedral coordination between Si and oxygens. However, if the large nitrogens (1.71 \AA) were really substituting for the tetrahedral oxygens then one would expect to see more pronounced changes in the interatomic distances of individual tetrahedra, especially in the comparison of, for instance, tetrahedral O(3)- and non-tetrahedral

Figure 2. Changes observed in the interatomic distances and angles of the silicate tetrahedra upon doping as opposed to constant Ce(2) - O(4) distances in both samples



O(4)-sites. The filling up of the vacancies in the 9-coordinated (all being silicon-bonded oxygens) Ce(1) positions seemed to have a more definite influence in the geometric rearrangements to be observed within the silicate tetrahedra.

The interatomic distances between the 3-coordinated "free", non-tetrahedral oxygens (O(4)-sites) and the Ce(2) atoms did not show any changes after doping with N and remained constant at 2.28 Å as also indicated in Figure 2. This exemplifies the significantly electropositive character of the heavy cerium atoms and the extent of strong polarizing forces exerted by them on the oxygens or nitrogens that would occupy the 0,0,1/4 or 0,0,3/4 positions which would keep those equal interatomic distances at a value even less than the sum of the individual ionic radii. These positions which are surrounded only by ceriums form the main tunnels along the 6_z axes of the cerium apatite lattice (Figure 3) and they would be the most favourable oxygen sites for nitrogen to substitute for. At nitrogen levels below 14100 ppm (the level of nitrogen dictated by the formula $\text{Ce}_{10}[\text{SiO}_4]_6\text{N}_2$), we believe, it would be more unlikely for N to replace O in the silicon tetrahedra since this would mean the formation of oxygen vacancies in the "free" oxygen sites surrounded by three highly electropositive cerium atoms. At higher nitrogen levels such as 21700 and 24400 ppm, as reported by Gaude⁴, the apatite structure was no longer stable, and it decomposed to Ce_2SiO_5 and $\text{Ce}_2\text{Si}_2\text{O}_7$. We believe that it would be quite unlikely to be able to ascertain the exact positions occupied by N in the apatite lattice just by thermogravimetric analysis and powder XRD as attempted for cerium apatite by Gaude⁴ and recently for yttrium apatite by Veyret et al.⁸.

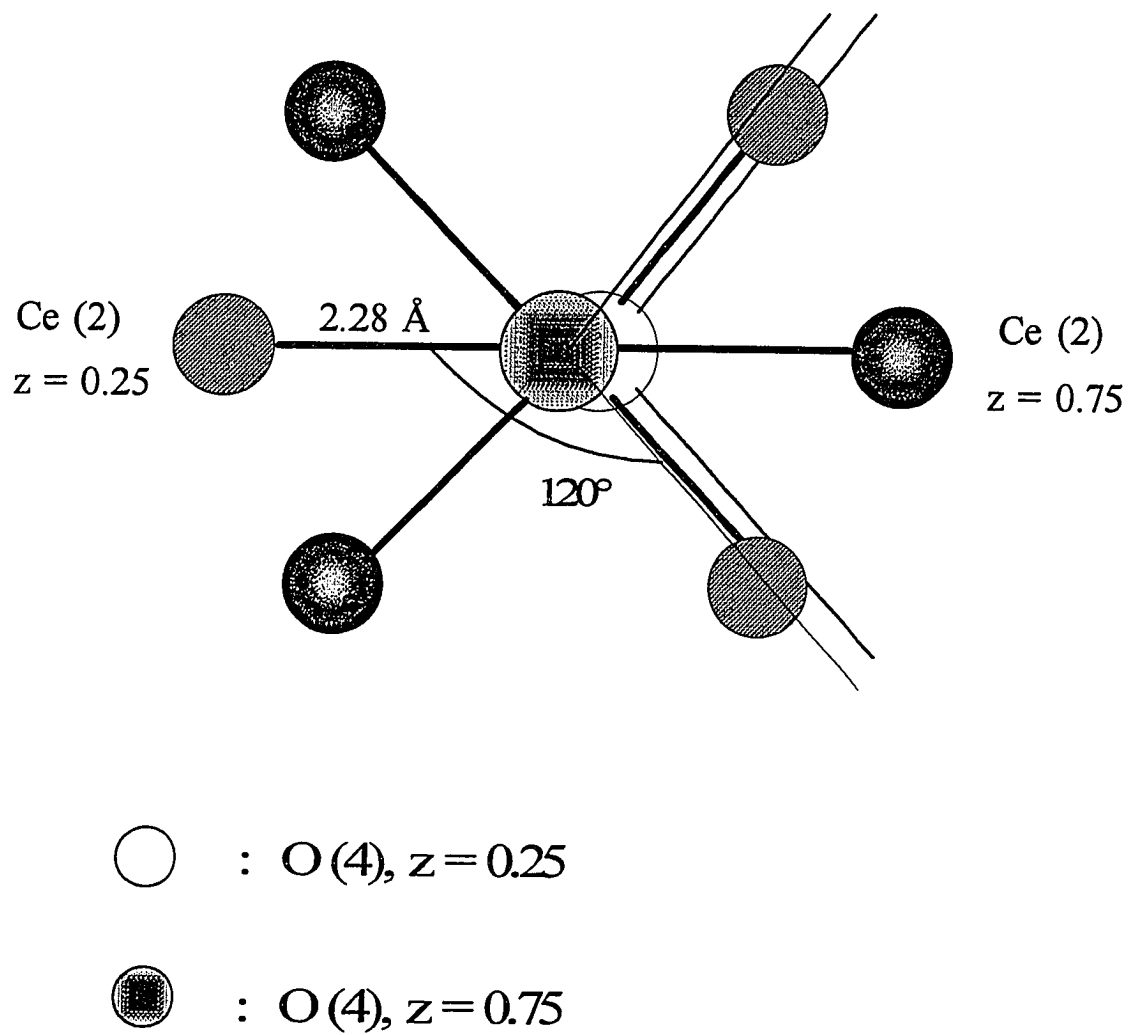


Figure 3. The main tunnels of the cerium apatite structure along the 6_z axes

CONCLUSIONS

Neutron diffraction experiments were carried out on samples of pure ($\text{Ce}_{9.33}[\text{SiO}_4]_6\text{O}_2$) and N-doped ($\text{Ce}_{9.553}[\text{SiO}_4]_6\text{O}_{1.341}\text{N}_{0.659}$) cerium apatite phase. Rietveld analyses were performed on both pure and N-doped cerium apatite. The effective ionic radius of Ce^{3+} cation in the apatite structure was found to be 1.177 Å. The interatomic distances and angles in the silicate tetrahedra were found to change slightly upon N-doping but they remained insensitive to the placement of N on the individual tetrahedral oxygen sites; O(1)- and O(3)-sites. Placing nitrogen on the non-tetrahedral O(4)-sites also produced the same interatomic distances and angles. The rearrangements observed in the structure upon N-doping could be explained by the filling up of the vacant sites in Ce(1)-sites. The density measurements were found to be inadequate in determining the levels of vacancy elimination in those sites at such low levels of N-doping investigated here. The most likely positions for nitrogen to substitute for oxygens of the lattice were deduced to be the 0,0,1/4 and 0,0,3/4 sites (O(4)-sites) at low levels of N-doping, such as 4800 ppm, since these sites are located at the center of the main tunnels of the lattice and are surrounded only by trivalent ceriums. The strongly electropositive character of Ce caused the Ce(2)-O(4) distances (in pure sample) and Ce(2)-N distances (in N-doped sample) to remain constant at 2.28 Å.

ACKNOWLEDGEMENT

We are grateful for the use of the HIPD instrument at LANSCE. Los Alamos National Laboratory is operated under a U.S. Government contract (W-7405-ENG-36) by the University of California for the U.S. Department of Energy.

REFERENCES

- ¹ A.C. Tas and M. Akinc, "Cerium Oxygen Apatite ($\text{Ce}_{4.67}[\text{SiO}_4]_3\text{O}$) X-Ray Diffraction Pattern Revisited," *Powder Diffraction*, **7**, 219-222 (1992).
- ² J.P. Guha, "The Silicon-cerium-oxynitride $\text{Ce}_5(\text{SiO}_4)_3\text{N}$ with Fluoroapatite Structure," *J. Mater. Sci.*, **15**, 521-522 (1980).
- ³ J. Felsche, "The Crystal Chemistry of the Rare Earth Silicates," *Structure and Bonding*, **13**, 99-197 (1973).
- ⁴ J. Gaude, "Nouveaux Resultats sur les Apatites Azotees. I. - Le Type $\text{Ln}_{10}\text{Si}_6\text{N}_2\text{O}_{24}$ Relatif au Cerium," *Revue de Chimie Minerale*, **24**, 22-27 (1987).
- ⁵ GSAS, A.C. Larson and R.B. VonDreele, LANSCE, MS-HB05, Los Alamos National Laboratory, Los Alamos, NM 87545, Copyright 1985-1993 : The Regents of the University California.
- ⁶ E.L. Belokoneva, T.L. Petrova, M.A. Simonov and N.V. Belov, "Crystal Structure of Synthetic TR Analogs of Apatite $\text{Dy}_{4.67}[\text{SiO}_4]_3\text{O}$ and $\text{Ce}_{4.67}[\text{SiO}_4]_3\text{O}$," *Soviet Physics - Crystallography*, **17**, 429-431 (1972).

- ⁷ A.C. Tas and M. Akinc, "Phase Relations in the System Ce_2O_3 - $\text{Ce}_2\text{Si}_2\text{O}_7$ in the Temperature Range 1150° to 1970°C in Reducing and Inert Atmospheres," To be published.
- ⁸ J.B. Veyret, M. Voorde and M. Billy, "Oxidation Behavior of Silicon Yttrium Oxynitride," *J. Am. Ceram. Soc.*, **75**, 3289-3292 (1992).

GENERAL SUMMARY

Prior to this study, the available phase diagram for the binary Ce_2O_3 - SiO_2 did only include two of the three binary compounds that existed in this system. The missing compound from this binary, i.e., $\text{Ce}_{4.67}[\text{SiO}_4]_3\text{O}$, had two slightly different XRD patterns listed in the JCPDS database referring to the same structure. $\text{Ce}_2\text{Si}_2\text{O}_7$ was known to exhibit only the high temperature, pseudo-orthorhombic polymorph as opposed to the other light lanthanide pyrosilicates which all also had a low temperature, tetragonal polymorph. Ce_2SiO_5 was expected to have a monoclinic structure similar to those in the other light lanthanide oxyorthosilicates. Ce_2SiO_5 did not have an XRD pattern listed in JCPDS database. The stability ranges and the melting points of all the three silicates were unknown prior to this study. CeAlO_3 , 1:1 compound in Ce_2O_3 - Al_2O_3 binary, was claimed to exhibit two polymorphic forms (cubic, high-temperature and rhombohedral, low-temperature) both appeared to be perovskite-like structures. $\text{Ce}_2\text{O}_3 \cdot 11\text{Al}_2\text{O}_3$ also did not have an XRD pattern like Ce_2SiO_5 and its crystal structure has needed to be decided between the two candidates magnetoplumbite and beta-alumina. There were no phase equilibria studies in the CeO_2 (Ce_2O_3) - Al_2O_3 - SiO_2 ternary. Few compositions studied (by O'Brien and Akinc, see paper 2, Ref.8), in an air atmosphere, in this ternary produced unique microstructures displaying web-like $\text{Ce}_2\text{Si}_2\text{O}_7$ strands in a liquid matrix together with large corundum and ceria grains. Such microstructures were found to improve the resistance of ceria-doped alumino-silicate refractories to the transport of molten alloys.

It was found that cerium pyrosilicate, $\text{Ce}_2\text{Si}_2\text{O}_7$, like other light lanthanide pyrosilicates, has two polymorphic forms. The high-temperature polymorph was shown, for the first time, to be monoclinic rather than pseudo-orthorhombic. The low-temperature, tetragonal polymorph of $\text{Ce}_2\text{Si}_2\text{O}_7$ has been found to form upon very slow cooling the high-temperature form to and below $1274 \pm 5^\circ\text{C}$. Two new XRD patterns were suggested for both polymorphs of $\text{Ce}_2\text{Si}_2\text{O}_7$. The melting of $\text{Ce}_2\text{Si}_2\text{O}_7$ was found to occur at $1788 \pm 5^\circ\text{C}$. A binary phase diagram for the Al_2O_3 - $\text{Ce}_2\text{Si}_2\text{O}_7$ system has been suggested for the first time. A eutectic reaction was found to occur, between the end members of this system, at $1375 \pm 5^\circ\text{C}$ and 51 mol% $\text{Ce}_2\text{Si}_2\text{O}_7$. No solid solubility has been detected between the phases of this system. The enthalpy of melting of cerium pyrosilicate was calculated as 36.81 kJ/mol from the slope of the $\text{Ce}_2\text{Si}_2\text{O}_7$ -liquidus.

The high temperature phase relations have been investigated in the Ce_2O_3 - $\text{Ce}_2\text{Si}_2\text{O}_7$ system and a binary phase diagram has been constructed, for the first time, in the temperature range 1150° to 1970°C . Three eutectic reactions were found to occur between the end members and the two other binary compounds; Ce_2SiO_5 and $\text{Ce}_{4.67}[\text{SiO}_4]_3\text{O}$, of this system. The eutectic reaction between Ce_2O_3 and Ce_2SiO_5 was observed to occur at $1664 \pm 8^\circ\text{C}$ and 27 mol% SiO_2 . Ce_2SiO_5 was found to melt congruently at $1970 \pm 30^\circ\text{C}$. The eutectic reaction between Ce_2SiO_5 and $\text{Ce}_{4.67}[\text{SiO}_4]_3\text{O}$ was found to occur at $1870 \pm 25^\circ\text{C}$ and 54 mol% SiO_2 . $\text{Ce}_{4.67}[\text{SiO}_4]_3\text{O}$ melted congruently at $1950 \pm 30^\circ\text{C}$. The third eutectic reaction of this system was found to occur between $\text{Ce}_{4.67}[\text{SiO}_4]_3\text{O}$ and $\text{Ce}_2\text{Si}_2\text{O}_7$ at $1762 \pm 10^\circ\text{C}$ and 65 mol% SiO_2 . The enthalpy of melting of both Ce_2SiO_5 and $\text{Ce}_{4.67}[\text{SiO}_4]_3\text{O}$ were calculated from the slopes of

the relevant liquid as 102.3 kJ/mol and 222.5 kJ/mol, respectively. No solid solubility has been detected between the phases of this system.

$\text{Ce}_{4.67}\square_{0.33}[\text{SiO}_4]_3\text{O}$, by having vacancies in the cation-sites which allows the charge - coupled substitutions to occur more readily as compared to the other two binary Ce-silicate compounds, was predicted to be able to absorb and tolerate nitrogen in its structure upto a level of 14100 ppm. Nitrogen-contaminated samples of the nominal apatite stoichiometry have been shown to retain the same hexagonal crystal structure of pure cerium oxygen apatite with similar lattice parameters. The similarity in the lattice parameters of pure and N-doped samples was shown to be a source of confusion in the literature in distinguishing between the two. A new XRD pattern has been suggested for pure $\text{Ce}_{4.67}[\text{SiO}_4]_3\text{O}$ in this study. Neutron diffraction experiments performed on both pure and N-doped samples of cerium oxygen apatite, for the first time on any of the lanthanide silicates, showed nitrogen to prefer the non-silicon bonded oxygen sites in the cerium oxygen apatite structure to substitute for oxygen rather than the tetrahedral, silicon-bonded sites.

One of the two binary compounds that we were able to synthesize in the Ce_2O_3 - Al_2O_3 system, CeAlO_3 , was shown to be stable in a perovskite-like structure with a slight tetragonal distortion from room temperature to 1950°C. A new XRD pattern, for the first time, has been suggested for CeAlO_3 with the lattice parameters $a = 3.763 \text{ \AA}$ and $c = 3.792 \text{ \AA}$. The second binary compound of this system, $\text{CeAl}_{11}\text{O}_{18}$, was shown to melt incongruently at $1915 \pm 25^\circ\text{C}$ confirming the findings of the previous researchers. An XRD pattern is suggested, for the first time, for pure $\text{CeAl}_{11}\text{O}_{18}$ having a hexagonal crystal structure with $a = 5.558 \text{ \AA}$ and

$c = 22.012 \text{ \AA}$. Its crystal structure was predicted to resemble that of magnetoplumbite rather than Na- β' -alumina. Eutectic-like microstructures, with sub-micron spaced lamellae, were observed and reported, for the first time in any of lanthanide-aluminate systems. The most recent version of the binary phase diagram for the $\text{Ce}_2\text{O}_3 - \text{Al}_2\text{O}_3$ system was confirmed to be accurate by this study.

Considering the fact that in none of the lanthanide alumino-silicate systems the ternary phase equilibria have not yet been studied, future research in the ternary system $\text{CeO}_2 (\text{Ce}_2\text{O}_3) - \text{Al}_2\text{O}_3 - \text{SiO}_2$ should focus on the ternary phase relations including the study of the joins such as $\text{Al}_2\text{O}_3 - \text{Ce}_{4.67}[\text{SiO}_4]_3\text{O}$, $\text{Al}_2\text{O}_3 - \text{Ce}_2\text{SiO}_5$, and $3\text{Al}_2\text{O}_3 \cdot 2\text{SiO}_2 - \text{CeO}_2 (\text{Ce}_2\text{O}_3)$ to complement the outcome of this study. Many structural similarities that were previously reported to exist between the silicates and aluminates of light lanthanides would also warrant the further x-ray or neutron diffraction studies of the light lanthanide (La, Pr, Nd, Sm, etc.) pyrosilicate phases which were all reported to have pseudo-orthorhombic high-temperature forms. Comparative structural and phase stability studies would also be required among the light lanthanide mono- or hexa-aluminates to achieve a better understanding of these materials.

ACKNOWLEDGEMENTS

I would like to thank my major professor, Dr. Mufit Akinc, for his help, guidance, patience, friendship, and genuine concern throughout my time here.

I would like to give special thanks to Dr. Victor G. Young, Jr. , Dr. Scott M. Schlorholtz and Dr. Warren E. Straszheim for the considerable amount of expertise and advice they shared with me regarding the experimental aspects of my work.

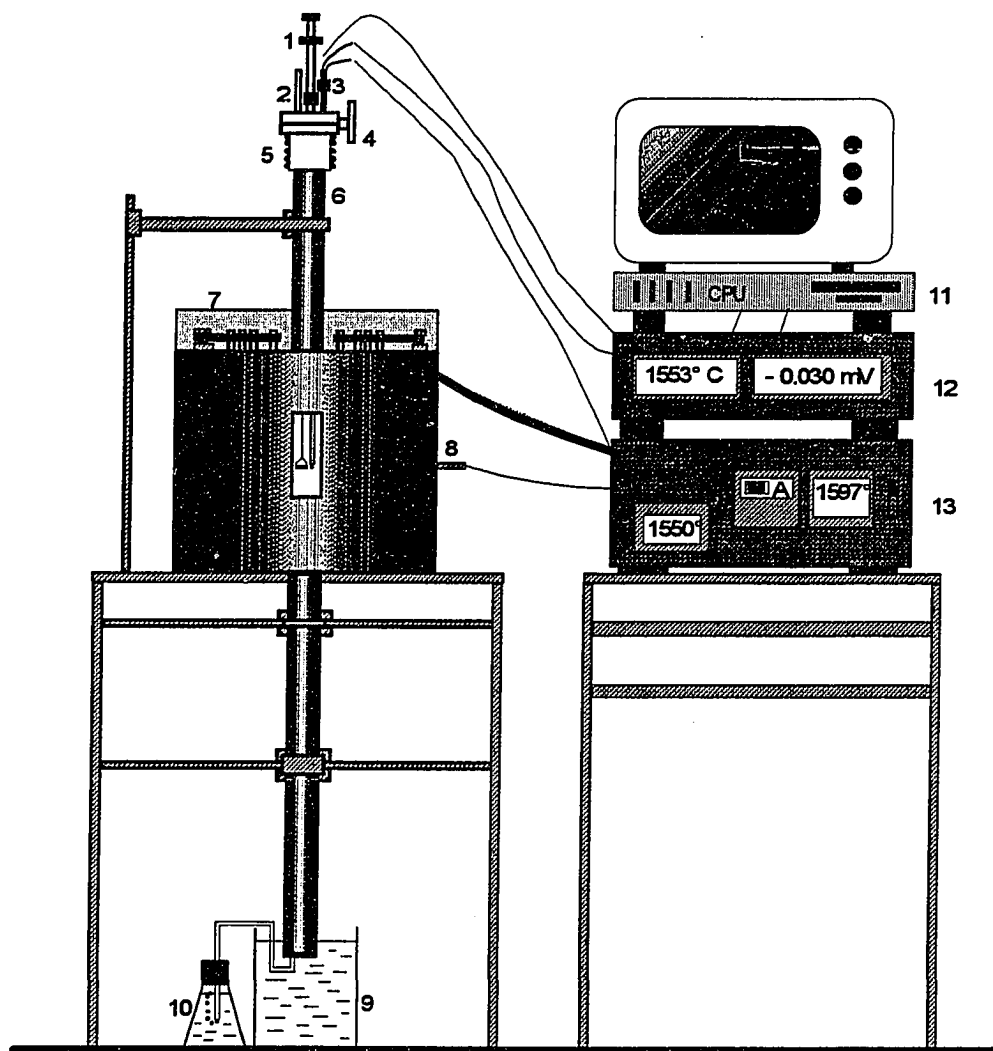
I also wish to thank my family for their support and understanding through my years at Iowa State University.

The financial support for this work was provided by Middle East Technical University, Ankara, Turkey, McKnight Foundation, St. Paul, MN and Iowa State University.

**APPENDIX A. SCHEMATIC OF THE QUENCHING FURNACE AND DTA
ACCESSORIES USED IN THIS STUDY**

Figure 1. Schematic of the quenching furnace used

- 1. Pick up tool used to drop the sample crucibles**
- 2. Gas inlet**
- 3. Sample thermocouple or DTA unit inlet**
- 4. Half-nipple, flange, O-ring and clamp assembly**
- 5. Water-cooling**
- 6. Mullite or alumina furnace tube**
- 7. MoSi_2 heating elements**
- 8. B-type furnace control thermocouple inlet**
- 9. Quench bath sealing the bottom end of the furnace tube**
- 10. Bubbler**
- 11. Microcomputer used in collecting the DTA data**
- 12. High sensitivity multimeters fed by the DTA thermocouples**
- 13. Sample thermocouple temperature indicator, SCR unit and temperature controller housing**



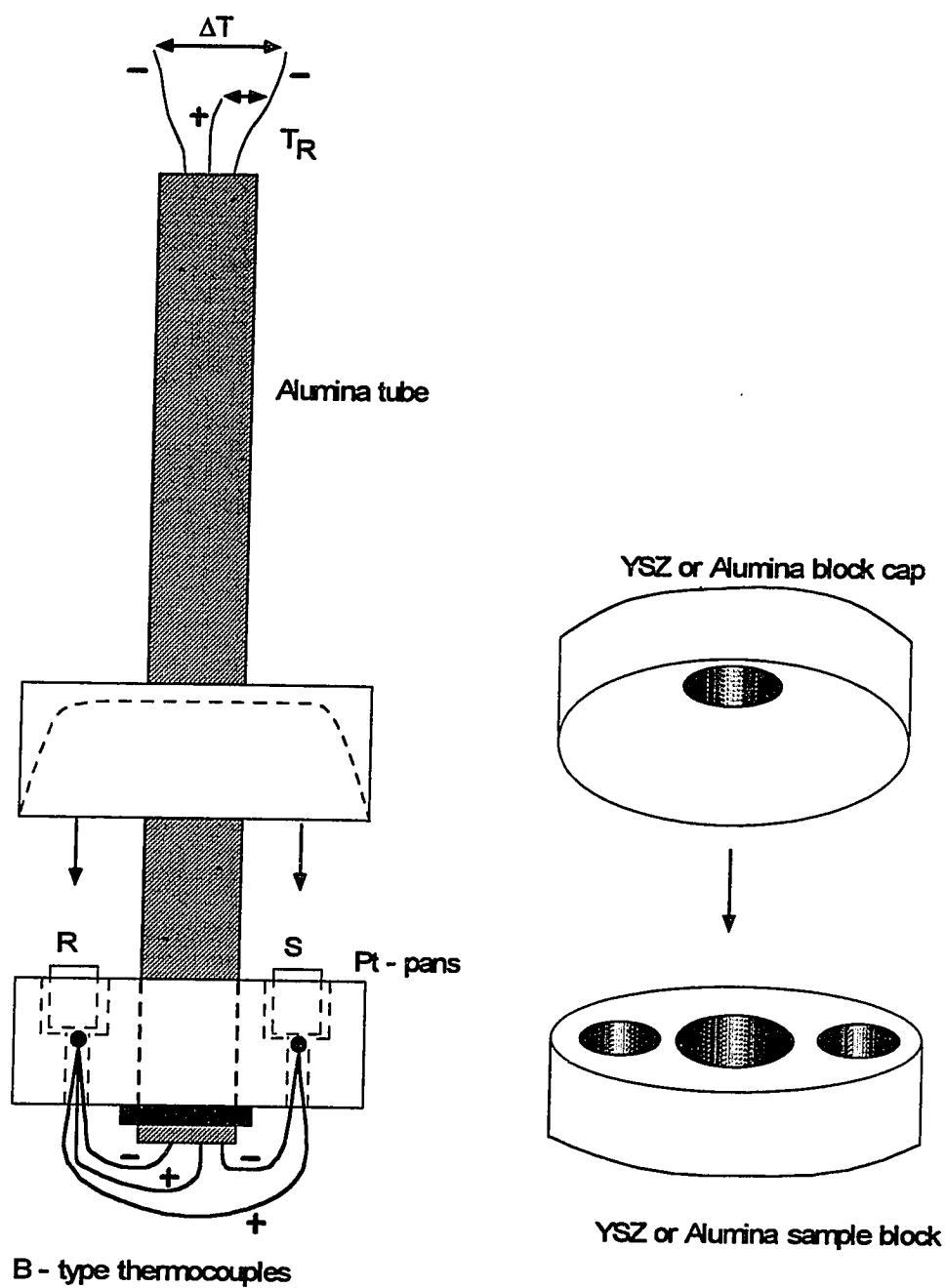


Figure 2. DTA unit built for use in the MoSi_2 quench furnace under controlled atmosphere. This unit was designed to operate in the temperature range 700° to 1700°C

**APPENDIX B. LISTINGS OF THE PROGRAM WRITTEN IN BASIC FOR THE DTA
MODULES OF THIS STUDY**

```

COMMON SHARED thermocouple$
COMMON SHARED baddata
COMMON SHARED firsttime
COMMON SHARED escape
COMMON SHARED dtainterval, degreechange
COMMON SHARED filename$
COMMON SHARED centerspot, filestringlocation
COMMON SHARED fileexistsvar
COMMON SHARED newfileperiod, newfile
COMMON SHARED dayflag, days
DECLARE SUB makeextensionfilename (tempfilename$, outputfilename$)
DECLARE SUB retrievedata (fromaddress$, datastring$)
DECLARE FUNCTION fileexists! (tempfile$)
DECLARE SUB readline (outputstring$, temprow!, tempcol!, length,
escapepressed)
DECLARE SUB tidyfilename (trialfilename$, filenameok!)
DECLARE SUB getfilename ()
DECLARE SUB changedtainterval ()
DECLARE SUB getescape ()
DECLARE SUB notes ()
DECLARE SUB bailout (escapenotpressed!)
DECLARE SUB drawwindow (lhcol!, lhrow!, rhcol!, rhrow!)
DECLARE SUB getoption (option$, optionset$)
DECLARE SUB mainmenu ()
DECLARE SUB getinterrupt ()
DECLARE SUB takedata ()
DECLARE SUB initglobalvars ()
DECLARE SUB resetclock ()
DECLARE SUB gettime (timevar!)
DECLARE SUB clearkeyboardbuffer ()
DECLARE SUB titlescreen ()
DECLARE SUB center (tempcol!, temprow!, inputstring$)
DECLARE SUB symbol (temprow!, tempcol!, inputstring$)
CLS

```

```

CALL initglobalvars
CALL titlescreen
CALL mainmenu
DO
  optionset$ = "RFNITQ"
  CALL getoption(option$, optionset$)
  IF option$ = "R" THEN
    oktogo = 0
    CALL bailout(oktogo)
    IF oktogo THEN
      CALL takedata
    END IF
    CALL mainmenu
  ELSEIF option$ = "N" THEN
    CALL notes
    CALL mainmenu
  ELSEIF option$ = "F" THEN
    CALL getfilename
    CALL mainmenu
  ELSEIF option$ = "I" THEN
    CALL changedtainterval
  ELSEIF option$ = "T" THEN
    IF thermocouple$ = "C-TYPE" THEN
      thermocouple$ = "OTHER "
    ELSE
      thermocouple$ = "C-TYPE"
    END IF
    CALL center(40, 9, "{h}T{h}hermocouple type: " + thermocouple$)
  ELSEIF option$ = "Q" THEN
    EXIT DO
  END IF
LOOP
CLS
CLOSE #1
END

```

errorhandler:

```
IF ERR = 53 THEN
  fileexistsvar = 0
  RESUME NEXT
ELSE
  fileexistsvar = 2
  RESUME NEXT
END IF
```

```
SUB bailout (escapenotpressed)
  CALL clearkeyboardbuffer
  CALL drawwindow(10, 7, 70, 9)
  CALL center(40, 8, "You have 5.0 seconds to hit {h}[ESC]{} to abort the
run.")
```

```
escape = 0
CALL resetclock
DO
  CALL getinterrupt
  CALL gettime(temptimevar)
  IF escape THEN
    escapenotpressed = 0
    EXIT DO
  ELSEIF temptimevar >= 5 THEN
    escapenotpressed = 1
    EXIT DO
  END IF
LOOP
END SUB
```

```
SUB center (tempcol, temprow, inputstring$)
  lengthofstring = LEN(inputstring$)
  highlightstart = INSTR(inputstring$, "{h}")
  highlightend = INSTR(inputstring$, "{}")
  IF highlightstart <> 0 THEN
    lengthofstring = lengthofstring - 3
```



```

END IF
IF highlightend <> 0 THEN
    lengthofstring = lengthofstring - 2
END IF
centerspot = tempcol - INT(lengthofstring) / 2
CALL symbol(centerspot, temprow, inputstring$)
END SUB

SUB changedtainterval
    escaped = 0
    CALL readline(dtintervalstr$, 55, 7, 5, escaped)
    IF escaped = 0 THEN
        dtinterval = VAL(dtintervalstr$)
    END IF
    CALL symbol(54, 7, STR$(dtinterval))
END SUB

SUB clearkeyboardbuffer
    DO
        IF INKEY$ = "" THEN
            EXIT DO
        END IF
    LOOP
END SUB

SUB drawwindow (lhcol, lhrow, rcol, rrow)
    REM draw top left-hand corner
    LOCATE lhrow, lhcol, 0
    PRINT CHR$(201);

    REM draw top line
    FOR temploop = lhcol + 1 TO rcol - 1
        PRINT CHR$(205);
    NEXT temploop

    REM alternate drawing left-hand line then right-hand line

```

```

LOCATE lthrow + 1, lhcol, 0
FOR temploop = lthrow + 1 TO rthrow - 1
  LOCATE temploop, lhcol, 0
  PRINT CHR$(186)
  LOCATE temploop, rhcol, 0
  PRINT CHR$(186)
NEXT temploop

```

```

REM draw top right-hand corner
LOCATE lthrow, rhcol, 0
PRINT CHR$(187);

```

```

REM draw bottom left-hand corner
LOCATE rthrow, lhcol, 0
PRINT CHR$(200);

```

```

REM draw bottom line
FOR temploop = lhcol + 1 TO rhcol - 1
  PRINT CHR$(205);
NEXT temploop

```

```

REM draw bottom right-hand corner
LOCATE rthrow, rhcol, 0
PRINT CHR$(188);
END SUB

```

```

FUNCTION fileexists (tempfile$)
ON ERROR GOTO errorhandler
fileexistsvar = 1
OPEN tempfile$ + ".001" FOR INPUT AS #4
fileexists = fileexistsvar
IF fileexistsvar = 2 THEN
  CALL center(40, 5, "      File ERROR. Try different name.      ")
  CALL center(40, 6, "Hit {h}[ESC]{} to continue.")
  CALL getescape
END IF

```

```
CLOSE #4
EXIT FUNCTION
```

```
END FUNCTION
```

```
SUB getescape
CALL clearkeyboardbuffer
DO
  IF INKEY$ = CHR$(27) THEN
    EXIT DO
  END IF
LOOP
END SUB
```

```
SUB getfilename
  escaped = 0
  nameok = 1
  CALL readline(tempfilename$, filestringlocation, 4, 30, escaped)
  IF escaped = 0 THEN
    CALL tidyfilename(tempfilename$, nameok)
    IF nameok THEN
      temp = fileexists(tempfilename$)
      IF temp = 2 THEN
        nameok = 0
      ELSEIF temp = 1 THEN
        CALL drawwindow(22, 3, 58, 5)
        CALL center(40, 4, "File Exists. Overwrite(Y/N)?")
        CALL clearkeyboardbuffer
        DO
          response$ = INPUT$(1)
          response$ = UCASE$(response$)
          IF response$ = "Y" THEN
            nameok = 1
            EXIT DO
          ELSEIF response$ = "N" THEN
            nameok = 0
          END IF
        LOOP
      END IF
    END IF
  END IF
END SUB
```

```

        EXIT DO
    END IF
LOOP
END IF
END IF
ELSE
    nameok = 0
END IF

IF nameok THEN
    filenam$ = tempfilename$
END IF
END SUB

SUB getinterrupt
    IF INKEY$ = CHR$(27) THEN
        escape = 1
    END IF
END SUB

SUB getoption (outkey$, set$)
    CALL clearkeyboardbuffer
    DO
        tempkey$ = INPUT$(1)
        tempkey$ = UCASE$(tempkey$)
        keyinset = INSTR(set$, tempkey$)
        IF (keyinset > 0) THEN
            EXIT DO
        END IF
    LOOP
    outkey$ = tempkey$
END SUB

SUB gettime (timevar)
    timestring$ = TIME$
    temphours = VAL(MID$(timestring$, 1, 2))

```

```

tempminutes = VAL(MID$(timestring$, 4, 2))
tempseconds = VAL(MID$(timestring$, 7, 2))
temptimevar = temphours * 3600 + tempminutes * 60 + tempseconds
timevar = 65536 * 2: REM To make sure compiler makes timevar DOUBLE or
REAL
timevar = temptimevar - firsttime

```

```

IF timevar < 0 THEN
  IF dayflag = 1 THEN
    days = days + 1
    dayflag = 0
  END IF
ELSE
  dayflag = 1
END IF
timevar = timevar + 24! * 60! * 60! * days
END SUB

```

```

SUB initglobalvars
  OPEN "COM2:4800,O,7,1,CS,DS,RS" FOR RANDOM AS #1
  REM -- No handshaking. CS, DS lines are disconnected.

  FOR x = 1 TO 300
  NEXT x
  PRINT #1, "*00W2000"
  escape = 0
  filenam$ = "C:\NEWPORT\DTATEST"
  dtainterval = 2
  degreechange = 2
  newfile = 0
  newfileperiod = 1
  dayflag = 1
  days = 0
  thermocouple$ = "C-TYPE"
  REM two thermocouple types exist in this program, "C-TYPE" and "OTHER"
END SUB

```

```

SUB mainmenu
  CLS
  CALL center(40, 1, "MENU")
  CALL center(40, 4, "{h}F{}ilename: " + filename$)
  filestringlocation = centerspot + 10
  CALL symbol(23, 7, "{h}I{}nterval between DTA readings: " +
STR$(dtainterval)

  CALL center(40, 9, "{h}T{}hermocouple type: " + thermocouple$)
  CALL center(40, 12, "{h}R{}un ")
  CALL center(40, 13, "{h}Q{}uit")

  CALL center(40, 17, "Experiment {h}N{}otes:")
  LOCATE 15, 1, 0
  FOR temploop = 1 TO 80
    PRINT CHR$(205);
  NEXT temploop
END SUB

SUB makeextensionfilename (tempfilename$, outputfilename$)
  extension$ = STR$(newfileperiod)
  IF LEFT$(extension$, 1) = " " THEN
    extension$ = RIGHT$(extension$, LEN(extension$) - 1)
  END IF

  IF LEN(extension$) = 1 THEN
    extension$ = "00" + extension$
  ELSEIF LEN(extension$) = 2 THEN
    extension$ = "0" + extension$
  END IF
  outputfilename$ = tempfilename$ + "." + extension$
END SUB

SUB notes
  escaped = 0

```

```

CALL drawwindow(5, 18, 75, 24)
CALL center(40, 19, "Press {h}[RETURN]{} to save line")
CALL center(40, 20, "Press {h}[ESC]{} to exit")
notefile$ = filename$ + ".NOT"
OPEN notefile$ FOR OUTPUT AS #3
CALL readline(line1$, 8, 21, 64, escaped)
IF escaped = 0 THEN
    PRINT #3, line1$
    CALL readline(line2$, 8, 22, 64, escaped)
END IF
IF escaped = 0 THEN
    PRINT #3, line2$
    CALL readline(line3$, 8, 23, 64, escaped)
END IF
IF escaped = 0 THEN
    PRINT #3, line3$
END IF
CLOSE #3
END SUB

SUB readline (outputstring$, tempcol, temprow, length, escapepressed)
    escapepressed = 0
    outputstring$ = ""
    COLOR 15, 0, 0
    tempfirsttime = 1
    templength = 0
    ch$ = ""
    CALL clearkeyboardbuffer
    LOCATE temprow, tempcol, 1

    DO
    IF (tempcol > 80) OR (templength >= length) THEN
        EXIT DO
    END IF

    LOCATE temprow, tempcol, 1

```

```

ch$ = INPUT$(1)
tempch$ = LEFT$(ch$, 1)
ch$ = tempch$
CALL clearkeyboardbuffer

IF (tempfirsttime = 1) THEN
  tempfirsttime = 0
  blanks$ = ""
  FOR temploop5 = 1 TO length
    blanks$ = blanks$ + " "
  NEXT temploop5
  CALL symbol(tempcol, temprow, blanks$)
  LOCATE temprow, tempcol, 1
END IF

IF (ch$ = CHR$(8)) AND (LEN(outputstring$) > 0) THEN
  tempcol = tempcol - 1
  templength = templength - 1
  outputstring$ = LEFT$(outputstring$, LEN(outputstring$) - 1)
ELSEIF (ch$ = CHR$(8)) THEN
  REM do nothing
ELSEIF (ch$ = CHR$(13)) THEN
  EXIT DO
ELSEIF (ch$ = CHR$(27)) THEN
  escapepressed = 1
  EXIT DO
ELSE
  CALL symbol(tempcol, temprow, ch$)
  tempcol = tempcol + 1
  templength = templength + 1
  outputstring$ = outputstring$ + ch$
END IF
LOOP

COLOR 7, 0, 0
END SUB

```


SUB resetclock

 timestring\$ = TIME\$

 temphours = VAL(MID\$(timestring\$, 1, 2))

 tempminutes = VAL(MID\$(timestring\$, 4, 2))

 tempseconds = VAL(MID\$(timestring\$, 7, 2))

 firsttime = temphours * 3600 + tempminutes * 60 + tempseconds

 dayflag = 1

 days = 0

END SUB

SUB retrievedata (fromaddress\$, datastring\$)

 temploop = 0

 okdata = 1

 datastring\$ = ""

 PRINT #1, "*" + fromaddress\$ + "X04": REM + CHR\$(13)

 REM -- Adding a carriage return at the end of the mnemonic would

 REM -- occasionally cause a meter to return the message

 REM -- "<ADDRESS>X46<CR>", meaning the mnemonic was of incorrect length.

DO

 IF (LOC(1) = 13) THEN

 datastring\$ = INPUT\$(13, #1)

 IF RIGHT\$(datastring\$, 1) = CHR\$(13) THEN

 tempstring2\$ = LEFT\$(datastring\$, LEN(datastring\$) - 1)

 datastring\$ = tempstring2\$

 ELSE

 okdata = 0

 END IF

 EXIT DO

END IF

IF (temploop > 2000) THEN

 datastring\$ = INPUT\$(LOC(1), 1)

 okdata = 0

```

    EXIT DO
  END IF
  temploop = temploop + 1
LOOP
  IF okdata = 1 THEN
    tempaddress$ = LEFT$(datastring$, 2)
    IF tempaddress$ <> fromaddress$ THEN
      okdata = 0
    END IF
    datastring$ = RIGHT$(datastring$, LEN(datastring$) - 5)
  END IF

  IF okdata = 1 THEN
    negative = 0
    DO
      IF (LEFT$(datastring$, 1) <> "0") AND (LEFT$(datastring$, 1) <> "-")
THEN
        EXIT DO
      END IF
      IF LEFT$(datastring$, 1) = "-" THEN
        negative = 1
      END IF
      datastring$ = RIGHT$(datastring$, LEN(datastring$) - 1)
    LOOP

    IF negative = 1 THEN
      datastring$ = "-" + datastring$
    END IF

    DO
      IF LEN(datastring$) >= 7 THEN
        EXIT DO
      END IF
      datastring$ = " " + datastring$
    LOOP

```

```

IF RIGHT$(datastring$, 1) = "." THEN
    tempstring2$ = " " + LEFT$(datastring$, LEN(datastring$) - 1)
    datastring$ = tempstring2$
END IF
END IF

```

```

IF okdata = 0 THEN
    IF LOC(1) > 0 THEN
        tempstring2$ = INPUT$(LOC(1), 1)
    END IF
    PRINT #1, "*00Z04" + CHR$(13)
    PRINT "***** HARD RESET: "; fromaddress$; " *****"
    FOR temploop2 = 1 TO 3000
        NEXT temploop2
    IF LOC(1) > 0 THEN
        tempstring2$ = INPUT$(LOC(1), 1)
    END IF
    baddata = 1
END IF
REM PRINT fromaddress$; "X"; datastring$; "X"
END SUB

```

```

SUB symbol (tempcol, temprow, inputstring$)
    highlighted = INSTR(inputstring$, "{h}")
    LOCATE temprow, tempcol, 0
    COLOR 7, 0, 0
    index = 1
    printdone = 0
    DO
        IF highlighted = index THEN
            index = index + 3
            EXIT DO
        ELSEIF index > LEN(inputstring$) THEN
            printdone = 1
            EXIT DO
        ELSE

```

```

    PRINT MID$(inputstring$, index, 1);
    index = index + 1
END IF
LOOP

```

```

IF printdone = 0 THEN
COLOR 15, 0, 0
stophighlight = INSTR(index, inputstring$, "{}")
DO
    IF stophighlight = index THEN
        index = index + 2
        EXIT DO
    ELSEIF index > LEN(inputstring$) THEN
        printdone = 1
        EXIT DO
    ELSE
        PRINT MID$(inputstring$, index, 1);
        index = index + 1
    END IF
LOOP
END IF

```

```

IF printdone = 0 THEN
    COLOR 7, 0, 0
    FOR temploop = index TO LEN(inputstring$)
        PRINT MID$(inputstring$, temploop, 1);
    NEXT temploop
END IF

```

```

    COLOR 7, 0, 0
END SUB

```

```

SUB takedata
CLS
CALL clearkeyboardbuffer
escape = 0

```

```

newfile = 1
newfileperiod = 1
firstreading = 1
needtoresetclock = 1
fileopened = 0

```

```

IF LOC(1) > 0 THEN
  dummystring$ = INPUT$(LOC(1), 1)
END IF
PRINT #2, "Resetting controllers..."
PRINT "Resetting controllers..."
PRINT #1, "*00Z04"
FOR temploop9 = 1 TO 3000
NEXT temploop9
IF LOC(1) > 0 THEN
  dummystring$ = INPUT$(LOC(1), 1)
END IF

```

```

CALL resetclock
CALL symbol(4, 3, "Press {h}[ESC]{} to stop taking data.")
LOCATE 4, 1

```

```

DO
  CALL getinterrupt
  IF (escape = 1) OR (newfile = 1) THEN
    IF (escape = 1) THEN
      IF fileopened = 1 THEN
        CLOSE #2
      END IF
      EXIT DO
    ELSE
      IF fileopened = 1 THEN
        CLOSE #2
      END IF
      CALL makeextensionfilename(filename$, extensionfilename$)
      OPEN extensionfilename$ FOR OUTPUT AS #2
    END IF
  END IF

```

```

PRINT #2, "  TIME      TEMP.  TEMP. DIFF."
PRINT #2, "  ----      ----  ----"
PRINT
PRINT "  TIME      TEMP.  TEMP. DIFF."
PRINT "  ----      ----  ----"
newfile = 0
fileopened = 1
END IF
END IF

```

```

CALL gettime(currenttime)
IF ((currenttime - lasttime) >= dtainterval) OR (firstreading = 1) THEN
  firstreading = 0
  lasttime = currenttime

  baddata = 0
  CALL retrievedata("01", tempstring$)
  IF baddata = 0 THEN
    IF thermocouple$ = "C-TYPE" THEN
      t = VAL(tempstring$)

      actualtemp = 292.35418018# - 11.1002522# * t + 7.5030893028# * t ^ 2
      - .491259386# * t ^ 3 + .0181360782# * t ^ 4 - .000344443# * t ^ 5 +
      .000002711
      8283# * t ^ 6
    
```

```

    IF actualtemp <= 804 THEN
      actualtemp = 804
    END IF
    IF actualtemp >= 2016 THEN
      actualtemp = 2016
    END IF
  
```

```

  actualtempstring$ = STR$(actualtemp)
  IF LEFT$(actualtempstring$, 1) = " " THEN

```

```

        actualtempstring$ = RIGHT$(actualtempstring$, LEN(actualtempstring$
) - 1)

```

```

    END IF

```

```

    DO

```

```

        IF LEN(actualtempstring$) >= 7 THEN

```

```

            EXIT DO

```

```

        END IF

```

```

        actualtempstring$ = " " + actualtempstring$

```

```

    LOOP

```

```

        tempstring$ = LEFT$(actualtempstring$, 7)

```

```

    END IF

```

```

    CALL retrievedata("02", tempdiffstring$)

```

```

END IF

```

```

IF (baddata = 0) THEN

```

```

    IF (needtoresetclock = 1) THEN

```

```

        needtoresetclock = 0

```

```

        CALL resetclock

```

```

        currenttime = 0

```

```

    ELSE

```

```

        CALL gettime(currenttime)

```

```

        lasttime = currenttime

```

```

    END IF

```

```

currtime$ = STR$(currenttime)

```

```

DO

```

```

    IF LEN(currtime$) >= 7 THEN

```

```

        EXIT DO

```

```

    END IF

```

```

    currtime$ = " " + currtime$

```

```

LOOP

```

```

PRINT currtime$, tempstring$, tempdiffstring$

```

```

PRINT #2, currtime$, tempstring$, tempdiffstring$

```

```

    END IF
  END IF
LOOP
END SUB

```

```

SUB tidyfilename (trialfilename$, filenameok)

```

```

  letters$ = "ABCDEFGHIJKLMNOPQRSTUVWXYZ"

```

```

  symbols$ = ":0123456789"

```

```

  slashes$ = "^"

```

```

  filenameok = 1

```

```

  colontest1 = INSTR(3, trialfilename$, ":")

```

```

  colontest2 = INSTR(trialfilename$, ":")

```

```

  IF (colontest1 <> 0) OR ((colontest2 <> 2) AND (colontest2 <> 0)) THEN

```

```

    filenameok = 0

```

```

  ELSE

```

```

    trialfilename$ = UCASE$(trialfilename$)

```

```

    temploop = 1

```

```

    inslashes = 0

```

```

    DO

```

```

      char$ = MID$(trialfilename$, temploop, 1)

```

```

      inletters = INSTR(letters$, char$)

```

```

      insymbols = INSTR(symbols$, char$)

```

```

      lastinslashes = inslashes

```

```

      inslashes = INSTR(slashes$, char$)

```

```

      IF ((temploop = 1) AND (insymbols <> 0)) THEN

```

```

        filenameok = 0

```

```

        EXIT DO

```

```

      ELSEIF ((temploop = 3) AND (colontest2 = 2) AND (insymbols <> 0))

```

```

      THEN

```

```

        filenameok = 0

```

```

        EXIT DO

```

```

      ELSEIF ((lastinslashes > 0) AND (insymbols > 0)) THEN

```

```

        filenameok = 0

```



```

EXIT DO
ELSEIF ((inslashes = 0) AND (insymbols = 0) AND (inletters = 0)) THEN
    filenameok = 0
EXIT DO
END IF
IF temploop = LEN(trialfilename$) THEN
    EXIT DO
END IF
temploop = temploop + 1
LOOP

IF filenameok = 1 THEN
DO
    slashlocation = INSTR(trialfilename$, "/")
    IF slashlocation = 0 THEN
        EXIT DO
    END IF
    startstring$ = MID$(trialfilename$, 1, slashlocation - 1)
    endstring$ = MID$(trialfilename$, slashlocation + 1, LEN(trialfilename$)
- slashlocation)
    trialfilename$ = startstring$ + "\" + endstring$
LOOP

DO
    doubleslashlocation = INSTR(trialfilename$, "\\")
    IF doubleslashlocation = 0 THEN
        EXIT DO
    END IF
    startstring$ = MID$(trialfilename$, 1, doubleslashlocation - 1)
    endstring$ = MID$(trialfilename$, doubleslashlocation + 2, LEN(trialfilen
ame$) - doubleslashlocation - 1)
    trialfilename$ = startstring$ + "\" + endstring$
LOOP
END IF

IF LEN(trialfilename$) = 1 THEN

```

```

inletters = INSTR(letters$, trialfilename$)
IF inletters = 0 THEN
    filenameok = 0
END IF
END IF
END IF
END SUB

```

```

SUB titlescreen
CALL clearkeyboardbuffer
CALL drawwindow(20, 3, 60, 7)
CALL center(40, 5, "{h}DTA DATA RETRIEVAL PROGRAM")
CALL center(40, 11, "{h}Program created by Jeff Meyer")
CALL center(40, 12, "{h}for Ames Laboratory")
CALL center(40, 13, "{h}Ames, Iowa 50010")
CALL center(40, 15, "{h}Under supervision of Cuneyt A. Tas")
CALL center(40, 19, "Temperature controllers: Newport Infinity")
CALL center(40, 20, "communications via COM2 and RS485")
CALL center(40, 24, "Version: 1.1    Release Date: May 16, 1992")
CALL resetclock
DO
    CALL gettime(temptime)
    IF (temptime >= 10) OR (INKEY$ <> "") THEN
        EXIT DO
    END IF
LOOP
CALL clearkeyboardbuffer
END SUB

```

APPENDIX C. X-RAY DIFFRACTION PATTERN OF Ce_2SiO_5

X-ray Diffraction Pattern of Ce_2SiO_5

$a = 9.278 \pm 1.44 \times 10^{-3} \text{Å}$, $b = 7.382 \pm 1.13 \times 10^{-3} \text{Å}$, $c = 6.956 \pm 1.61 \times 10^{-3} \text{Å}$, $\beta = 108^\circ 20'$
 $V = 452.261 \pm 9.20 \times 10^{-2} \text{Å}^3$, $Z = 4$, $D_x = 5.702 \text{ gm/cm}^3$, Monoclinic
 Non-extinction conditions : $h0l$ ($l=2n$), $0k0$ ($k=2n$), $00l$ ($l=2n$) Space group : $P12_1/c1$ (#14)

hkl	d_{calc}	d_{obs}	I/I_0
1 0 0	8.81	8.78	2
-1 1 0	5.66	5.65	12
0 1 1	4.92	4.92	3
-1 1 1	4.80	4.82	5
2 0 0	4.40	4.40	22
1 1 1	3.92	3.92	4
2 1 0	3.78	3.78	7
-2 1 1	3.75	3.74	2
-1 0 2	3.47	3.47	3
0 2 1	3.22	3.22	24
-1 2 1	3.19	3.19	16
-2 0 2	3.16	3.16	63
-1 1 2	3.14	3.14	16
0 1 2	3.014	3.015	3
3 0 0	2.936	2.934	26
1 2 1	2.886	2.886	69
-2 2 1	2.814	2.814	100
3 1 0	2.728	2.726	7
-3 1 2	2.490	2.490	1

(continued)

hkl	d_{calc}	d_{obs}	I/I_0
-3 2 1	2.358	2.359	2
0 3 1	2.306	2.308	4
-4 1 1	2.212	2.22	16
4 0 0	2.202	2.2	2
-4 0 2	2.174	2.175	15
-4 1 2	2.086	2.089	4
3 2 1	2.021	2.021	14
2 2 2	1.961	1.962	13
-2 3 2	1.942	1.942	16
-3 3 1	1.919	1.918	13
1 3 2	1.853	1.851	12
-3 3 2	1.802	1.802	22
0 4 1	1.777	1.778	10
-5 1 2	1.756	1.756	8
1 0 -4	1.724	1.726	2
2 4 0	1.702	1.701	1
-2 1 4	1.689	1.690	2
-4 2 3	1.675	1.676	5
-5 2 1	1.656	1.656	3
-2 4 2	1.594	1.596	3
-3 4 1	1.581	1.580	4

(continued)

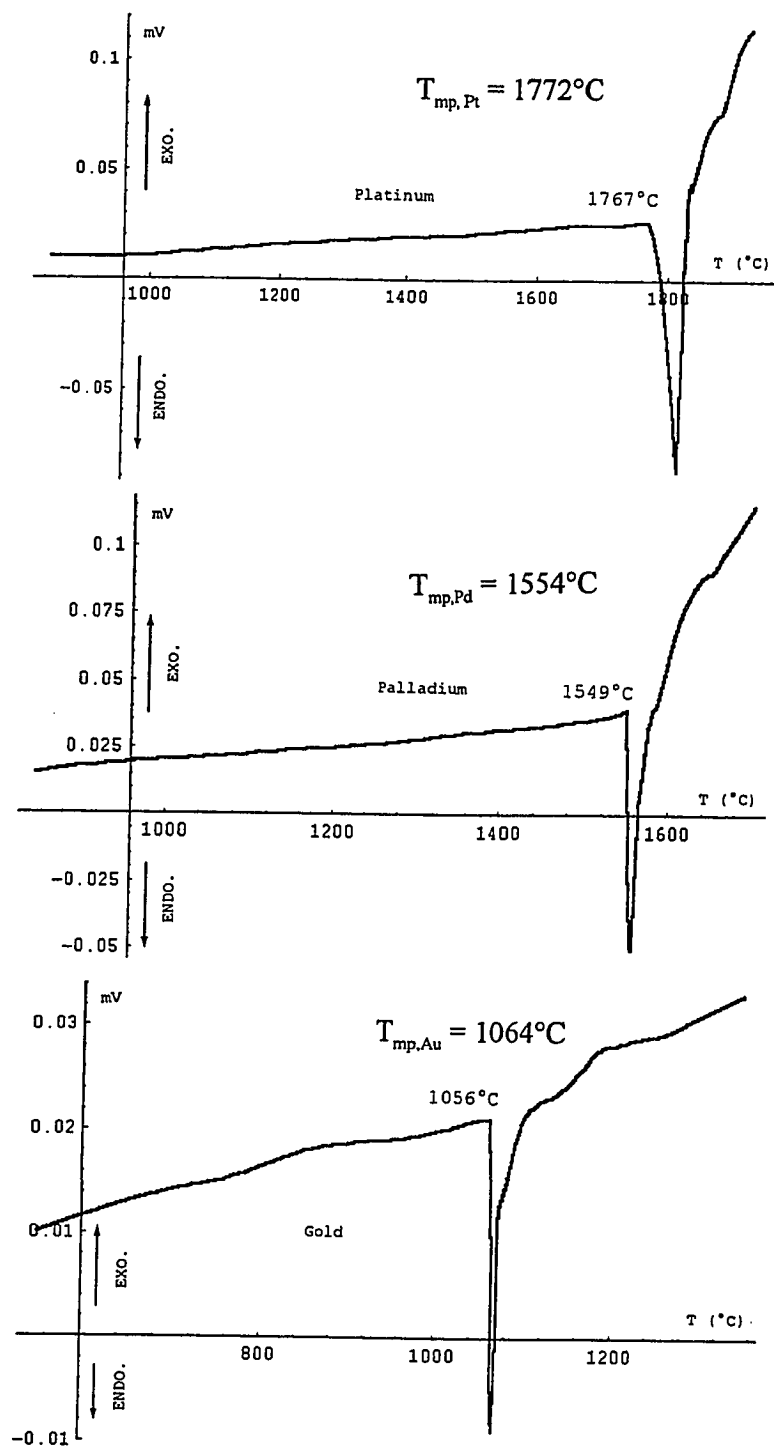
hkl	d_{calc}	d_{obs}	I/I_0
1 3 3	1.549	1.549	9
-3 4 2	1.514	1.513	11
0 2 4	1.507	1.507	2
-6 1 2	1.500	1.499	4
3 4 1	1.467	1.466	6
1 5 0	1.456	1.457	1
6 1 0	1.440	1.440	1
-4 4 2	1.407	1.408	3
2 1 4	1.382	1.383	2
1 4 3	1.354	1.355	2
-6 2 3	1.349	1.349	3
5 3 1	1.331	1.331	3
6 1 1	1.324	1.324	1
2 2 4	1.315	1.316	3
-5 4 2	1.292	1.292	2
2 4 3	1.274	1.274	10
-6 3 0	1.261	1.261	2
2 5 2	1.2449	1.2451	2
-7 2 1	1.2381	1.2383	2
1 6 1	1.1891	1.1893	2
2 6 0	1.1849	1.1847	1

(continued)

hkl	d_{calc}	d_{obs}	I/I_0
1 4 4	1.1813	1.1814	3
-6 3 4	1.1650	1.1658	2
-7 3 1	1.1593	1.1594	2
5 2 3	1.1439	1.1444	2
- 5 4 4	1.1421	1.1429	2
-8 1 1	1.1324	1.1324	3
-2 5 4	1.1245	1.1231	2
5 4 2	1.1072	1.1075	2
6 4 1	1.0876	1.0876	1
-6 5 1	1.0654	1.0660	2
6 1 3	1.0640	1.0645	2
7 1 2	1.0582	1.0575	2
8 2 0	1.0550	1.0558	2

Note : This pattern has not been included in any of the papers to be published from this dissertation since a similar pattern for the same compound was published by Van Hal and Hintzen (Paper III, reference 7) , for the first time, while this work was still in progress. The above pattern has extended the 2θ range for the reflections to 93° as compared to the maximum 2θ reported (53°) by Van Hal and Hintzen.

APPENDIX D. SAMPLES OF DTA CALIBRATION RUNS



DTA runs of Au, Pd, and Pt in vacuum ($P_{\text{O}_2} \approx 6 \times 10^{-9}$ atm) for calibration purposes